



**PV-Powered Vehicle Strategy Committee
Report
- Current Status and Future Outlook of
PV-Powered Vehicles -**

June 2025

New Energy and Industrial Technology Development Organization

Table of Contents of the PV-Powered Vehicle Strategy Committee Report

Introduction

Chapter 1: Trends in PV-Powered Vehicles and Expected Effects	1
1.1 Trends in PV-Powered Vehicles	1
1.1.1 Trends in Commercialization and Related Developments	1
1.1.2 Efforts to Promote Commercialization and Deployment in Japan and Abroad	5
1.2 Expected Effects of PV-powered Vehicles	11
1.2.1 Preconditions	11
1.2.2 Expected Benefits of PV-powered Vehicles (per unit vehicle)	12
1.2.3 Effects of Widespread Adoption of PV-powered Vehicles (Scenario Analysis)	15
【Chapter 1 References】	17
Chapter 2: Findings Derived from Demonstration Driving of PV-powered vehicles	20
2.1 Installation of PV on Passenger Vehicles	21
2.1.1 Installation of Photovoltaic Systems on Plug-in Hybrid Electric Vehicles (PVEVs): Evaluation of Generated Power, Driving Range, and Solar Irradiance/ Power Generation on Curved Vehicle	21
2.1.2 Installation of PV Systems on Electric Vehicles: Evaluation of Power Generation, Charging Frequency Reduction, and Performance against Fluctuations in Solar Irradiance	30
2.2 Installation of PV Systems in Commercial Vehicles	42
2.2.1 Installation of PV systems on Electric Commercial Vehicles	43
2.2.2 Installation of PV Systems on Internal Combustion Engine Trucks and Trailers	51
2.3 Reliability Evaluation of PV Modules for Passenger Vehicles	62
2.3.1 Organization of Environmental Load Test Items and Points to Note	62
2.3.2 Implementation of Reliability Tests for Automotive Components	66
2.3.3 Summary	69
2.4 Resilience Provided by Vehicle-mounted PV	70
2.4.1 Resilience Scenario	70
2.4.2 Effectiveness of Vehicle-mounted PV as Resilience Hubs	73
2.4.3 Required Number of Vehicles According to the Amount of Surplus Electricity Shared from PV-powered Vehicles	74
2.4.4 Summary	75

【Chapter 2 References】	76
Chapter 3: Conclusions (Findings and Future Challenges and Outlook).....	78
3.1 Findings	78
3.1.1 Trends in PV-powered Vehicles and Their Expected Benefits	78
3.1.2 Demonstration Driving of PV-Powered Vehicles for Passenger Use	78
3.1.3 Demonstration Driving of Commercial Vehicles Equipped with PV Systems	80
3.1.4 Reliability Evaluation of PV modules for passenger vehicles	81
3.1.5 Resilience Effects of Installing PV Systems on Passenger Vehicles	81
3.2 Future Challenges and Prospects	82
3.2.1 Future Challenges	82
3.2.2 Future Prospects	85
【Chapter 3 References】	88
[PV-Powered Vehicle Strategy Committee]	89

Introduction

The transport sector will have to play a significant role in achieving carbon neutrality by 2050, and measures by the automotive sector will be of great importance. In order to reduce greenhouse gas emissions from cars, initiatives aiming at a rapid rollout of the electrification of vehicles have begun in countries across the world. However, unless clean power derived from renewable energy sources can be supplied, such vehicles will have a limited effect in reducing greenhouse gas emissions.

Emissions of greenhouse gases are falling in the power generation sector due to the accelerated introduction of renewable energy, such as solar (hereinafter, photovoltaic or “PV”) and wind. In the transport sector however, which relies on fossil fuel for most of its energy needs, revolutionary technological development will be required to outperform current greenhouse gas reduction targets.

In response to this situation, NEDO has been conducting public road demonstration driving of PV-powered vehicles equipped with innovative, high-performance solar cells (very-high-efficiency solar cells) developed through NEDO projects since 2019^{i,ii}. Furthermore, under the “Development of Technologies to Promote Photovoltaic Power Generation as a Main Power Source” initiative launched in FY 2020, NEDO has been advancing various technological developments and research activities that form the foundation for the full-scale commercialization of PV-powered vehicles.

In addition, NEDO established the PV-Powered Vehicle Strategy Committee (secretariat: Mizuho Research & Technologies, Ltd.). This committee investigated the potential benefits and outstanding issues for installing high-efficiency PV on automobiles and reported in January 2018 on its potential for reducing the CO2 emissions in the transport sectorⁱⁱⁱ. This report also indicated that solar irradiation and generated power differ between PV on vehicle and PV installed on the roof or rooftop of a building, and stressed the need for quantitative analysis into this difference. In keeping with this recommendation, the solar irradiation of vehicles was measured at two locations in Japan (in Hokkaido and Miyazaki Prefectures), and the results of these measurements were reported in April 2019^{iv}. In February 2023, a comprehensive overview was compiled on the trends surrounding PV-powered vehicles, including the key findings obtained from the public road demonstration driving of PV-powered vehicles that began in 2019, as well as the status of efforts related to the core technologies forming the foundation for their full-scale commercialization in the future^v.

This PV-Powered Vehicle Strategy Committee report provides an overview of trends related to PV-powered vehicles as examined by the Committee. It includes an estimation of the potential benefits expected from their widespread adoption, highlights key outcomes from projects led primarily by NEDO aimed at

ⁱ NEDO: Press Release "Public Road Demonstration of Electric Vehicles Equipped with World's Highest-Efficiency Solar Cells Commences" (July 4, 2019) (https://www.nedo.go.jp/news/press/AA5_101150.html)

ⁱⁱ NEDO: Press Release "Production of Solar Panels for Electric Vehicles Utilizing World's Highest-Efficiency Solar Cells" (July 6, 2020) (https://www.nedo.go.jp/news/press/AA5_101326.html)

ⁱⁱⁱ NEDO, PV-Powered Vehicle Strategy Committee Interim Report, January 2018 (<https://www.nedo.go.jp/content/100885778.pdf>)

^{iv} NEDO, PV-Powered Vehicle Strategy Committee Interim Report (2) - Preliminary Study on Solar Irradiation of PV-Powered Vehicles-, April 2019 (<https://www.nedo.go.jp/content/100896335.pdf>)

^v NEDO, PV-Powered Vehicle Strategy Committee Interim Report (3) - Demonstration Driving of PV-Powered Vehicles, and Research for Practical Realisation-, February 2023 (<https://www.nedo.go.jp/content/100967545.pdf>)

promoting the practical implementation of PV-powered vehicles, and outlines remaining challenges and prospects.

Chapter 1: Trends in PV-Powered Vehicles and Expected Effects

In recent years, countries around the world have been intensifying their efforts to reduce CO₂ emissions. The automobile industry, as well, is dedicating itself to decarbonisation initiatives. At the start of the 21st century, the number of global annual vehicle production was around 60 million, but by 2023 it had risen to over 90 million¹. The number of vehicles owned worldwide surpassed 1.6 billion by 2018. As developing nations advance economically, their annual production and ownership numbers of vehicles are expected to grow².

To reduce CO₂ emissions from automobiles, companies are accelerating their efforts to develop environmentally-friendly (electric) vehicles, such as Hybrid Electric Vehicles (HEVs), Plug-in Hybrid Electric Vehicles (PHEVs), Fuel Cell Electric Vehicles (FCEVs), and Battery Electric Vehicles (BEVs). In particular, since 2022, the number of new BEV sales has been increasing, driven by efforts to mitigate economic security risks associated with oil dependence and by cost reductions. In 2022, sales rose by 54% YoY, followed by a 35% YoY increase in 2023³.

On the other hand, looking outside the transport sector, advances are being made in the use of renewable energy such as solar power as a promising approach for cutting CO₂ emissions in the residential and electricity sectors. Renewable energy is now the most inexpensive power source in many nations, and its importance continues to rise.

When a PV system is installed on an electric vehicle (including a plug-in hybrid vehicle) and the generated power is used to drive the vehicle, there are expected benefits such as a reduction in CO₂ emissions compared to when a vehicle is externally charged using grid, and a reduction in the frequency of external charging operations⁴. This aligns with the global trends of promoting the vehicle electrification. Although the output of PV is not large, PV-powered vehicles are gradually advancing toward commercial release. Technological development, such as the improvement of PV performance, is also being carried out to assist with the full-fledged practical application of PV-powered vehicles.

An overview of initiatives for the commercialization and practical implementation of PV-powered vehicles, along with estimated benefits expected from their widespread adoption are presented below.

1.1 Trends in PV-Powered Vehicles

1.1.1 Trends in Commercialization and Related Developments

(1) Installation of PV on Passenger Vehicles

The installation of PV on automobiles was originally proposed in the 1980s and began in early 1990s. The Mazda Sentia, launched in 1991, and the Audi A6, launched in 1993, had PV built onto their sunroofs. The rated output of the PV was several tens of watts, and used to power fans for ventilating the interior. The third generation Prius, launched in 2009, also had a similar PV system installed. The Nissan Leaf, released in the following year, made it possible to charge the auxiliary (12V) battery with installed PV. However, automobiles run on solar power from installed PV were not sold until recently. In January 2014, Ford announced a concept car that used PV as its energy source. Various car manufacturers then began to investigate the potential of PV as a power source for electric vehicles.

Table 1.1-1 shows examples of passenger cars that currently on market and those planned for equipped with PV systems for power for driving (including those currently on the market, under development, as well

as those for which development has been discontinued).

Table 1.1-1 Examples of PV-powered passenger cars

Name and manufacturer	Category	PV output (W)	Battery capacity (kWh)	Vehicle weight (kg)	Kilometres per kWh	Cruising Range (km)	PV system price	Status ^{*1}
Prius (4 th) ⁵ (Toyota)	PHEV	180 W ⁶	8.8	1,510	—	—	¥ 288,000 ⁷	On sale (from 2017)
Prius (5 th) ⁸ (Toyota)	PHEV	(186 W) ²	51 (Ah)	1,570	6.6~8.9	—	¥ 286,000	On sale (from 2023)
Karma Revero ^{9,10} (Karma)	PHEV	200 W	28	2,296	—	—	—	On sale (2020)
Sonata ¹¹ (Hyundai)	HEV	205 W	—	1,584 - 1,595	—	—	\$ 5,400 ^{*3}	On sale (from 2020)
bz4x ¹² (Toyota)	BEV	225 W ¹³	71.4	2,195 ~2,285	6.8~8.8	540~559	¥ 286,000	On sale (from 2022)
IONIQ 5 ¹⁴ (Hyundai)	BEV	205 W	58~72.6	1,870 - 2,100	7.0~7.6	498~618	\$ 3,000	On sale (from 2022)
Cybertruck ¹⁵ (Tesla)	BEV	Currently not equipped with PV	—	—	—	—	—	On sale (from 2023)
Vision EQXX ¹⁶ (Mercedes)	BEV	—	100	1,755	11.5	Over 1,000	—	—

*1: As of October 2024, *2: Estimation based on PV output from the Prius (4th generation) model, according to a report¹⁷

*3: Note that this represents the price difference between models with and without PV systems, not the pure cost difference of the PV systems themselves

The world's first mass-produced automobile to use vehicle-mounted PV to charge high voltage batteries for propulsion was the Prius PHEV launched in 2017. The Prius PHEV had an optional crystalline silicon PV module with an output of 180 W. Although the PV alone was not enough to drive the vehicle, the expected driving range under power generated using the PV per day was calculated as being up to 6.1 km/day. Additionally, the 5th generation Prius, launched in 2023, was announced to have reduced the module area by 10% while improving efficiency by 15%¹⁷.

This was followed by the launches of models using power generated by onboard PV, such as the 2020 Karma Revero (rated output 200 W) and the 2020 Hyundai Sonata HEV. The Sonata HEV's chassis roof had a 205 W LG-made PV module (only available for the top end model) made up of 46 cells, with a curved glass surface. Power generated by the PV was used to charge the direct-drive battery, a very different system than the Prius PHEV, which used PV to charge the sub-battery for buffering.

Looking at the trends from 2022 onward, the capacity of PV modules being installed has grown larger, and the range of mass-market product variations has grown more diverse. In 2022, Toyota Motor Corporation began selling the bz4x, a SUV-type BEV. One of the vehicle's options are a charging system that uses PV electricity (solar charging system). The bz4x has both a drive battery and an auxiliary battery. While parked,

the solar charging system charges the drive battery, and while driving, it supplements the power consumption of the auxiliary battery system, helping provide the vehicle with a longer driving distance. In Europe, the German startup Sono Motors had been developing the Sion, while the Dutch startup Lightyear had been developing the Lightyear 0. Both were BEVs. In the case of the Sono Motors Sion, PV were installed not only on the top of the chassis, but also on its sides and rear, for a PV output of 1.2 kW (1,200 W)¹⁸. The PV cover did not use glass, as in previous vehicles, but instead abrasion-resistant, lightweight polymer. The Lightyear 0, on the other hand, had PV covering from the bonnet to the entire upper chassis, achieving a capacity of 1 kW¹⁹. However, in February 2023, Sono Motors suspended its development plans for PV-powered BEVs and shifted its business model as a solution company to focus on providing retrofit PV kits for larger vehicles such as buses and trucks, as well as passenger cars. Similarly, Lightyear also halted the development of the Lightyear 0 and announced that it would concentrate its efforts on the development of its successor, the Lightyear 2. Additionally, Fisker, a company that had been selling PV-powered vehicles, filed for Chapter 11 bankruptcy protection in June 2024, following a slowdown in EV demand and a recall related to software issues in its "Ocean" model. In recent years, there has been a noticeable shift in development and sales strategies, with some manufacturers withdrawing from production altogether. This trend suggests that startup companies, in particular, are facing significant challenges in the commercialization and mass production of PV-powered vehicles.

(2) Installation of PV on Heavy Duty Vehicles

In recent years, an increasing number of companies—including Sono Motors, which has shifted its focus to providing PV kits for vehicles—have been actively developing PV systems for large vehicles such as buses, trucks, and trailers (HDVs: Heavy Duty Vehicles). Examples of large vehicles equipped with PV systems are shown in Table 1.1-2.

UK-based Trailar Ltd, a spin-off of logistics giant DHL, has developed and commercially launched a system with CIGS thin film solar cells on the roofs of trailers to reduce vehicle fuel consumption. This system can be used in a wide range of applications, such as trucks, trailers, buses, and refuse collection trucks. One of the advantages of installing thin film PV is its slimness, so vehicles do not need to be re-registered after the modules are installed. In addition to DHL, this system is being adopted by Loyal Mail (UK) and Go-Ahead Group (UK) and by ALBA Group (Singapore). As of October 2024, the number of partner companies has reached 16.

The Dutch company IM Efficiency is also carrying out initiatives to install PV on the roofs of box-type trailers²⁰. Currently, the PV being used is crystalline Si PV module, and in addition to installation on trailer roofs, the company is also studying the potential and effectiveness of installation on the sides of trailers. As previously mentioned, Sono Motors is leveraging its expertise in developing vehicles equipped with PV modules to create kits for installation on HDVs such as buses. The company has already introduced these kits to hybrid buses and is evaluating their effectiveness through on-road driving. In Europe, the German research institute Fraunhofer ISE is conducting demonstration tests of electric cargo transport trucks equipped with PV modules. The electric cargo transport trucks used in the tests have a 3.5-kW PV module and an 800-V high-voltage battery, reputedly capable of supplying 5 to 10% of the energy used by the trucks. In addition, research and development of HDVs is being conducted in several European countries, including Sweden, Switzerland, Italy, and the United Kingdom. In China, Hong Kong buses has installed PV modules on BYD's BEV buses. The electricity generated is used to power

onboard lighting and air conditioning systems, and compared to buses without PV modules, km per kWh is estimated to improve by 5 to 8%.

Efforts to use PV on trucks have also begun in Japan. Nagasaki Logistics Co., Ltd. has provided demonstration trucks for the trials which have PV modules on top of 10 tonne refrigerator van trailers. Thin film PV has been installed, and it is reported that fuel consumption has been reduced by over 10%. The company plans to begin commercializing this solution in September 2024.

Table 1.1-2 Examples of PV-powered vehicles (HDVs) utilizing PV-generated electricity

Company Name	Category	Country	PV capacity	Battery capacity	Estimated Effects
Trailer ^{21,22}	Trailer/ bus/ truck	UK	Varies by category	Depends on vehicle	For buses equipped with 1.5 kW PV systems, annual reduction of 4,800 t-CO ₂ (equivalent to 1.8 kL fuel) is possible.
IM efficiency	Trailer	Netherlands	430 W per module	Up to 4 kWh	Can reduce fuel consumption by 1 - 3 kL and CO ₂ emissions by 3 - 9 t annually.
Nagasaki Logistics ²³	Refrigerated trailer	Japan	125 W × 4 modules ²⁴	Unknown	Depends on driving conditions and vehicle type, but can improve fuel efficiency by about 10%.
PLM Fleet ²⁵	Refrigerated trailer	USA	Unknown	137 kWh	Battery alone enables over 14 hours of operation; with PV, over 20 hours is possible.
Fraunhofer ISE ^{26,27}	Truck	Germany	3.5 kW	Unknown	Can supply 5 - 10% of the truck's total energy consumption.
Hong Kong Buses/ BYD	Bus	China	Unknown	Unknown (Cruising Range 300 km)	PV electricity is used for onboard lighting and air conditioning; km per kWh improves by approx. 5 - 8%.
Sono Motors	Bus	Germany	1.4 kW	Depends on vehicle	Effectiveness is being verified through implementation in hybrid buses by running tests on actual regular routes.
Scania	Trailer	Sweden	13.2 kW	300 kWh	Annual PV generation expected to reach 8,000 kWh.
Peak Evolution	Truck	Switzerland/ Austria	7.4 kW	90 kWh	Four modules permanently installed on the ground and roof; 16 additional modules deployed for charging at high-altitude.
Multitrax/ Volvo/ FOUR	Trailer	Italy	5.16 kW	540 kWh	PV electricity used for lifting and lowering the loading platform.
Capsolar	Trailer	Canada	5.6 kW	Unknown	Can extend driving range per charge by 30 - 40%.
SUNSWAP/ JS Davidson	Trailer	UK	Unknown	Unknown	Can be installed on existing refrigerated trailers; no impact on refrigerated delivery operations.
PXP/ Topre	Truck	Japan	Unknown	Unknown	If 452 MW of PV is installed annually on domestic logistics vehicles, 408 kt of CO ₂ reduction is possible per year.

As for trends among Japanese companies, since December 2020, a U.S.-based PLM Fleet, a refrigerated trailer leasing and rental company jointly funded by Mizuho Leasing Company, Limited and Marubeni Corporation, has been supplying refrigerator and freezer unit-equipped trailers designed and manufactured by Advanced Energy Machines with installed PV modules and battery storage systems²⁸. The power generated by the PV modules is supplied to a battery storage system installed beneath the trailer and is used exclusively for the refrigerated trailer. These activities were prompted by moves in the U.S., especially in California, toward achieving zero emissions, and the increased attention being turned to the hybridisation and electrification of trailers using diesel engines and other similar vehicles.

(3) Installation of PV Modules in Compact Cars

In addition to general passenger vehicles and truck trailers, PV is increasingly being installed in compact cars.

U.S.-based startup Aptera Motors is developing the Aptera, a three-wheeled BEV that will be able to operate using PV alone. Thanks to a design focused on aerodynamics and reducing rolling resistance, the model with a 100-kWh battery capacity will have a cruising range of 1,000 km²⁹. Furthermore, as it is a three-wheeled BEV, it will be classified as a motorcycle, not an automobile, making it comparatively easier to meet safety standards³⁰. A Dutch company, Squadmobility, is developing a lightweight four-wheeled vehicle with PV mounted on its chassis roof. The company's vehicle will also not be categorized as an automobile, but instead will be in the light quadricycle (L6e) category. It will have a maximum speed of roughly 45 km/h, and is drawing interest as one type of next-generation mobility³¹. TUX Mobility, a Dutch company, is developing a compact three-wheeled EV for cargo transport equipped with PV modules, which has been attracting attention³². The company is working in collaboration with partners such as DHL and Amazon to advance the development.

In Japan, there is a growing trend of installing PV modules on compact cars. EV Genesis has launched a demonstration test for its three-wheeled electric vehicle, “3 RUOTA,” which is equipped with chalcopyrite solar cells³³. With these PV modules, the vehicle is capable of generating enough electricity to power approximately 15 to 20 km of driving per day. The solar cells, manufactured by PXP, are extremely lightweight at approximately 1mm thick. Furthermore, if upgraded to PXP’s perovskite tandem solar cells currently under development, the same surface area could potentially generate enough power for 25 to 30 km of travel per day.

1.1.2 Efforts to Promote Commercialization and Deployment in Japan and Abroad

(1) Overview of NEDO’s Research and Development Projects

Under the “Development of Technologies to Promote Photovoltaic Power Generation as a Main Power Source” (FY2020 - 2024), NEDO has been conducting research and development aimed at the practical application of low-cost, high-performance solar cells intended for installation on mobile platforms such as vehicles, or for related applications. Efforts have also included the development of technologies to estimate power generation of PV-powered vehicles, methods to assess market compatibility, and approaches for designing market introduction models that maximize effectiveness in target markets (Table 1.1-3).

This research and development project is being led by PV manufacturers and conducted together with

participating companies, research organizations, and universities. Furthermore, to accelerate the development of these technologies, research and development, market trend studies, and market trend analyses are being conducted both inside Japan and overseas. Trend studies are also being conducted in order to deliberate regarding the future directions. The IEA PVPS Task17: PV and Transport project conducted as part of this trend study, in which NEDO is participating, is an international cooperative project under the IEA. Japan is leading the project as *Task manager (chair)* (Refer to section (4)(i)).

Prior to these research and development efforts, NEDO collaborated with Toyota Motor Corporation, Nissan Motor Co., Ltd., and Sharp Corporation, in the development of PV-powered vehicles in FY 2019 and 2020 (Figs. 1.1-1 and 1.1-2). These demonstration vehicles are equipped with ultra-high-efficiency solar cells with a power generation efficiency of over 30%, and public road trials are still being carried out. In addition to data concerning the power generation performance of PV themselves, a variety of other data is also being collected in preparation for the full-fledged use of PV as a vehicle drive power source.

Chapter 2 of this report provides a summary—albeit partial—of the insights obtained thus far through the related research and development, demonstration trials, and trend analyses.

Table 1.1-3 Research and development conducted by NEDO on solar cells for transportation-related applications and PV-powered vehicles³⁴

Research and development of solar cells for transportation-related applications / Development of ultra-high-efficiency module technology	Develop high efficiency technologies, cost reduction technologies, new cell and module structures, and modularisation technologies for mounting on vehicles, etc. of PV (such as III-V compound multi-junction solar cells, III-V/Si and other tandem PV) that do not require tracking to match the sun's irradiance direction, and will have a module efficiency of over 35% at AM1.5 spectrum.
Research and development of solar cells for transportation-related applications / Development of next-generation module technology	Develop low-cost crystalline silicon-based PV modules that have a conversion efficiency of over 30% and the ability to conform to curved surface. This includes, for example, the development of tandem technologies for perovskite/Si, etc., and 3D curved surface module technologies.
Development of solar cells targeting multi-junction and related technologies	To explore the diverse potential of solar cells and promote broader adoption, development on multi-junction solar cells capable of achieving high conversion efficiency even in compact areas, as well as solar cells designed to balance the trade-off between light transmittance and conversion efficiency is conducted. In addition, to overcome the technical limitations of solar cells currently available in the market, high-efficiency solar cells such as multi-junction solar cells and mini modules—are developed.
Development of power generation forecasting technologies for new market deployment	Establish a technology to estimate the annual-basis power generation and other effects of PV power generation, and develop a method for assessing compatibility with the intended market (such as transport sector).
Trend survey of solar cells for transportation-related applications	Participate in activities such as IEA PVPS Task17 (PV and Transport), investigate and analyse R&D trends and market movements, both in Japan and overseas, related to PV for use in transport such as electric vehicles, deliberate regarding future directions, and accelerate research and development in the transport sector.



Fig. 1.1-1 PV-powered demonstration vehicle
1) Prius PHEV (Toyota Motor Corporation)³⁵



Fig. 1.1-2 PV-powered demonstration vehicle
2) eNV200 (Nissan Motor Co., Ltd.)³⁶

(2) Initiatives for Solar Cells for Transportation-related Applications in Japan

Based on technology development projects by NEDO, Japanese companies have been advancing solar cell technologies with the goal of integrating them into transportation-related applications such as vehicles.

In the project titled “Research and development of solar cells for transportation-related applications /Development of ultra-high-efficiency module technology,” Sharp Energy Solutions Corporation³⁷ has taken the lead in promoting solar cell innovation using III-V compound semiconductors. A PV-powered vehicle developed under this initiative was equipped with a high-efficiency PV module rated at 31.17%, which was the highest in the world at the time³⁶. Furthermore, in October 2023, Sharp achieved a world-record energy conversion efficiency of 33.66% with a compound–silicon stacked PV module³⁸.

In the “Research and development of solar cells for transportation-related applications /Development of next-generation module technology”, Kaneka Corporation is leading efforts to develop practical technologies for perovskite/silicon tandem solar cells³⁷. Evaluation assuming application to transportation sector has been conducted using prototype modules, verifying their effectiveness.

Under the “Development of solar cells targeting multi-junction and related technologies,” Toshiba Corporation is working on the development of Cu₂O tandem solar cells³⁷. By enhancing the efficiency of the Cu₂O top cell, they aim to achieve a tandem cell conversion efficiency exceeding 26%.

Additionally, EneCoat Technologies Inc., which is advancing the development and commercialization of perovskite solar cells with support from NEDO’s Green Innovation Fund, has initiated joint development of perovskite solar cells to be mounted on vehicles with Toyota Motor Corporation³⁹.

In addition to the aforementioned NEDO projects, PXP Corporation - possessing proprietary manufacturing technology for chalcopyrite solar cells - is developing film-type CIGS solar cells suitable for application in transportation-related applications such as vehicles. The company is conducting trials of mounting these solar cells on passenger vehicle rooftops and exploring their integration into refrigerated containers⁴⁰. Moreover, PXP is also engaged in the development of tandem solar cells that combine CIGS bottom cell with perovskite top cell. In April 2024, they reported achieving a conversion efficiency of 26.5%.

(3) Initiatives in Europe and the United States for PV-Powered Vehicles

In addition to Japan, efforts toward the practical implementation of PV-powered vehicles are also being promoted in Europe and the United States.

(i) Europe

In Europe, the EU's Solar Energy Strategy⁴¹ explicitly identifies the installation of PV systems into transportation-related applications such as vehicles as a key application area for expanding PV utilization in the future. Additionally, the Strategic Research and Innovation Agenda for Photovoltaics⁴², which serves as a guideline for PV research and development, outlines targets such as cost reduction (Table 1.1-4).

Furthermore, the SolarMOVES project⁴³ launched in Europe in 2023 evaluates energy consumption across 23 types of passenger and commercial cars of various sizes, based on representative driving patterns. The project also estimates the expected contribution of PV system when installed on these vehicles⁴⁴. In the next phase, several vehicle models will be selected, and demonstration driving with PV-powered vehicles are scheduled to be carried out.

Table 1.1-4 Europe: KPIs related to Vehicle-integrated PV (VIPV) as outlined in the Strategic Research and Innovation Agenda for Photovoltaics⁴²

KPI	Target value	Year
Standardization		
Performance Rating Methods	Methodology defined for accurate comparisons of systems in terms of additional power generation on a daily or monthly basis to help with customer understanding and comparisons. This must include differentiated use cases and understandable to customers.	2030
Homologation	Standards for Safety and Reliability to guide Road registration process in multiple countries.	2027
Vehicle Power Management	Shared and safe protocols defined for input to VPM for efficient charging while parked.	2030
Cost		
Manufacturing	Manufacturing concepts compatible with existing automotive supply chain requirements and processes including safety and traceability.	2028
System Additional Cost	Passenger Car: <800 EUR/m ²	2025
	Passenger Car: <500 EUR/m ²	2030
	Passenger Car: <250 EUR/m ²	2035
	Commercial Vehicles: <400 EUR/m ²	2028
	Commercial Vehicles: <200 EUR/m ²	2035
Technology		
BOS	Development of power conversion electronics suited for dynamic irradiance and vehicle integration, and gamification of technology use.	2030
Battery Impact	Theoretical and real world validation of impact on battery longevity, recyclability and temperature management.	2035
Circularity	Improved recyclability, repairability, reusability, and recoverability to exceed EU ELV requirements at component level.	2035
New Technologies	Investigation of integration of new PV technologies into vehicle environment (i.e. thin-film resistance to partial shading, Pb-free perovskite, (semi-)transparency, tandems, etc.)	2035
Data		
On-road	Demonstrate and validate on-road performance and reliability in various environments.	2028
Grid/Infrastructure	Large fleet modeling with grid integration and pilot studies.	2030

(ii) United States

In the United States, prior to initiating efforts toward PV-powered vehicles, the Department of Energy (DOE)'s Solar Energy Technologies Office conducted a Request for Information (RFI) in the summer of 2022 to broadly gather opinions on the potential, expectations, and challenges surrounding such technologies⁴⁵.

Based on the findings, the DOE concluded that Vehicle-Added PV (VAPV), such as installation on the rooftops of commercial vehicles like trucks, and Vehicle-Integrated PV (VIPV), such as integration into the rooftops of passenger and commercial cars, are both promising. In the short term, VAPV for trucks is seen as particularly feasible, while VIPV holds significant medium-to-long-term potential. The DOE expressed its intention to explore and promote these opportunities in coordination with relevant automotive divisions^{46,47}.

Subsequently, demonstration projects for various PV applications - including installation on vehicles - were launched, with a call for proposals starting in July 2023. Regarding PV-powered vehicles, a project was selected (announced in May 2024) to install PV systems on refrigerated trailers⁴⁸. Lightweight and flexible PV modules are mounted on the refrigerated trailer roofs (VAPV), and demonstrations are being conducted to evaluate the effects of PV systems, as well as reliability, environmental durability, and maintenance aspects^{48,49}.

(4) International Initiatives on PV-Powered Vehicles

Although not directly related to the aforementioned technological development or demonstration projects, international initiatives aimed at contributing to the commercialization and deployment of PV-powered vehicles are also being carried out under the frameworks of the International Energy Agency (IEA) and the International Electrotechnical Commission (IEC).

(i) IEA PVPS Task17

“IEA PVPS Task 17: PV and Transport” (IEA PVPS: International Energy Agency, Photovoltaic Power Systems Programme) is an international collaborative project launched under the IEA framework based on a proposal by Japan. Its objective is to contribute to the medium-to-long-term expansion of PV market and to reduce greenhouse gas emissions in the transport sector (especially in the automotive field) by promoting the integration of PV systems into transportation sector.

Japan, together with France, serves as Task manager (chair), and the task conducts analyses on trends and the expected impacts of the practical implementation of PV-powered vehicles and PV-powered electric vehicle charging stations. The task is composed of the following Subtasks⁵⁰.

- Subtask 1: Benefits and requirements for PV-powered vehicles
- Subtask 2: PV-powered applications for electric systems and infrastructures
- Subtask 3: Potential contribution of PV in transport
- Subtask 4: Dissemination

As of the end of 2024, ten countries are participating in Task 17, with experts from universities, research institutes, and companies engaging in active discussions. Technical reports produced to date are available on the IEA PVPS website and are recommended for reference as needed.

(ii) IEC TC82 PT600

IEC TC82 develops international standards related to PV systems and their components.

PV modules mounted on vehicle roofs (such as passenger cars) often feature curved (three-dimensional) shapes and are subject to partial shading from the surrounding environment while driving. As a result, the methods and conditions required to evaluate the performance of vehicle-mounted PV differ from those used

for conventional PV systems on buildings or the ground.

To address this, PT600 was established as an international collaborative project aimed at standardizing energy rating procedures for vehicle-mounted PV. Led by Japan, this project is driving the discussions and is working on the development of the following Technical Report⁵¹.

- EC TR 6XXXX: Monitoring three-dimensional solar irradiance around the automobile using array of pyranometers
- IEC TR 6XXXX: Modelling solar irradiance and its distribution and its distribution to VIPV affected by shading by buildings

1.2 Expected Effects of PV-powered Vehicles

By installing PV systems on Battery Electric Vehicles (BEVs) and Plug-in Hybrid Electric Vehicles (PHEVs), several benefits can be expected: a reduction in grid electricity usage through substitution with PV-generated power for charging, decreased charging frequency, and lower CO₂ emissions. On the other hand, the addition of PV systems increases vehicle weight, which must be taken into account as it can impact energy consumption. Moreover, the effects of mounting PV systems on vehicles varies depending not only on driving patterns but also on the installed PV capacity and battery size.

This section estimates the benefits per PV-powered vehicle and conducts scenario analysis for future widespread adoption of PV-powered vehicles.

1.2.1 Preconditions

The vehicle specifications for electric vehicles, etc. used in this analysis fundamentally follow those from previous years. For the base vehicles, a 40-kWh storage battery is assumed to be installed for BEVs and a 15-kWh battery for PHEVs. The installed PV capacity is assumed to range from 200 W to 1,000 W (1 kW), consistent with the previous year. The storage battery manufacturing emission intensity adopts the value for Japanese NMC batteries published by ICCT⁵². The impact of vehicle weight changes on electric (km per kWh) and fuel consumption was calculated using the correlation between vehicle weight and fuel efficiency as defined in Japan's Top Runner Program⁵³ under the Energy Conservation Act. Although the Top Runner Program provides a relationship between vehicle weight and fuel economy (km per L), it was adapted for electric consumption (km per kWh) by calculating the rate of change in fuel economy with weight and applying this to the electric consumption. Six driving patterns, consistent with previous years, were considered:

- Holiday use: A-1 (150 km/day, 2 days/week, (annual mileage: 15,600 km/year)) and A-2 (50 km/day, 2 days/week (annual mileage: 5,200 km/year))
- Weekday & holiday use: B-1 (50 km/day, 4 days/week (annual mileage: 10,450 km/year)) and B-2 (5 km/day, 4 days/week (annual mileage: 1,045 km/year))
- Weekday use: C-1 (50 km/day, 5 days/week (annual mileage: 13,050 km/year)) and C-2 (15 km/day, 5 days/week (annual mileage: 3,915 km/year))

When considering the installation of PV modules on vehicles, increased frontal projected area may lead to greater air resistance and reduced electric consumption (km per kWh) and fuel economy. However, given that urban driving dominates in Japan, the relative impact of air resistance is smaller. Therefore, only the influence of increased vehicle weight is considered in this study.

For grid charging assumptions, in the case of BEVs, the scenario was designed to maximize the benefits of installed PV, whereby grid charging occurs only when the remaining battery charge becomes insufficient during driving. For PHEVs, the scenario maximizes the advantage of gasoline backup: if the remaining battery charge is insufficient based on the scheduled driving distance for the next day, the vehicle charges at home using grid electricity; if battery capacity becomes insufficient during driving, the vehicle switches to gasoline-powered operation. Additionally, future scenarios were calculated assuming the widespread adoption of PV-powered vehicles, including changes over time in the grid electricity emission intensity, CO₂ emissions from PV and battery manufacturing, and the weight of PV modules.

1.2.2 Expected Benefits of PV-powered Vehicles (per unit vehicle)

(1) Grid Charging Reduction Effects (power-saving impact)

Figures 1.2-1 and 1.2-2 illustrate the effects of mounting PV systems on vehicles in reducing charging power from the grid. In the case of BEVs, although km per kWh deteriorates due to the additional PV modules, grid electricity consumption is reduced across all preconditions. Conversely, for PHEVs, the reduction effect is minimal under preconditions A-1 and B-2. This is attributed to the low utilization rate of PV electricity. In precondition A-1, the long driving distance per trip necessitates grid charging on the previous day, resulting in limited benefit from PV. Consequently, the advantage of mounting PV systems is offset by worsened electric consumption (km per kWh) and fuel efficiency. In precondition B-2, the short driving distance per trip leads to excess PV-generated electricity being unused (effectively wasted). In other preconditions, however, PHEVs also demonstrate contribution to reducing grid electricity.

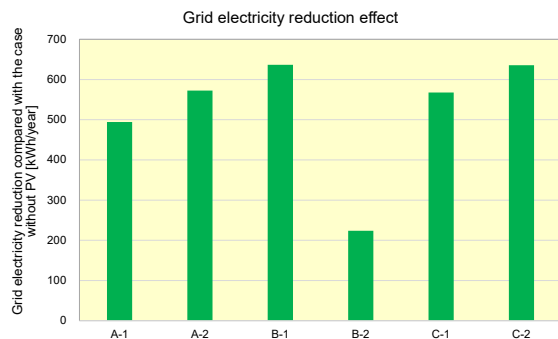


Fig. 1.2-1 per PV-powered Vehicle (BEV)
(BEV with 1-kW PV and 40-kWh battery)

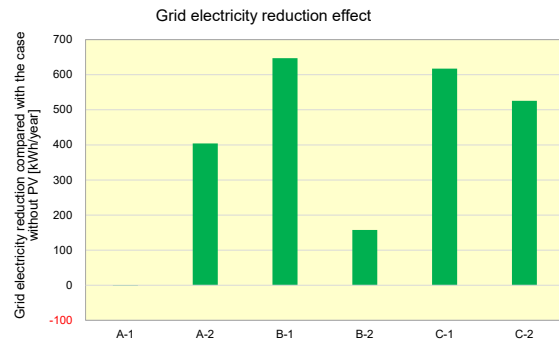


Fig. 1.2-2 Grid electricity reduction effect per
PV-powered Vehicle (PHEV)
(PHEV with 1-kW PV and 15-kWh battery)

(2) Charging Frequency Reduction Effect

Figures 1.2-3 and 1.2-4 illustrate the reduction in the number of charging from the grid achieved through the installation of PV systems on vehicles. In the case of BEVs, all preconditions lead to a decreased frequency of charging. Notably, under precondition B-2, the required electricity for driving can be fully supplied by PV, resulting in zero grid charging. Conversely, for PHEVs, precondition A-1 shows an increase in charging frequency. Due to the long driving distance per trip in A-1, the battery is fully depleted during driving days. Moreover, to cover the power consumption of the ECU for PV modules, charging from grid electricity becomes necessary on the following day of the driving, resulting in a net increase in the number of charging from the grid. In other preconditions, however, PHEVs demonstrate a significant contribution to reducing the number of charging.

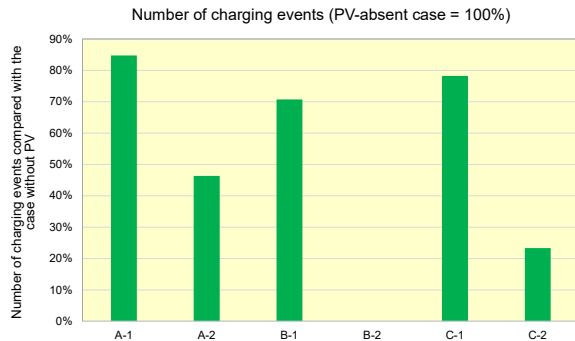


Fig. 1.2-3 Charging frequency reduction effect by mounting PV on BEV
(BEV with 1-kW PV and 40-kWh battery)

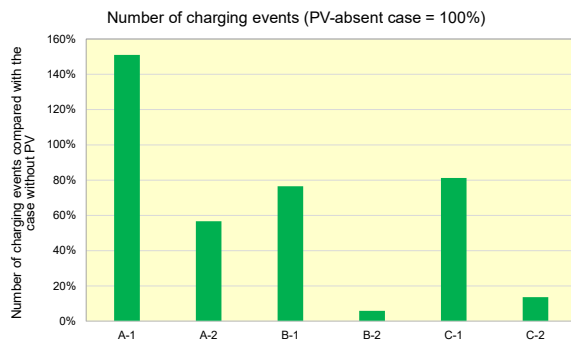


Fig. 1.2-4 Charging frequency reduction effect by mounting PV on PHEV
(PHEV, with 1-kW PV and 15-kWh battery)

(3) CO₂ Emission Reduction Effect

The CO₂ emission reduction effect per PV-powered vehicle is shown in Figures 1.2-5 to 6. In all preconditions, a CO₂ emission reduction effect can be observed, and except for A-1, this effect is generally at a similar level for both BEVs and PHEVs. This is attributed to the fact that in all preconditions from A-2 to C-2, the utilization rate of PV-generated electricity is generally at a same level (excluding the shorter driving range in B-2, the utilization rate of PV-generated electricity is high across all preconditions). On the other hand, A-1 shows significantly different results between BEVs and PHEVs, which, as with the reasons mentioned above, is due to the longer driving distance per trip. In the case of driving under the A-1 pattern with PHEVs, most of the travel is done using gasoline, resulting in a significant impact from the deterioration in fuel economy due to the increased vehicle weight.

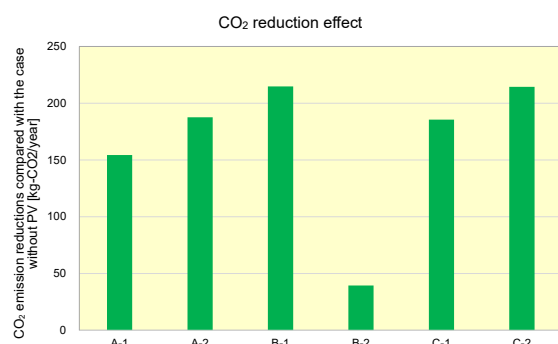


Fig. 1.2-5 CO₂ reduction effect per PV-powered vehicle (BEV)
(BEV with 1 kW PV capacity and 40 kWh battery capacity)

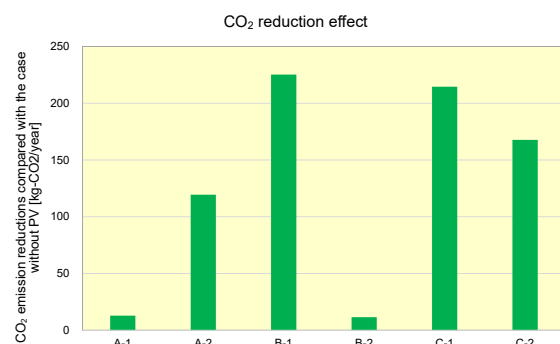


Fig. 1.2-6 CO₂ reduction effect per PV-powered Vehicle (PHEV)
(PHEV with 1 kW PV capacity and 15 kWh battery capacity)

(4) Trial Calculation of Effect Variation due to Electricity Consumption (kilometres per kWh)

In the aforementioned trial calculation, it is assumed that PV systems are mounted on existing BEVs and PHEVs. On the other hand, while it is anticipated that the widespread adoption of PV-powered vehicles will take time, it is highly probable that the electricity consumption and fuel efficiency of BEVs and PHEVs will

have improved beyond their current levels by the time widespread adoption occurs. Therefore, we decided to trial calculate the effect of installing PV systems assuming an improvement in the electricity and fuel efficiency of the base vehicles. For BEVs, the improved electric consumption was estimated by taking the ratio between the current BEV reference value and the reference value projected for 2030 and beyond, as defined in the Top Runner Program for energy conservation and multiplied that ratio by the electricity consumption of the existing base vehicle. For PHEVs, the same approach as for BEVs was adopted for electricity consumption, while for fuel efficiency, the improvement rate required by the Top Runner Program for energy conservation for a vehicle weighing approximately 1,400 kg (subtracting the assumed battery weight from the base vehicle's curb weight) was adopted and multiplied by the fuel efficiency of the existing base vehicle to adopt it as the improved fuel efficiency value.

The respective effects for BEVs are shown in Figures 1.2-7 to 1.2-9. Patterns with relatively longer driving distances show a greater reduction in grid electricity consumption and CO₂ emissions, while shorter driving patterns exhibit the opposite results. In the scenario analysis presented in section 1.2.3, similar calculations were performed for PHEVs, using the estimation results based on the improved electricity and fuel efficiency.

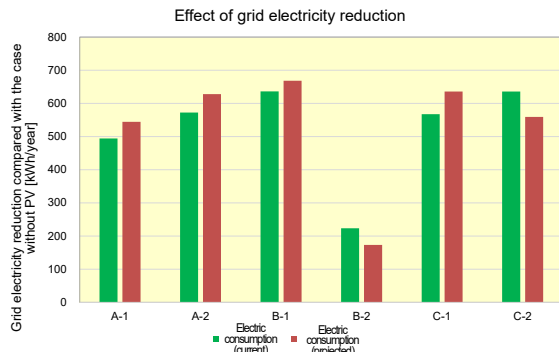


Fig. 1.2-7 Effect of grid electricity reduction by differences in electricity consumption (BEV with 1 kW PV capacity and 40 kWh battery capacity)

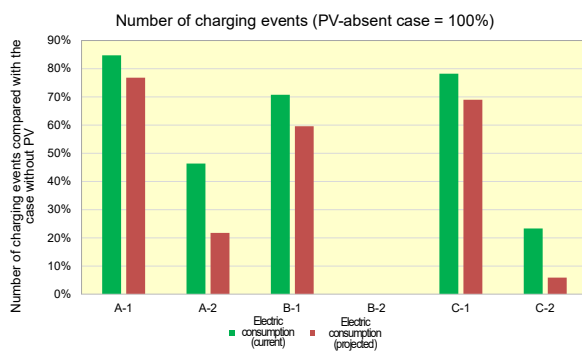


Fig. 1.2-8 Effect of reduced charging frequency by differences in electricity consumption (BEV with 1 kW PV capacity and 40 kWh battery capacity)

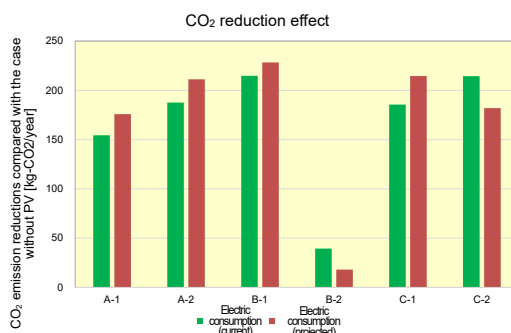


Fig. 1.2-9 Effect of CO₂ reduction by differences in electricity consumption (BEV with 1 kW PV capacity and 40 kWh battery capacity)

1.2.3 Effects of Widespread Adoption of PV-powered Vehicles (Scenario Analysis)

Assuming future projections for the widespread adoption of PV-powered vehicles, a scenario analysis was conducted regarding the effects of their widespread adoption in Japan.

Assuming the sales volume forecast trends from Fuji Keizai's "2023 Edition: Thorough Market Analysis of HEV and EV-Related Markets"⁵⁴ for the period of 2030 - 2035 are maintained, the sales volume forecast for EVs and PHEVs in Japan were calculated. However, in light of the goal to achieve 100% electric vehicle sales among new car sales by 2035, a correction was made assuming that a portion of the internal combustion engine vehicle sales forecast would be replaced by electric vehicles by 2035. Based on recent trends, the average vehicle lifespan was assumed to be 13 years, and from the aforementioned sales volume forecast, the forecast for the number of vehicles in use were calculated.

The penetration forecast for PV-powered vehicles in Japan was created by setting three patterns for the ratio of PV-powered vehicles among electric vehicles:

Early Adoption: 100% penetration rate by 2050

Medium Adoption: 100% penetration rate by 2060

Low Adoption: 100% penetration rate by 2070

The capacity of the PV modules installed per vehicle was set at 200W for vehicles sold in 2025, based on recent commercialization examples. An analysis was conducted using two patterns for the increase rate of installed capacity, with an upper limit of 1,000W:

High installed capacity: an annual increase of 40W

Low installed capacity: an annual increase of 20W

Furthermore, for grid electricity's CO₂ emissions, the assumed values for CO₂ emission intensity of grid electricity from the Stated Policies Scenario (STEPS) in the International Energy Agency's (IEA) World Energy Outlook 2023 (WEO2023) were used⁵⁵. The expected effects per PV-powered vehicle utilized the aforementioned analysis results. Although the CO₂ emission reduction effect may sometimes be negative depending on the driving pattern, it was assumed that PV systems would only be installed if the CO₂ emission reduction effect was positive at the time of vehicle sale. The analysis per vehicle was conducted across six types of driving patterns, and the total number of vehicles in Japan was apportioned among these six driving patterns. For this apportionment, the results of a survey on the driving patterns of 5,000 vehicles in Japan from the research by Kimura et al.^{56,57} were used.

Based on these assumptions, Figures 1.2-8 and 1.2-9 illustrate the CO₂ emission reduction effect and grid electricity consumption reduction effect from the widespread adoption of PV-powered vehicles in Japan. By 2050, the number of BEVs and PHEVs in use is projected to range from 16 to 28 million for BEVs and 1.7 to 3.6 million for PHEVs, depending on the case. The CO₂ emission reduction effect in the early adoption combined with high installed capacity scenario is projected to exceed 500,000 tCO₂ by the 2040s. Subsequently, in the A-1 and B-2 patterns, as the CO₂ emission factor of grid electricity decreases, the CO₂ reduction effect becomes negative. Consequently, the CO₂ emission reduction effect of PV-powered vehicles in Japan will decline. However, in the early adoption combined with high installed capacity scenario, the CO₂ emission reduction effect for FY 2050 will still be approximately 350,000 tCO₂. According to the Announced Pledges Scenario (APS) in the WEO2023, CO₂ emissions from Japan's transportation sector by 2050 are projected to be 19 million tCO₂. The introduction of PV-powered vehicles could lead to an additional

emissions reduction of approximately 2% beyond the transition from internal combustion engine vehicles to electric vehicles.

As mentioned above, while the CO₂ emission reduction effect is projected to decrease from mid-2040s due to the reduction in the CO₂ emission factor of grid electricity, the grid electricity reduction effect is expected to show an increasing trend in all cases towards FY 2050, reaching an estimated 6,300 to 17,000 GWh in 2050. The projected electricity consumption for the transport sector in Japan in 2050, according to the Announced Pledges Scenario (APS) of WEO2023, is 593 PJ (164,722 GWh). The aforementioned trial calculation results for grid electricity reduction effect correspond to 3.8% to 10.3% of this figure. Furthermore, while the installation of PV systems in vehicles is expected to reduce the number of EV charging cycles, based on the aforementioned assumptions, the number of charging cycles initially increases due to the weight increase associated with PV module installation. However, by 2050, a reduction of 200 million to 540 million charging cycles is expected. This reduction in charging cycles is also believed to contribute to a decrease in social costs, such as the charging infrastructure, that will be required with the widespread adoption of electric vehicles.

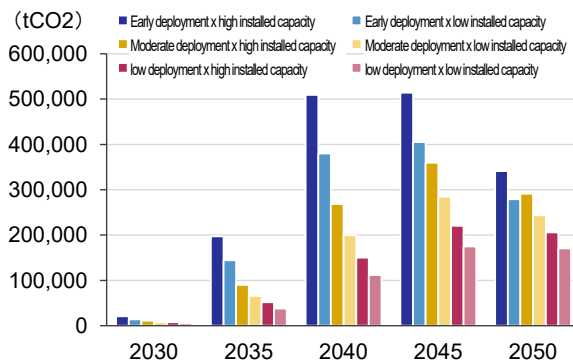


Fig. 1.2-8 Projection of CO₂ reduction effects by PV-powered vehicles in Japan

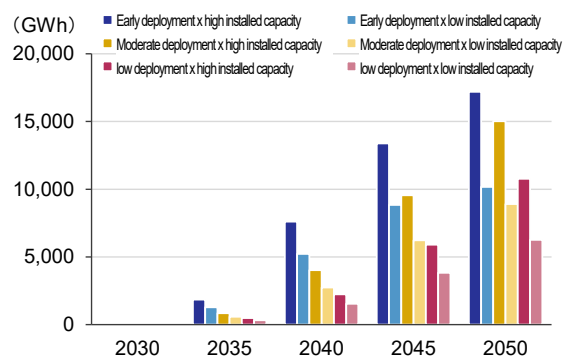


Fig. 1.2-9 Projection of grid electricity consumption reduction effects by PV-powered vehicles in Japan

【Chapter 1 References】

¹ Japan Automotive Manufacturers Association, “World production, sales, possession, penetration and exports” (Japanese Only), (Confirmed on January 10, 2025)

² IEA, Tracking Transport 2020 (2020) (<https://www.iea.org/reports/tracking-transport-2020>)

³ IEA, Global EV Outlook 2024 (2024) (<https://www.iea.org/reports/global-ev-outlook-2024>)

⁴ NEDO, ”PV-Powered Vehicle Strategy Committee Interim Report” (January 2018) (<https://www.nedo.go.jp/content/100961854.pdf>)

⁵ Toyota Motor Corporation, ”Toyota Launches Redesigned "Prius PHV" in Japan” (<https://global.toyota/jp/newsroom/toyota/21821789.html>) (Confirmed on January 10, 2025)

⁶ Panasonic Holdings Corporation, “Panasonic's Photovoltaic Module HIT™ adopted for Toyota Motor's New Prius PHV” (February 28, 2017) (<https://news.panasonic.com/jp/press/jn170228-2>) (Confirmed on January 10, 2025)

⁷ Response Company, “The solar charging system is available at a standard price of JPY 280,000(Translated title” (Japanese Only) (Article on February 15, 2017) (Confirmed on March 10, 2025)

⁸ Toyota Motor Corporation, Web Catalogue (https://toyota.jp/pages/contents/request/webcatalog/prius/prius_main_202502.pdf) (Japanese Only) (Confirmed on March 10, 2025)

⁹ Karma Automotive “Revero” Homepage (<https://karmaautomotive.com/revero/>) (Confirmed on January 10, 2025)

¹⁰ Society of Automotive Engineers of Japan, Inc. (<https://guide.jsae.or.jp/topics/252994/>) (Japanese Only) (Confirmed on January 10, 2025)

¹¹ Hyundai Motor America Webpage (<https://www.hyundaiusa.com/us/en/vehicles/sonata-hybrid/compare-specs>) (Confirmed on January 10, 2025)

¹² Toyota Motor Corporation “bz4x” Web Catalogue (https://toyota.jp/pages/contents/request/webcatalog/bz4x/bz4x_main_202410.pdf) (Japanese Only) (Confirmed on January 10, 2025)

¹³ Toyota Motor Corporation, TOYOTA Technical Review vol.68 (Confirmed on January 10, 2025)

¹⁴ Hyundai Motor UK Webpage (<https://www.hyundai.com/uk/ioniq-5/ioniq5/specifications.html#>) (Confirmed on January 10, 2025)

¹⁵ Tesla “Cybertruck” Webpage (https://www.tesla.com/ja_jp/cybertruck) (Japanese Only) (Confirmed on January 10, 2025)

¹⁶ Mercedes-Benz “Vision EQXX” Webpage (https://media.mercedes-benz.com/vision_eqxx) (Confirmed on January 10, 2025)

¹⁷ Toyota Motor Corporation, TOYOTA Technical Review vol.69 (Confirmed on January 10, 2025)

¹⁸ Lightyear, “Lightyear 0” Webpage (<https://lightyear.one/lightyear-0>) (Confirmed on January 10, 2025)

¹⁹ Sono motors, “Sion” Information Sheet (https://sonomotors.com/site/assets/files/1621/sonomotors_informationssheet_sion_1.pdf) (Confirmed on January 10, 2025)

²⁰ IM Efficiency Webpage (<https://imefficiency.com/>) (Confirmed on October 4, 2022)

²¹ Trailer Webpage (<https://www.trailar.co.uk/products>) (Confirmed on January 10, 2025)

²² MiaSolé Press Release (<https://miasole.com/miasole-hanergy-and-trailor-deutsche-post-dhl-unveil-solutions-to-global-logistic-green-energy-power-showcase/>) (Confirmed on January 10, 2025)

²³ Nagasaki Logistics Webpage (<https://nagalogi.co.jp/info/5919246>) (Japanese Only) (Confirmed on January 10, 2025)

²⁴ Megasolar Business (<https://project.nikkeibp.co.jp/ms/atcl/19/news/00001/02824/?ST=msb>) (Japanese Only) (Confirmed on January 10, 2025)

²⁵ PLM fleet Webpage (<https://www.plmfleet.com/fleet-solutions/zero-emissions->)(Confirmed on January 10, 2025)

²⁶ Fraunhofer ISE, Lade-PV – Development of Vehicle-Integrated Photovoltaics for On-Board Charging of Electric Utility Vehicles

(<https://www.ise.fraunhofer.de/en/research-projects/lade-pv.html>) (Confirmed on January 10, 2025)

²⁷ STROM-FORSCHUNG, E-truck runs on solar energy from its own vehicle roof (November 11, 2021) (Confirmed on January 10, 2025)

²⁸ Mizuho Leasing Company, Marubeni Corporation Press Release (<https://www.mizuho-ls.co.jp/ja/news/news2021020501/main/0/link/Delivery%20of%20Zero-Emission%20Refrigerated%20Trailers%20for%20Leasing%20by%20PLM%20Fleet,%20LLC..pdf>) (Japanese Only) (Confirmed on January 10, 2025)

²⁹ Aptera Motors Webpage (<https://www.aptera.us/about>) (Confirmed on January 10, 2025)

³⁰ Aptera Motors Webpage (<https://www.aptera.us/faq>) (Confirmed on January 10, 2025)

³¹ Squadmobility Webpage (<https://squadmobility.com/>, <https://www.squadmobility.com/#specs>) (Confirmed on January 10, 2025)

³² TUX mobilityWebpage (<https://www.tuxmobility.com/>) (Confirmed on January 10, 2025)

³³ Smart Mobility JP (https://smart-mobility.jp/_ct/17701259) (Japanese Only) (Confirmed on January 10, 2025)

³⁴ NEDO, Master plan on ‘Development of Technologies to Promote Photovoltaic Power Generation as a Primary Power Source’, updated in July 2024

(<https://www.nedo.go.jp/content/100930776.pdf>) (Japanese Only) (Confirmed on January 8, 2025)

³⁵ NEDO Press Release, “NEDO, Sharp, and Toyota to Begin Public Road Trials of Electrified Vehicles Equipped with High-efficiency Solar Batteries“ (4 July 2019)

(https://www.nedo.go.jp/english/news/AA5en_100408.html) (Confirmed on January 8, 2025)

³⁶ NEDO Press Release “Solar Battery Panel for Electrified Vehicles Using World-Class, High-Efficiency Solar Battery Cells” (6 July 2020)

(https://www.nedo.go.jp/news/press/AA5_101326.html) (Japanese Only) (Confirmed on January 8, 2025)

³⁷ NEDO, Enforcement policy on ‘Development of Technologies to Promote Solar Power Generation as a Primary Power Source’ in FY2024

(<https://www.nedo.go.jp/content/100972461.pdf>) (Confirmed on January 8, 2025)

³⁸ NEDO Press Release

(https://www.nedo.go.jp/news/press/AA5_101700.html) (Japanese Only) (Confirmed on January 8, 2025)

³⁹ EneCoat Technologies Co.,Ltd., Press Release (Japanese Only) (Confirmed on January 8, 2025)

⁴⁰ PXP Corporation website (<https://pxpco.jp/>) (Confirmed on January 8, 2025)

⁴¹ EU, Solar Energy Strategy, 2022 (<https://eur-lex.europa.eu/legal>-

content/EN/TXT/?uri=COM%3A2022%3A221%3AFIN&qid=1653034500503)(Confirmed on January 8, 2025)

⁴² ETIP/EERA, Strategic Research and Innovation Agenda for Photovoltaics, Aug. 2024 update (https://media.etip-pv.eu/filer_public/f5/8b/f58b06d7-60fa-457a-8562-80eb71fa667c/etip_pv_-sria_report_update_-august24.pdf) (Confirmed on January 8, 2025)

⁴³ SolarMoves brochure (<https://publications.tno.nl/publication/34642389/SKwCWv/tno-2024-solarmoves.pdf>) (Confirmed on January 8, 2025)

⁴⁴ A. J. Carr, Modelling the impact of VIPV, Conference & Exhibition on Vehicle Integrated PV (PV in Motion 2024), Neuchatel, Switzerland, March 2024

⁴⁵ U.S.DOE, SETO, Challenges and Opportunities for Vehicle Photovoltaics, July 2022

⁴⁶ U.S.DOE, SETO, Summary: Vehicle-Integrated Photovoltaics Request for Information (<https://www.energy.gov/eere/solar/summary-vehicle-integrated-photovoltaics-request-information>) (Confirmed on January 8, 2025)

⁴⁷ J. DiStefano, et al., Challenges and Opportunities for VIPV: The Perspective of the U.S. Department of Energy, Conference and Exhibition on Solutions for Vehicle Integration (PV in Motion 2023), s-Hertogenbosch, the Netherlands, February 2023

⁴⁸ U.S.DOE, SETO, Silicon Solar Manufacturing and Dual-use Photovoltaics Incubator Funding Program (<https://www.energy.gov/eere/solar/silicon-solar-manufacturing-and-dual-use-photovoltaics-incubator-funding-program>) (Confirmed on January 8, 2025)

⁴⁹ Wabash National Corporation, News “Wabash Partners with University of Delaware to Advance Solar Solutions in Commercial Transportation” (<https://ir.onewabash.com/news/news-details/2024/Wabash-Partners-with-University-of-Delaware-to-Advance-Solar-Solutionsin-Commercial-Transportation/default.aspx>) (Confirmed on January 8, 2025)

⁵⁰ IEA PVPS Task17 Webpage

(<https://iea-pvps.org/research-tasks/pv-for-transport/>) (Confirmed on January 8, 2025)

⁵¹ IEC TC82 Webpage

(https://www.iec.ch/ords/f?p=103:14:527618088944::::FSP_ORG_ID,FSP_LANG_ID:27684,25#) (Confirmed on January 8, 2025)

⁵² ICCT, White Paper a Global Comparison of the Life-Cycle Greenhouse Gas Emissions of Combustion Engine and Electric Passenger Cars

⁵³ Agency for Natural Resources and Energy Webpage, “Energy conservation regulations for energy consumption equipment manufacturers(Translated Title)” (Japanese Only) (Confirmed on January 8, 2025)

⁵⁴ FUJI KEIZAI GROUP CO.,LTD., “2023 Edition: HEV and EV-related market in-depth analysis survey” (Japanese Only)

⁵⁵ IEA, World Energy Outlook 2023 (2023)

⁵⁶ Kazutaka Kimura et al, Techno-Economic Analysis of Solar Hybrid Vehicles Part 1: Analysis of Solar Hybrid Vehicle Potential Considering Wellto-Wheel GHG Emissions (2016)

⁵⁷ Kazutaka Kimura et al, Techno-Economic Analysis of Solar Hybrid Vehicles Part 2; Comparative Analysis of Economic, Environmental, and Usability Benefits (2016)

Chapter 2: Findings Derived from Demonstration Driving of PV-powered vehicles

CO₂ emissions from the transport sector account for roughly 21% of global emissions, of which, roughly 39% are reported to come from passenger vehicles¹. Companies around the world are accelerating their development of environmentally friendly (electric) vehicles to reduce CO₂ emissions. Plug-in Hybrid Electric Vehicles (PHEVs) and Battery Electric Vehicles (BEVs), which equipped with high-capacity batteries, are good matches for renewable energy. PV modules are the form of plates, so they are especially well-suited for mounting on vehicles.

Although many studies have been reported on the application of solar energy in the transportation sector (using PV power generated on board), the technology remains in a developmental stage at the mass-production level. However, NEDO, in collaboration with automobile manufacturers, has developed a passenger vehicle equipped with PV systems that utilizes solar power as a driving power source (supplying the vehicle's drive power with solar power), and is conducting demonstration driving on public roads.

There is a perspective that the commercialization of PV-powered vehicles may progress faster for commercial vehicles than for passenger vehicles. Various initiatives are beginning to take place both domestically and internationally, and NEDO is also conducting demonstration projects to develop effective methods for introducing these systems to the market.

Additionally, as the installation of PV systems in vehicles involves different conditions compared to the installation in buildings or on the ground, efforts such as reliability assessments and resilience measures are also being carried out simultaneously to support the commercialization and widespread adoption of PV-powered vehicles.

This chapter outlines the key findings obtained from NEDO's projects, including demonstration driving of PV-powered vehicles.

Table 2-1 Projects and key points related to PV-powered vehicles covered in this chapter

Integrating PV into passenger vehicles	Plug-in hybrid electric vehicles (PHEVs)	Evaluation of generated power, driving range, and solar irradiance/ power generation on curved vehicle surfaces.
	Battery electric vehicles (BEVs)	Evaluation of generated power, reduction in charging frequency, and performance under solar irradiance fluctuations.
Integrating PV into commercial vehicles	Electric commercial vehicles	Development of quantitative evaluation techniques for the effects of PV integration.
	Internal combustion engine trucks/ trailers	Conducting demonstration driving and developing design technologies for PV integration.
Reliability assessment of PV modules for passenger vehicles		Study and review of reliability assessment items and implementation of reliability test.
Resilience effect of vehicle-mounted PV		Effectiveness as an independent power source in emergencies such as natural disasters

2.1 Installation of PV on Passenger Vehicles

European startup companies were at the forefront of developing PV-powered passenger vehicles for practical use. However, in Japan as well, with the support of a technology development project conducted by NEDO and the cooperation of automobile manufacturers (Toyota Motor Corporation and Nissan Motor Co., Ltd.), Japan became the first in the world to begin demonstration driving of PV-powered vehicles on public roads.

The purpose of this project is to verify the effects of installing high-efficiency solar cells on electric vehicles in terms of extended driving range and improved fuel efficiency through public road demonstration driving. Additionally, the project aims to evaluate data such as the electricity generation amount of PV modules and the amount of electricity charged to the batteries for propulsion, which will be used to promote the future development of PV-powered vehicles.

The base vehicles (passenger vehicles) used in the demonstration are PHEVs and BEVs, equipped with PV modules using world-class high-efficiency solar cells (with conversion efficiency exceeding 34%) and rated power output of approximately 1 kW. This report outlines the key findings obtained so far from the demonstration driving of PV-powered PHEVs and BEVs, as well as the challenges that remain for future development.

Table 2.1-1 PV-powered demonstration vehicle for passenger use

Base vehicle	PHEV	BEV
	Prius (Toyota Motor Corporation)	eNV200 (Nissan Motor Co., Ltd.)
Rated output of PV module	860 W	1,150 W
Solar cells	III-V compound solar cells (Sharp), conversion efficiency: >34%	
Battery capacity	8.8 kWh	40 kWh

2.1.1 Installation of Photovoltaic Systems on Plug-in Hybrid Electric Vehicles (PHEVs): Evaluation of Generated Power, Driving Range, and Solar Irradiance/ Power Generation on Curved Vehicle Surfaces

(1) Objectives of Demonstration and Vehicle Specifications

Toyota Motor Corporation, together with NEDO and Sharp Corporation, manufactured a demonstration vehicle with a rated power generation output of approximately 860 W by installing III-V compound triple-junction solar cells with a conversion efficiency of over 30% on the roof, bonnet, and rear hatch door of a commercially available Prius PHEV (with a battery capacity of 8.8 kWh) (Fig. 2.1-1). The demonstration vehicle was used in public road driving, starting in July 2019, to demonstrate the possible driving distance and the effect of reduced charging frequency of using on-board PV-generated power.

A Prius PHEV model equipped with one unit of single crystalline silicon PV module is sold on

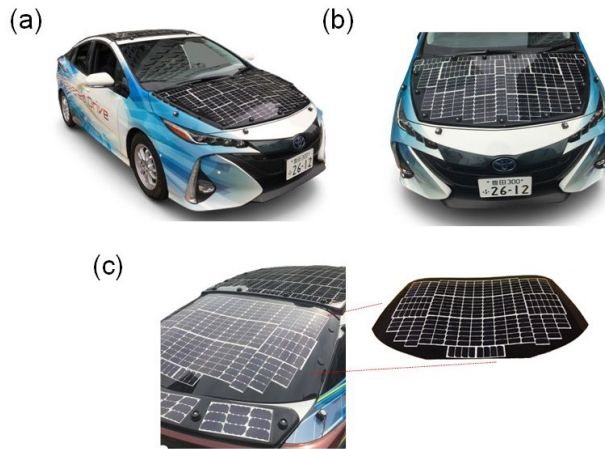


Fig. 2.1-1 PV-powered PHEV demonstration model

the market. However, in the demonstration vehicle, in addition to a significant improvement in generated electric power, a system that allows the main batteries for propulsion to be charged even while driving has been adopted, unlike the commercial vehicle where this is only done while parked. This is expected to significantly improve the vehicle's cruising range and fuel efficiency.

Table 2.1-2 Comparison of demonstration vehicle and conventional product

Vehicle Performance Item	"Prius PHV" (with charging system that uses solar power)	Demonstration vehicle
Solar cell conversion efficiency	22.5 %	Over 34 %
Rated power generation	180 W	Approx. 860 W
Maximum charge amount to drive battery (per day) when parked	Equivalent to 6.1 km of EV range	Equivalent to 44.5 km of EV range
Maximum charge/ supply amount to drive/ auxiliary battery systems (per day) while driving	Power supplied only to auxiliary battery systems for car navigation, etc.	Equivalent to 56.3 km of EV range

(2) Generated Power and Possible Driving Distance

Regardless of the capabilities of the PV, the effect of on-board PV was affected significantly by the actual driving patterns. Table 2.1-3 shows the driving patterns that were used in the demonstration driving in Aichi Prefecture. These were selected to reflect real-world driving patterns from actual market by actual users.

Table 2.1-3 Driving patterns used in demonstration driving

	Usage	Driving range (km/day)	Patterns
A	Highway	70	
B	Neighborhood driving (shopping, pick-up/drop-off)	5	
C	Commute	15	
D	City area	15	

A representative example of the results of the demonstration driving is obtained under driving pattern A, shown below. Pattern A consists of driving 35 km in the morning and 35 km in the afternoon (for a total driving distance of 70 km in a day). The power consumption rate for this pattern was measured as roughly 10.1 km/kWh.

Fig. 2.1-2 shows changes in the amount of PV generated power by the demonstration vehicle and its remaining battery level (state of charge, or SOC). The SOC fell from 66% to 24% as a result of the morning drive. But during the outdoor parking after driving (from 10:00 a.m. to 3:00 p.m.), the PV charged the batteries, restoring the SOC to 58%. This data was acquired in June 2020, and on that day the on-board PV generated approximately 4 kWh of power, and it was experimentally confirmed that the power generated by the PV could be used to drive 30 km per day.

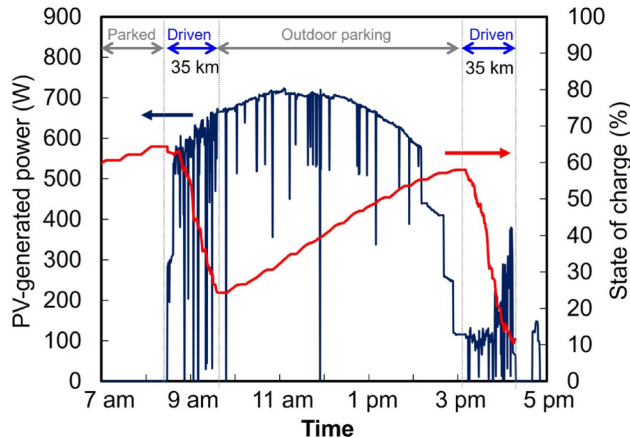


Fig. 2.1-2 Power generated by the PV on the demonstration vehicle and the changes in remaining drive battery level

Fig. 2.1-3 shows measurements of the driving distance using on-board PV derived power and solar irradiance per day. The amount of solar irradiance was determined by averaging the measurements taken in September 2021 from multiple pyranometers attached to the exterior of the demonstration vehicle. The driving distance by using PV power is proportional to the solar irradiance each day, and the constant proportionality was estimated at $5.9 \text{ (km/(kWh/m}^2\text{)}$. Tokyo, for example, receives approximately $1,200 \text{ kWh/m}^2$ of solar irradiance per year. A vehicle with an 860 W PV system would therefore, theoretically, be able to drive approximately 7,080 km per year.

Based on the above, it would be reasonable to conclude that the demonstration driving experimentally confirmed the effect of mounting PV on vehicles.

Furthermore, based on these results, and using solar irradiance data in Nagoya for estimation, it was found that CO₂ emissions could be reduced by 62%².

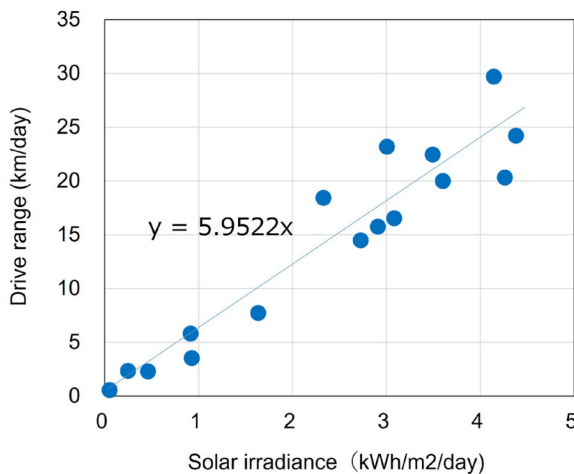


Fig. 2.1-3 Relationship between driving distance by solar energy and solar irradiance

(3) Analysis of Solar Irradiance and Power Generation on Curved Vehicle Surfaces

(i) Approach to power generation prediction

To predict the amount of power generated, it is necessary to measure solar irradiance data. However,

vehicle surfaces are susceptible to shadows from surrounding structures, and the orientation of the light-receiving surface can vary in many ways³. For this reason, various studies on solar irradiance on vehicle surfaces have been conducted by research institutions, including those overseas. Broadly, these can be classified into measurements using a single pyranometer or multiple pyranometers (Table 2.1-4). Each method has its pros and cons and must be used appropriately depending on the objective. For the purpose of calculating solar irradiance, it is necessary to use the measurement results from multiple pyranometers as a base and probabilistically model the various disturbances unique to vehicle surfaces (such as partial shading) to calculate the expected value of solar irradiance.

Table 2.1-4 Classification of measurement methods by pyranometer type

	Single pyranometer measurement ^{4,5,6}	Simultaneous measurement with multiple pyranometers ^{7,8}
Measurement/evaluation method	Measurement of solar irradiance on solar cell/ module plane → evaluation of power element efficiency and performance	3D solar irradiance measurement → comprehensive solar irradiance evaluation for curved surfaces, uneven shading, partial shading, etc.
Comparison with conventional methods	conventional PV evaluation methods are applied as is	Developed for solar irradiance for on-board PV; subsequently, its superiority was recognized and adopted by various research institutions in Japan, Germany, France, Spain, etc.
Examples of measurements	Commercial vehicle demonstration by AIST (NEDO) ⁹	University of Miyazaki and other European research institutions (five-axis orthogonal) ^{10,11} Toyota Motor Corporation and NEDO demonstration vehicle (oblique ten-axis)
Features/points to note	Model verification is easy; however, there is a risk that even an incorrect model may match measurement results for specific routes or seasons.	If the model is incomplete, redundant measurements can increase errors, but this allows for the detection of model incompleteness, which can be utilized for factor analysis.
	Convenient for learning about the power generation performance and characteristics of on-board PV (cells/ modules) through driving experiments; however, it is susceptible to misleading data and unconscious bias.	It becomes clear how on-board PV behaves in various solar irradiance and driving environments, and this information can be applied to design.

Also, regarding the collection of solar irradiance data, it is necessary to give due consideration to whether to measure it on a specific route or a random route, and to use them appropriately. Furthermore, to present a general power generation index, some kind of modeling is necessary because the solar irradiance observation results need to be extrapolated scientifically. While the aggregation of solar irradiance measurement results from

driving experiments can only yield results for a specific date and time on a specific route (Table 2.1-5), measurement on a specific driving route is effective for understanding complex phenomena. It is useful for analyzing on-board solar cells for passenger cars, which are strongly affected by curved surfaces (self-shading, mismatching loss) and partial shading.

Table 2.1-5 Classification of measurement and simulation methods by driving route

	Specific route	Random route	Probabilistic model
Measurement method	Repeatedly drive on a specific route (in different seasons and weather conditions)	Recruit volunteer users to drive freely and collect data remotely	Analyze shade environment by probabilistically modeling factors like shading probability
Examples of measurements	NEDO passenger vehicle demonstration NEDO commercial vehicle demonstration (AIST)	Fraunhofer Institute, University of Lisbon and NEDO commercial vehicle demonstration (University of Miyazaki, etc.)	University of Miyazaki, University of Lisbon and IEC international standard (under deliberation)
Features / points to note	Susceptible to unconscious bias and misleading data (further biased by seasonal, time, and weather variations).	Fair power generation data can be obtained, but the data is specific to a certain region, such as Lisbon.	A power generation metric applicable to various regions can be obtained, but the model itself requires careful examination and validation.
	Effective for developing power models but unsuitable for energy rating.	Difficult to extract the factors that influence power generation performance.	Effective for energy rating but unsuitable for power models

For passenger vehicles, which require implementation on a three-dimensional curved body and exhibit complex behavior, the evaluation of on-board solar cells for passenger vehicles aims to quantitatively understand complex phenomena and derive useful guidelines for design by having engineers repeatedly perform simultaneous measurements with multiple pyranometers on a specific route and conduct advanced analysis (Table 2.1-6).

Table 2.1-6 Approach to power generation prediction for passenger vehicles

- Multiple simultaneous solar irradiance measurements, oblique ten-axis
- Specific routes
- Curved solar cells
- Self-shading present
- Large influence of partial shading
- Multi-junction solar cells
- Measurements by in-house engineers
- In addition to power generation fluctuations due to shading while driving, power generation fluctuates due to partial shading, curvature loss, and spectral changes associated with the low-profile curved body
- Research and development of advanced mathematical models related to body curvature, such as differential geometry and partial shading probability
 - Development of design technology for PV-powered vehicles for passenger use

(ii) Driving route

Fig. 2.1-4 shows the driving routes that were the source of the data used for the analysis of solar irradiance and power generation. The drives for data acquisition were carried out in Shizuoka Prefecture.

Unless otherwise specified, each driving direction was analyzed by assuming it to be constant. However, this assumption is not always necessary, as the relative orientation of the vehicle body can be ascertained from a GPS or an electronic compass. Therefore, by analyzing the data using a local coordinate system, it is possible to calculate the amount of power generated for any vehicle orientation.



Fig. 2.1-4 Driving routes of the demonstration vehicle for solar irradiance and power generation analysis (in Shizuoka Prefecture)

(iii) Solar irradiance and power generation correction factors for curved vehicle surfaces

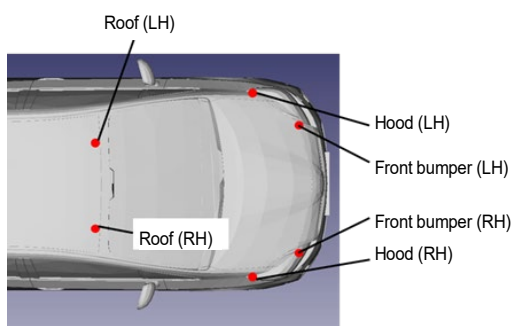
In the case of passenger vehicles, because the body is a three-dimensional curved surface, it is affected by the vehicle body's own self-shading and partial shading from nearby surrounding structures (such as guardrails), so the amount of power generated cannot be predicted simply from the amount of solar irradiance calculated from shading probability.

Fig. 2.1-5 shows the measurement results from a drive on a route with good solar conditions, where the south side is a coast, but the solar irradiance on each part of the curved vehicle body is less than the theoretical value of 1. However, if limited to the roof surface, the influence of loss due to partial shading is not so prominent compared to the loss from curved partial shading, except for the left side surface, as long as it is observed with an even distribution throughout the year and time of day. It is possible to calculate and verify this using a differential geometric approach for curved solar cells.

The exception is the amount of solar irradiance on the left side of the engine hood (hood LH position). This position is close to the left side and its mounting height is low, making it susceptible to the effects of irregular shading from guardrails, vegetation, etc. In this analysis, these irregular shadows were not considered, so the calculated values are overestimated. However, since information about such shading environments cannot be collected from maps, it would be necessary to include them as an expected value from a probabilistic model.

The degree of solar irradiance fluctuation caused by the curved vehicle body varies greatly depending on the weather and the sun's altitude. An example of the time-series fluctuation of solar irradiance is shown in Fig. 2.1-6.

<Pyranometer installation positions>



<Solar irradiance on each part of the curved vehicle body (comparison of calculation and measurement)>

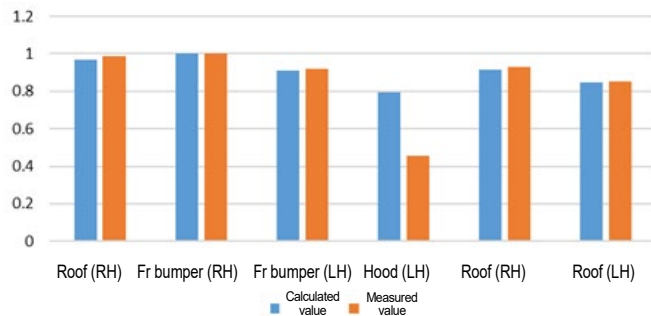


Fig. 2.1-5 Comparison of calculated and measured solar irradiance values on each part of a passenger vehicle's curved body

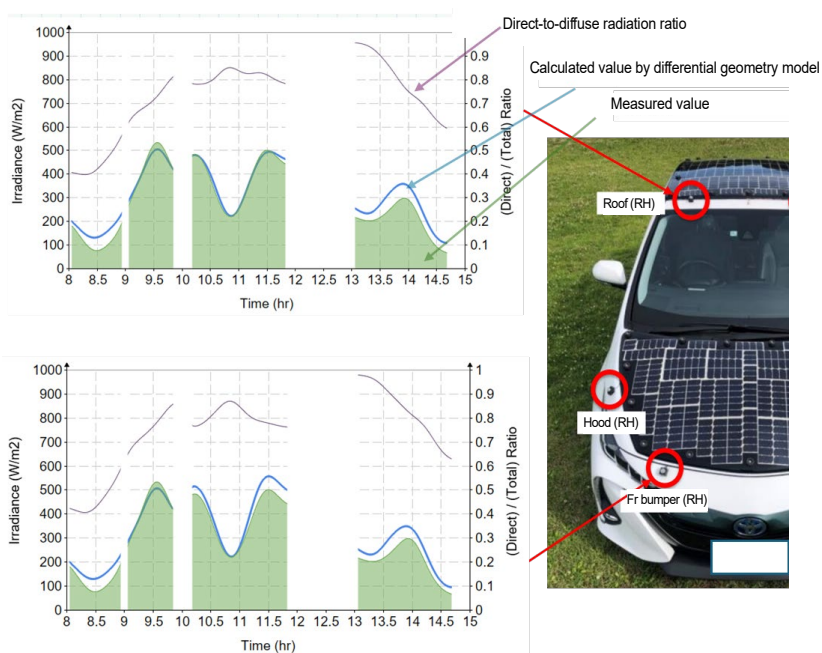


Fig. 2.1-6 Comparison of predicted and measured solar irradiance fluctuation on each part of the curved vehicle body

In this analysis, since it includes driving in a complexly curved urban area, it is difficult to assume that the vehicle orientation is constant for each section shown in Fig. 2.1-4. Also, as the analysis is for a long period of driving, it is unreasonable to assume that the weather conditions (especially the ratio of Direct Normal Irradiance (DNI) to Diffuse Horizontal Irradiance (DHI)) are constant. Therefore, using multivariate analysis techniques, the momentary vehicle orientation and the DNI and DHI in the sky were calculated (each assumed to be affected by momentary fluctuations due to shading from surrounding structures and sky obstruction, respectively) from the solar irradiance balance measured by an oblique ten-axis pyranometer, in a way that minimizes the square of the error with the model. Against this, the solar altitude was calculated for each part of the curved vehicle body using a differential geometric approach. However, the effects of close-proximity structures such as the aforementioned guardrails and vegetation were not included.

These losses vary greatly depending on the curved shape of the vehicle body. Therefore, PV-powered vehicles

must be designed with great care regarding their power generation behavior on curved surfaces. However, this curvature-derived loss can be calculated by a differential geometric approach, and since that calculation method has been verified, it can be applied to design.

The power output of solar cells covering a curved vehicle body is far more complex than the solar irradiance distribution, and it varies greatly depending on the vehicle orientation and the sun's altitude. Regarding this as well, it is possible to predict the amount of power generated with an analysis using differential geometry, but in particular, solar cells on the engine hood and rear part tend to be measured at lower values than the calculated values, as they are also strongly affected by partial shading.

The effect of the curved surface is complex and cannot be generalized, as it is strongly influenced by the curved shape, sun azimuth, solar altitude, driving direction, and partial shading, but the correction factors are calculated as shown in Tables 2.1-7 and 2.1-8. Note that the calculations in the table are the results for the area covered by the solar cells, not for the entire curved surface. Furthermore, the curved surface correction factor for power generation is strongly influenced not only by the shape of the curved surface but also by the weather conditions (the ratio of DNI to DHI), solar altitude, and driving direction. In this report, the calculation results for a vehicle orientation given by a random number using the standard irradiance database for the Temperate Coastal climate zone as specified in the international standard IEC 61853-4 is shown.

The curved surface loss worsens when shallow direct light hits it. On the other hand, shallow direct light is easily shaded by buildings. Therefore, it tends to be smaller in urban and mountainous areas where shading loss becomes large. Similarly, since it is strongly affected by self-shading, by blocking it into the engine hood, front part of the roof, rear part of the roof, and rear part, and operating each with its own MPPT, the effects of self-shading can be avoided and curved surface loss can be significantly reduced.

Table 2.1-8 contains correction factors for calculating the power generated from curved solar cells. These factors are applied to the module output measured using the IEC 60904-1-3 method, which is currently under deliberation. It is important to note that these factors are not applicable to the total output when the cells are arranged in a flat configuration to cover the same curved surface area.

Table 2.1-7 Correction factor for solar obstruction on a waterfront

IEC 61853-4 Climate classification	Suburbs	Residential areas	High-rise buildings / mountainous regions
High elevation	0.92	0.68	0.45
Subtropical arid	0.93	0.69	0.45
Subtropical coastal	0.92	0.71	0.49
Temperate coastal	0.90	0.67	0.46
Temperate continental	0.91	0.66	0.43
Tropical humid	0.93	0.74	0.54

Table 2.1-8 Correction factor for vehicle surface curvature

	Engine hood	Front part of the roof	Rear part of the roof	Rear part
Solar irradiance correction factor (random ray)	0.914	0.984	0.980	0.919
Power output correction factor, suburban areas IEC61853-4 Temperate Coastal	0.952	0.968	0.965	0.966
Power output correction factor, residential areas IEC61853-4 Temperate Coastal	0.969	0.971	0.966	0.968
Power output correction factor, high-rise buildings / mountainous regions IEC61853-4 Temperate Coastal	0.971	0.975	0.968	0.971

The probability of occurrence of loss from partial shading can be measured by counting how often power output drops suddenly while driving on a clear day. In summer, during midday driving when the solar altitude is high, it is generally a few percent, but in winter, during midday driving when the solar altitude is low, measurement results were 10%. However, in cases like residential areas where overhead electric wires frequently cause partial shading, the frequency of occurrence reaches nearly 20%. The sudden drop in power caused by partial shading is a power loss that occurs when a shaded part of the solar cell acts as a bottleneck for the current flowing through the series circuit. This phenomenon is commonly observed in general PV systems. Nevertheless, with PV systems mounted on vehicles, this effect appears more frequently and has a greater impact depending on the installation location and the driving environment. Therefore, this correction is necessary when evaluating power generation.

- If power generation decreases due to partial shading, the amount of solar irradiance has also decreased, so if this part is not inversely corrected, the solar irradiance correction due to shading shown in Table 2.1-7 will be double-counted. The distribution of the size of partial shading is random, and the decrease in solar irradiance at the time of occurrence is generally 50%, which corresponds to its expected value. Therefore, the degree of impact must be calculated as 1/2.
- Partial shading occurs only during clear weather. In cloudy weather, there is no direct sunlight, so partial shading loss does not occur. The occurrence rate of weather conditions where partial shading occurs generally corresponds to the sunshine duration rate, which is about 46% on a nationwide average in Japan. Therefore, when evaluating the impact on annual power generation, it must be multiplied by 0.46 as an inverse correction.
- Even if a cell is shaded by a partial shading, the amount of Diffuse Horizontal Irradiance (DHI) remains

largely unchanged. Therefore, power generation equivalent to the DHI ratio of Global Horizontal Irradiance (GHI) is still maintained; it does not drop to near zero.

- Street trees and signs that cause partial shading in suburban areas may cast shadows partially on a vehicle's body. However, in high-rise building districts or mountainous regions, vehicles are often in the complete shadow of buildings or mountains. Therefore, it is a misconception that the loss rate from partial shading is higher in areas with numerous shade-causing objects. Typically, the probability of partial shading is higher in residential areas than in areas with high-rise buildings or mountains.

Various research institutions have proposed PV modules that are robust against partial shading. Since partial shading is a common issue for all PV modules, not just PV systems mounted on vehicles, extensive research was conducted around 2010. Numerous papers were published on module structures designed to minimize its effects. However, experiments used to verify this effect often intentionally shade a part of the solar cells (ignoring the fact that some DHI still reaches the solar cells) or present results based only on observations from clear days (ignoring cloudy days). This can lead to results that may differ from real-world weather and shading conditions. Taking these experimental results at face value can give a misleading impression, making it seem that the impact of partial shading on annual power generation is far more significant than it actually is.

Similar to the evaluation of overall shading, the impact of partial shading can be calculated as an annual expected value by aggregating the effects over the entire year. This is done by weighting factors such as the distribution of obstacle heights (specifically, the height distribution along the shadow boundary, excluding cases of overlapping shadows), the sun's altitude, the seasonal distribution of weather conditions, and the time-of-day and seasonal variations in the DNI ratio. The results of this calculation are shown in Table 2.1-9.

Table 2.1-9 Correction factor for partial shading losses

Power output correction factor	Suburban area	Residential area	High-rise / mountainous area
All climate zones in IEC 61853-4	0.99	0.97	0.98

2.1.2 Installation of PV Systems on Electric Vehicles: Evaluation of Power Generation, Charging Frequency Reduction, and Performance against Fluctuations in Solar Irradiance

(1) Objectives of Demonstration and Vehicle Specifications

A demonstration driving was initiated on mounting a PV system on an electric vehicle, using the power generated by the PV to charge the vehicle's drive batteries and then driving the vehicle. Data regarding power generation performance was acquired during parking and public roads driving in order to perform the followings: 1) assessment of the actual amount of power generated and the actual reduction in charging frequency, 2) evaluation of performance against partial shading, and 3) evaluation of MPPT performance while driving.

Figs. 2.1-7 and 2.1-8 show the appearance of the demonstration vehicle and an overview of the PV system. Table 2.1-10 shows the vehicle's specifications. A Nissan eNV200 was used as the base vehicle, and the power generated by the PV system was stored in a 40-kWh vehicle drive battery. PV panels made up of multiple modules were installed in three locations: the roof, the bonnet, and the tailgate. The roof had six PV

panels and the bonnet and tailgate. The roof had six PV panels and the bonnet and tailgate each had two PV panels, with each panel consisting of two PV modules. Each of these modules consisted of multiple unit cells connected in a series-parallel configuration, and each module had its own connected MPPT converter for power control. The solar cells used were III-V compound triple junction PV cells with a module conversion efficiency of 31.17%, and were developed by Sharp Corporation¹². The maximum module voltage, even when sunlight is strongest during the year, was kept below 60 V for safety. The roof also had a pyranometer for measuring solar irradiance. A converter system was connected between the PV panels and the drive batteries to convert power, controlling the power generation of the PV panel and converting the voltage to supply power to the drive batteries.



Fig. 2.1-7 The demonstration vehicle



Fig. 2.1-8 The demonstration vehicle's PV system

Table 2.1-10 Specifications of the PV system installed in the vehicle

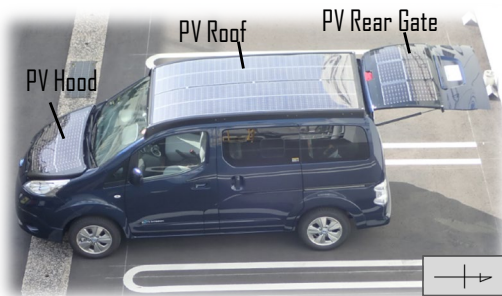
Base vehicle (eNV200) specifications			
Vehicle type	BEV		
Battery capacity	40 kWh		
PV panel specifications			
	Roof	Hood	Rear gate
PV cell structure	GaAs-based 3-layer tandem		
PV cell manufacturer	SHARP		
Nominal PV output	1,150 W		
No. of modules	6	2	2
Angle to the horizon	0–20°	20°	0–20°(open) 80°(close)

(2) Assessing Actual Capabilities - Amount of Power Generated, Possible Driving Distance, and Reduction in Charging Frequency

(i) Annual power generation and possible driving distance

i) Experiment and calculation conditions

The amount of power generated by the demonstration vehicle was evaluated over the course of a year. In order to determine the maximum capabilities of the on-board PV system, measurements were performed by opening the tailgate such that all of the PV panels were oriented horizontally¹³, as shown in Fig. 2.1-9.



Location
 : Yokosuka, Kanagawa Prefecture, Japan
 Vehicle placement
 : Parked facing south, rear gate opened horizontally
 Weather
 : Mainly measured on days with no rainfall

Fig. 2.1-9 Vehicle during power generation evaluation

The actual results of daily measurement were integrated with the calculation method shown below to calculate the potential monthly and yearly possible EV driving distances given the amounts of power generated. Specifically, the following formula was used to calculate the possible EV driving distance that could be achieved from the amount of energy generated per day (E_g), summed over the course of a year.

$$\text{Possible EV driving distance (amount of power generated per day)} \\ = \{ \text{amount of power generated per day } E_g \times c \} \text{ electric fuel economy} \\ E_g = \{ a \} \text{ daily solar irradiance } E_r \times b \text{ solar-power generation coefficient} \}$$

a) Daily solar irradiance (E_r)

- This was calculated using the information in the NEDO solar irradiance database (METPV-11)¹⁴.
- Solar irradiance data for representative years (average year, high-irradiation year, and low-irradiation year) was available for various locations in Japan (837 locations) for a 20-year period (1990 to 2009). Data regarding solar irradiance over the course of an entire year could be used on an hourly basis. (Fig. 2.1-10).

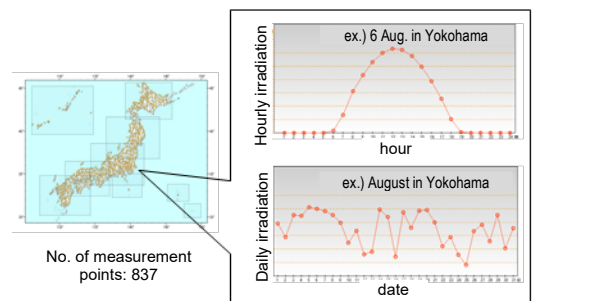


Fig. 2.1-10 NEDO solar irradiance database ¹⁴

b) Solar irradiance and solar-power generation coefficient (relationship between the solar irradiance (E_r) and the amount of power generated (E_g))

- The amount of power generated by the PV during the power generation evaluation experiment and the solar irradiance recorded by the on-board pyranometer were measured and the correlation was calculated (Fig. 2.1-11).
- The solar irradiance (E_r) and the amount of generated power (E_g) were generally proportional, regardless of the weather or time of year, so a linear approximate equation was used for calculations.

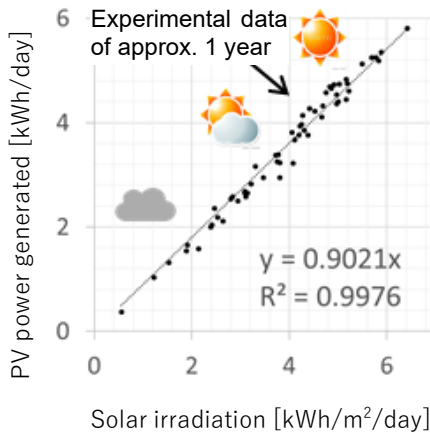


Fig. 2.1-11 Relationship between the amount of energy generated and solar irradiance during power generation evaluation

c) Electric fuel economy

- The electric fuel economy from public road demonstration driving was used. The annual average electric fuel economy is 6 km/kWh, but due to differences such as air conditioner usage frequency, electric fuel economy varies by season, so the calculations reflect these quarterly fluctuations.

ii) Calculation results for annual power generation and possible EV driving distance

Fig. 2.1-12 shows the amount of power generated each month and the monthly average daily power generated. These calculations were based on data from the solar irradiance database for an average year in Yokohama.

Fig. 2.1-13 shows the possible EV driving distance based on the amount of monthly power generated each month. It can be deduced that the total EV drivable distance was roughly 7,100 km per year, or an average of roughly 20 km per day. As Fig. 2.1-12 shows, the months with the highest power generation amounts were July and August, but the months with the longest possible EV driving distances were April and May. This is because of seasonal differences in electric fuel economy and differences in the number of sunny days. The shorter possible EV driving distance in June can be attributed to the prevalence of cloudy days during the rainy season. Also, the possible EV driving distance in winter is roughly half that of the summer.

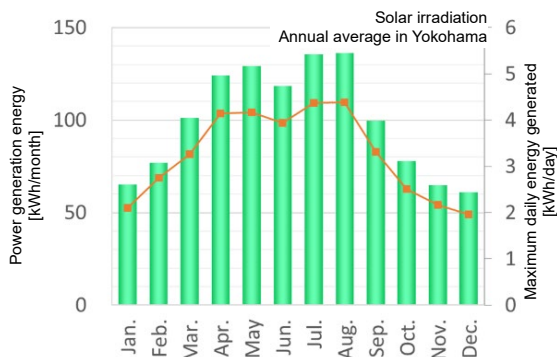


Fig. 2.1-12 Monthly power generation and daily power generation (monthly average)

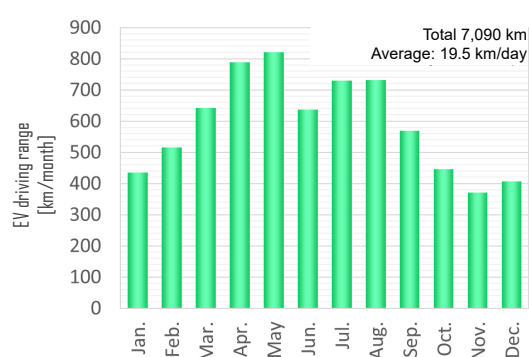


Fig. 2.1-13 Possible EV driving distance per month

(ii) Effect of reducing the frequency of charging

Using PV to charge EV's driving batteries is expected to reduce the frequency of charging. The demonstration vehicle was used to validate the benefit.

i) Calculation method and calculation conditions

The driving pattern used was "A: Weekend use, B: Weekday/ weekend use, C: Weekday commuting use" (Table 2.1-11), based on the representative vehicle usage patterns listed in the PV-Powered Vehicle Strategy Committee Interim Report (January 2018)¹⁵.

Table 2.1-11 Excerpt of representative car usage patterns¹⁵

Pattern	Type	Driving distance per journey (km)	User image
A. Weekend use	A-1: Long-distance weekend leisure	150 km for 2 days (Sat. and Sun.)	Use only on weekends (Sat./Sun.) for visiting distant locations for leisure, etc.
	A-2: Short-distance weekend leisure	50 km for 2 days (Sat. and Sun.)	Use only on weekends (Sat./Sun.) for visiting nearby locations for leisure, etc.
B. Weekday /weekend use	B-1: Active use	50 km for 4 days (Mon., Wed., Fri., and Sun.)	Use actively on weekdays and weekends
	B-2: Suburban use	5 km for 4 days (Mon., Wed., Fri., and Sun.)	Use for visiting shops and local destinations, on weekdays and weekends
C Weekday use	C-1 Long-distance commuting	50 km for 5 days (weekdays)	Use only on weekdays for commuting to distant workplace, etc.
	C-2 Short-distance commuting	15 km for 5 days (weekdays)	Use only on weekdays for commuting to nearby workplace, etc.

When starting with day n, the formula for determining the battery energy (state of charge (SOC)) for day n+1 and PV-generated electricity utilization rate is as shown below.

$$En_{Ba_{n+1}} = En_{Ba_n} - Di_{Dr_n} + En_{So_n}$$

$$En_{Dr_n} = Di_{Dr_n} \div Ef_{Dr_n}$$

$$En_{So_n} = Ef_{Sun_n} \times Ef_{So_n}$$

If $(En_{Ba_{n+1}} < En_{Ba_min})$... $En_{Ba_{n+1}}$ is overwritten with En_{Ba_max} (number of charges + 1)

If $(En_{Ba_{n+1}} > En_{Ba_max})$... $En_{Ba_{n+1}}$ is overwritten with En_{Ba_max} (simulating a full charge)

$$U = \frac{\sum_{n=1}^{365} Di_{Dr_n} \times Ef_{Dr_n} - \sum_{n=1}^{365} En_{Ca_n}}{\sum_{n=1}^{365} En_{So_n}}$$

En_{Ba_n} : Battery energy on day n
 En_{Dr_n} : Energy consumed by driving on day n
 En_{So_n} : PV energy generated on day n
 En_{Ca_n} : Charged energy on day n
 Di_{Dr_n} : Distance driven on day n
 Ef_{Dr_n} : Electric fuel economy on day n
 Ef_{Sun_n} : Solar irradiance on day n
 Ef_{So_n} : PV conversion efficiency on day n
 En_{Ba_max} : Maximum battery energy charge
 En_{Ba_min} : Minimum battery energy discharge threshold
 U : PV-generated electricity utilization rate

The calculation conditions were as shown on Table 2.1-12.

Table 2.1-12 Battery energy calculation conditions

Solar irradiance	NEDO solar irradiance database (Yokohama, average year)
PV conversion efficiency, electric fuel economy, and driving distance	Used values determined based on trials
Initial battery energy level	24 kWh
Maximum battery energy charge	40 kWh
Minimum battery energy discharge threshold	8 kWh

ii) Results of the calculation of effectiveness in reducing the frequency of charging

A Weekend use

Fig. 2.1-14 shows the annual number of charging events and the utilization rate of PV-generated power for cases with and without PV power generation, assuming weekend driving ranging from 25 km/day to 200 km/day. A charging-free operation can only be achieved when the driving distance is up to 50 km. As shown in Fig. 2.1-14, it is notable that the utilization rate and the reduction in the number of charging events vary depending on the conditions. This indicates that, because the vehicle is only used on weekends, the PV-generated power is not being fully utilized.

B Weekday /weekend use

Fig. 2.1-15 shows the annual number of charging events and the utilization rate of PV-generated power for cases with and without PV power generation, assuming weekday and weekend driving ranging from 5 km/day to 100 km/day. Charging-free operation can only be achieved when the driving distance is up to 25 km/day; however, even for those driving 50 km/day or more, the annual number of charging events can be significantly reduced. For example, in the 50 km/day driving range, the annual charging frequency is expected to be reduced by approximately 65%. In addition, when the driving distance is 50 km/day or more, the utilization rate is around 90%, indicating that, compared with weekend-only use (Case A), the greater number of usage days enables the PV-generated power to be utilized more effectively.

C Weekday use

Fig. 2.2-16 shows the difference in the charging frequency over the course of the year for one-way commuting distances of 10 to 30 km, comparing the scenarios with and without PV. This shows that, although the commuting distance for which charge-free operation is possible was 10 km or under, even for people who commute more than 10 km, the annual charging frequency could be reduced considerably. For example, for a commuting distance of 25 km, the number of charges per year could be reduced by roughly 48%. For commuting distances of 15km or more, the utilization rate is around 90%. This indicates that the PV electricity is being effectively used, as the vehicles are in use on more days compared to the weekend-only use (Case A).

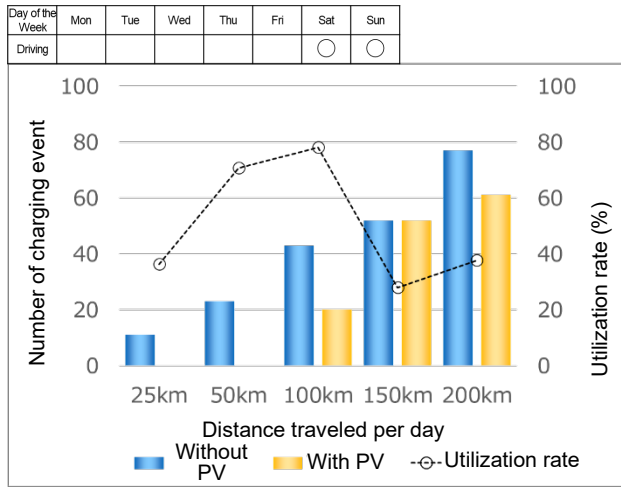


Fig. 2.1-14 Number of charges per year for weekend use

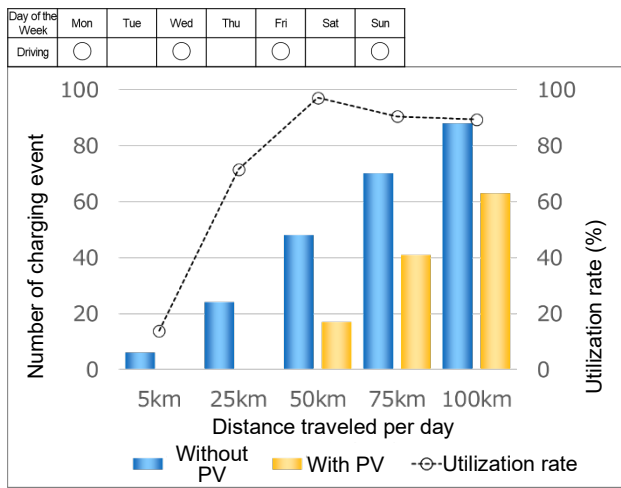


Fig. 2.1-15 Number of charges per year for weekday /weekend use

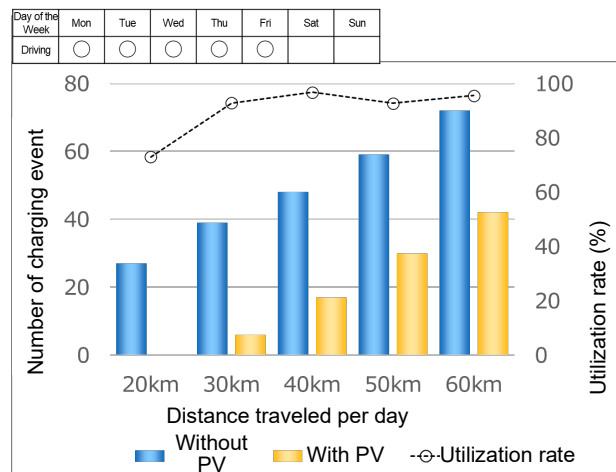


Fig. 2.1-16 Number of charges per year for commuting use

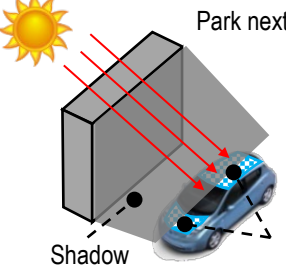
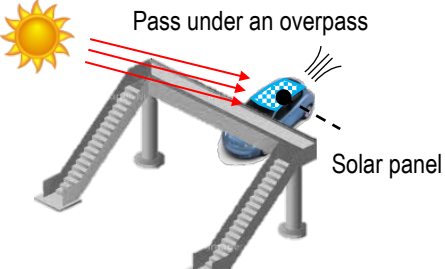
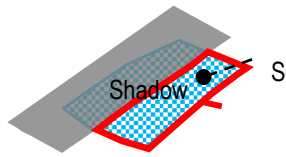
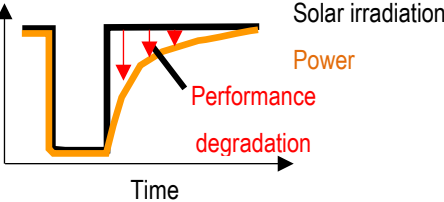
(3) Evaluation of Performance in Relation to Fluctuations in Solar Irradiance

(i) Issues related to fluctuations in solar irradiance

One of the unique challenges faced by on-board PV systems is that, due to being installed on the moving vehicles, solar irradiance received can be obstructed in unpredictable shapes and timings, leading to frequent

fluctuations in solar irradiance. Situations in which there are fluctuations in solar irradiance include i) when a part of the on-board PV is in the shade and ii) when there are sudden fluctuations in solar irradiance while driving (Table 2.1-13). Methods for dealing with these different forms of fluctuations in solar irradiance are described below.

Table 2.1-13 Situations in which fluctuations in solar irradiance occurs in onboard PV

	i) Partial shade	ii) Quick change of solar irradiation
Scene	 <p>Park next to a building</p> <p>Shadow</p> <p>Solar panel</p>	 <p>Pass under an overpass</p> <p>Solar panel</p>
Issue	 <p>Shadow</p> <p>Solar panel</p> <p>Performance degradation under sunlight due to influence of PV panel under the shadow</p>	 <p>Solar irradiation</p> <p>Power</p> <p>Performance degradation</p> <p>Time</p> <p>Delay of generation power due to solar irradiation change</p>

(ii) Response to Partial Shading

i) Countermeasures

Fig. 2.1-17 shows the converter system. In order to deal with partial shading, the PV modules are segmented and each is provided with its own converter. This structure makes it possible to perform Maximum Power Point Tracking (MPPT) control for each individual PV module. The step-up function for the high voltage system is provided by a subsequent converter. Therefore, even if there is partial shading, etc., the PV modules that are not in the shade will not be affected by those that are in the shade, and the subsequent converters connected to them are able to step up the voltage¹⁶.

Fig. 2.1-18 shows the connection configuration of solar cells in each PV module. Each PV string is made up of 16 PV cells connected serially, and 11 of these strings are connected in parallel, making up the PV module. Due to this connection configuration, when shading occurs like Shadow A in Fig. 2.1-18, the PV cells covered in shadow will be in parallel, so the PV module voltage will stay the same but the current will drop (Fig. 2.1-19). In contrast, when shading occurs like Shadow B, the PV cells covered in shadow will be in series direction, so as the area of the shadow increases, the PV module voltage will drop but the current will stay the same. Keeping the voltage the same makes it possible to maintain the optimal step-up ratio within the converter, so the PV would be more robust when shaded by a shadow such as Shadow A. When a vehicle is in motion, Shadow A-type moving shadows are dominant, so cells were arranged to provide robustness for this direction of shadows.

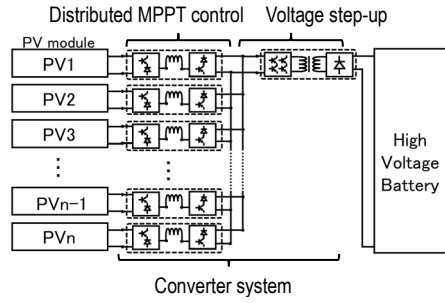


Fig. 2.1-17 Overview of the converter system¹³

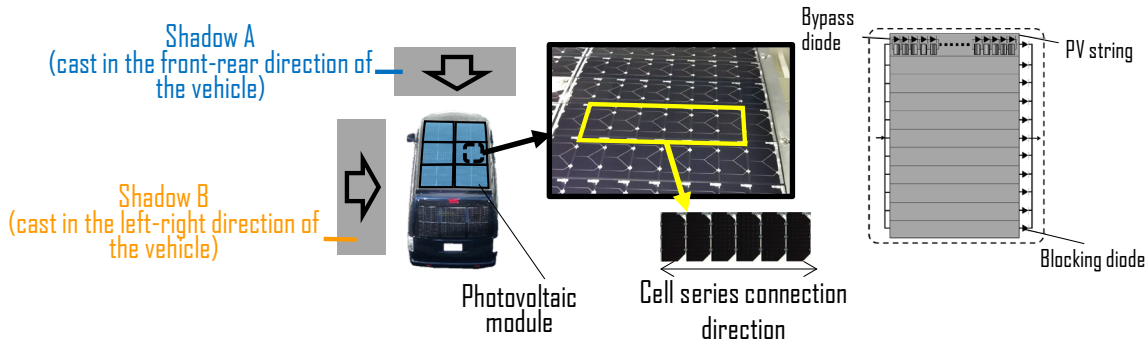


Fig. 2.1-18 PV cell layout and relationship between its positioning in relation to the vehicle body and shadow

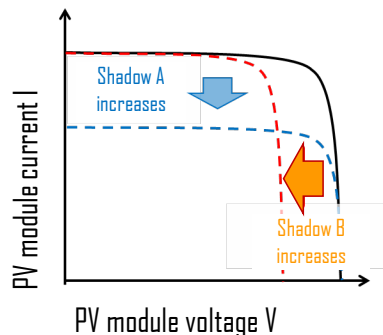


Fig. 2.1-19 PV module IV characteristics

ii) Evaluation results

For the two types of shadows shown in Fig. 2.1-18, artificial shadows using shading objects were created and trials were performed. Shadow A represented a shadow that moves from the front toward the rear of the vehicle, while Shadow B represented a shadow that moves from the left toward the right of the vehicle.

Fig. 2.1-20 shows the relationship between the normalized roof-generated power and the areas of Shadows A and B. This Normalization is based on the roof-generated power when the shadow coverage percentage is 0%. As the shadow area of Shadow A increased, the normalized roof-generated power fell linearly, but the normalized roof-generated power fell in steps for Shadow B. Compared to Shadow A, the decline in generated power for Shadow B is greater.

Fig. 2.1-21 (a) shows the normalized PV module power, voltage, and current when the shadow area of Shadow A is 17% (1/6). Half of PV1 and PV4 were in the shade, so the module current was halved, but the shadow covered the PV cells in their parallel direction, so the module voltage stayed the same. As the results show, module power only fell for the part covered by the shade.

Fig. 2.1-21 (b) shows the normalized PV module power, voltage, and current when the shadow area of Shadow B is 12.5% (1/8). 1/4 of PV1, PV2, and PV3 were in the shade, and the module voltage fell by more than 1/4 of the voltage when there was 0% shadow coverage. The current also fell slightly from the current when there was 0% shadow coverage. This is believed to be because when the current passed through the bypass diodes for the part in shade, the voltage fell, and the current was dropped during the transition to a new optimal operating point through MPPT control.

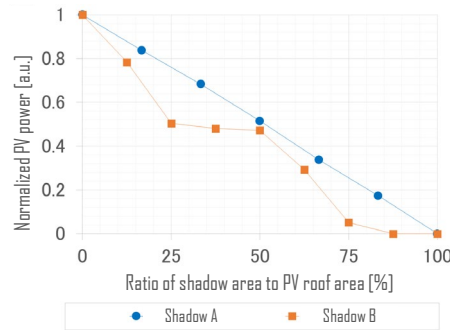


Fig. 2.1-20 Shade coverage percentage and normalized roof-generated power¹⁶

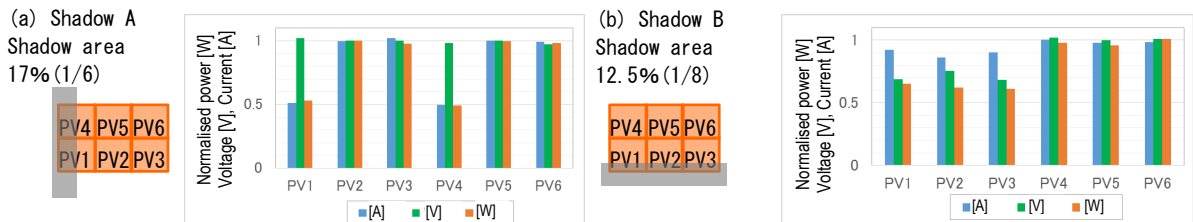


Fig. 2.1-21 Normalized PV module power, voltage, and current¹⁶

(ii) Response to Transient Fluctuations in Solar Irradiance

i) Countermeasures

For the converter system shown in Fig. 2.1-17, Maximum Power Point Tracking (MPPT) control was used to constantly update the operating point of each PV module. The operating points were determined by using the ordinary hill climbing method to change the operating voltage of the PV module and track the operating point that produces the greatest power. When there are complex fluctuations in solar irradiance occur over short durations, such as when the vehicle passes under a tree's shadow on the side of the road, the voltage-current characteristics of the PV module undergo multiple changes as the system looks for the maximum power point. It can take some time to find the maximum power point, resulting in power generation opportunity losses. Improving the control tracking performance in situations in which there are frequent solar irradiance changes by limiting the voltage search range of the MPPT control was attempted.

ii) Method (evaluation through driving on public roads)

MPPT control was evaluated in locations where there were trees on both sides of the road, like that shown in Fig. 2.1-22. Driving on these roads involves repeated switching between sunlight and shade, making it hard for MPPT control to track operating points. The trial method consisted of changing the initial search voltage as shown in Fig. 2.1-23 and measuring the MPPT achievement rate (see the formula below). The MPPT achievement rate is the rate of actual generated PV power to the amount of PV power that would be generated at the MPP estimated based on solar irradiance. It indicates the level of performance of the MPPT control.



Fig. 2.1-22 Evaluation scene

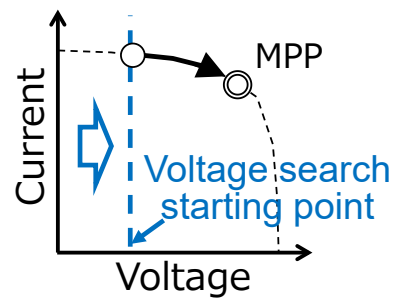


Fig. 2.1-23 MPPT control initial search voltage

$$AR_{MPP} = \frac{P_{AVE}}{S_{AVE}} \div R_{MPP} \times 100$$

AR_{MPP}

: MPPT achievement rate

P_{AVE}

: Average PV generated power

S_{AVE}

: Average solar irradiance

R_{MPP}

: Amount of PV power generated at MPP relative to solar irradiance

iii) Results

Fig. 2.1-24 shows the relationship between the MPPT achievement rate and the MPPT control initial search voltage. The higher the MPPT control initial search voltage is raised, the higher the MPPT achievement rates. This indicates that raising the MPPT control initial search voltage to limit the search range improves the MPPT control response. Moreover, when the MPPT control initial search voltage was raised to 40 V, the MPPT achievement rate dropped significantly, presumably because the MPP voltage is roughly 38 V, making it impossible to operate constantly at the MPP. Consequently, it is found that an MPPT achievement rate of 97% or greater could be achieved by setting the initial search voltage between 20 and 35 V.

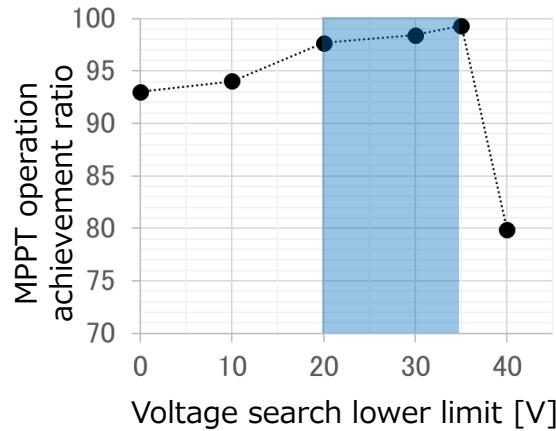


Fig. 2.1-24 Relationship between the MPPT control initial search voltage and the MPPT achievement rate¹³

Fig. 2.1-25 shows the results of the evaluation when the demonstration vehicle passing by trees along the side of the road. The graphs show the relationship between solar irradiance and the amount of power generated by the PV roof at the evaluation locations indicated above when searching range of MPPT control was set to the entire region (left) and when it was limited (right). When the search range was set to the entire region (left), the search for the MPP took a large amount of time, so even if solar irradiance returned to normal levels when the vehicle moved out from the shade to the sunlight, the amount of power generated by the PV roof did not recover completely. However, when the search range was limited (right), the amount of power generated by the PV roof fully recovered when solar irradiance returned to normal levels. In this way, appropriately limiting the MPPT control searching range successfully improved MPPT control tracking performance.

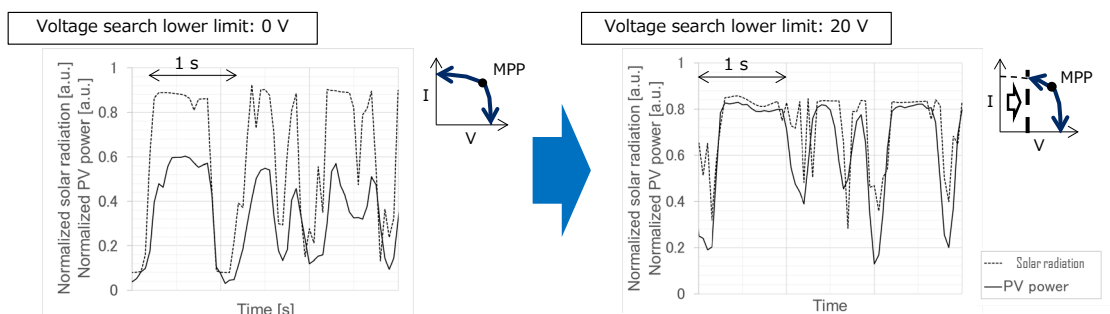


Fig. 2.1-25 Relationship between solar irradiance and the amount of power generated by the PV roof¹³

2.2 Installation of PV Systems in Commercial Vehicles

In recent years, initiatives to install photovoltaic power generation on commercial vehicles have been accelerating, mainly in Europe^{17,18}, and demonstration projects for installing PV systems on refrigerated trailers have also begun in the United States¹⁹.

For passenger vehicles, the installation of PV systems is basically assumed for electric vehicles (including Plug-in Hybrid Electric Vehicles (PHEVs)). However, in the case of commercial vehicles, it is possible to substitute the electric power consumed inside the vehicle, trailer, or container during driving with electricity generated by PV systems, even if the vehicle itself is powered by an internal combustion engine. By realizing and promoting the installation of PV systems on vehicles driven by internal combustion engines, not only electric vehicles, the range of target vehicle types and the market for PV installation can be expected to expand dramatically.

On the other hand, there are various types and uses of commercial vehicles, and in addition to vehicle configurations and vehicle operation modes, the forms of use of generated electricity are also diverse, resulting in many use cases. These use cases are considered to have a significant impact on power generation performance, and the effectiveness of installing PV systems is also expected to vary greatly. In order for PV-powered vehicles to become widespread, it is important to estimate the amount of power generation in various use cases taking these effects into account, as well as to estimate the impact of introducing PV-powered mobile bodies into the market.

Against this background, as “**Development of Power Generation Forecasting Technology for New Market Introduction**,” NEDO is implementing the following projects targeting commercial vehicles over fiscal years 2023 to 2024, with the aim of developing a method to examine more effective market introduction approaches for PV-powered vehicles, which are required to be put into practical use at an early stage (Table 2.2-1). In this report, an outline of these projects and a part of the results obtained so far are introduced.

Table 2.2-1 Projects implemented under NEDO’s initiative “Development of Power Generation Forecasting Technology for New Market Introduction”

Theme	Development of PV-powered EV system design technology	Demonstration of diverse commercial vehicle-integrated PV and development of effect prediction technology
Implementing organizations	National Institute of Advanced Industrial Science and Technology (AIST) (Subcontracted to Waseda University)	SYSTECH CO., LTD., University of Miyazaki, Photovoltaic Power Generation Technology Research Association (PVTEC)
Demonstration vehicles	Electric vehicles (e.g., trucks, vans)	Diesel vehicles (e.g., trucks, trailers)
Application of PV-generated electricity	Supplementary power for traction	Supplementary power for auxiliary electrical systems
Installed solar cells	Commercial crystalline silicon solar cells	Commercial CIGS solar cells
Development objectives	<ul style="list-style-type: none">- Power generation estimation methods through demonstration testing- Simulation technologies for secondary battery charging/discharging- Development of PVEV system design technologies based on the above, along with proposals for introduction effects and deployment models	<ul style="list-style-type: none">- Power generation estimation methods through demonstration testing- Estimation of fuel consumption reduction and CO₂ mitigation across diverse commercial vehicle operation patterns- Examination of retrofitting methods for PV systems (e.g., adhesive-based installation techniques)

2.2.1 Installation of PV systems on Electric Commercial Vehicles

Since FY2023, the National Institute of Advanced Industrial Science and Technology (AIST), with support from NEDO, has been promoting the project “Development of PV-Powered EV System Design Technology”, which focuses on the installation of PV systems on electric commercial vehicles. The overall framework of the project is illustrated in Fig. 2.2-1. At AIST, PV-equipped electric vehicles are referred to as PVEVs. The project consists of two sub-themes: (1) demonstration driving of PV-powered EVs, and (2) development of PVEV system design technologies. This section provides an overview of the activities and key achievements under each sub-theme.

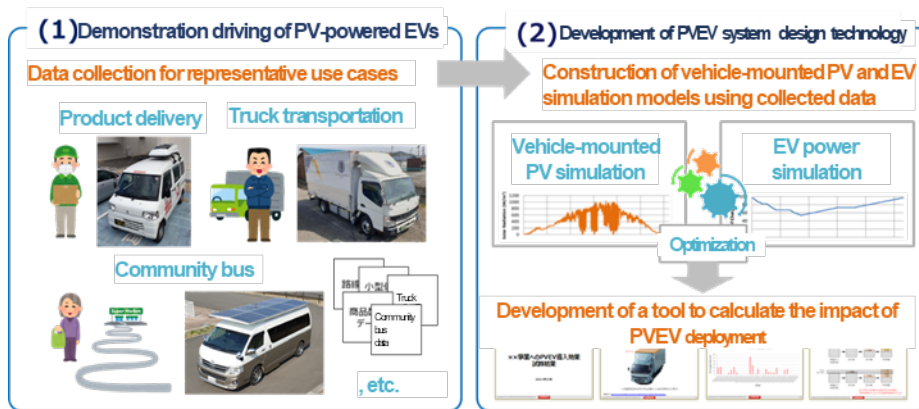


Fig. 2.2-1. AIST project: “Development of PV-Powered EV System Design Technology”

(1) Demonstration Driving with PV-Powered EVs

The effect of PV installation on vehicles is expected to vary depending on the type of vehicle used, the driving location, and the time of operation. To investigate this, demonstration vehicles developed by AIST were utilized. These included:

- PVEV: an EV equipped with PV modules, in which the generated PV power can be used for EV driving in practice;
- PYEV: an EV equipped with a pyranometer instead of PV modules, allowing estimation of PV contribution by comparing the assumed PV power derived from solar irradiance data with the EV's actual power consumption.

These vehicles were introduced into several real-world services in order to obtain data and conduct case studies for verifying the effects of PV installation.

(i) Product delivery

Short-distance delivery using light commercial vans (so-called last-mile delivery) is considered a particularly promising use case for PVEVs. With the cooperation of YORK-BENIMARU Co., Ltd., AIST introduced its PYEV into the company's delivery service vehicles and collected various data during actual service operations (implementation period: February 2022 to December 2024). Fig. 2.2-2 shows the exterior of the demonstration vehicle, a small van-type PYEV. The base vehicle used was Mitsubishi Motors Corporation's light commercial EV van (Minicab MiEV, battery capacity: 16 kWh). A PV-module-type solar irradiance sensor (with thermocouples attached to the back surface) installed on the roof box enabled measurement of solar irradiance

and module temperature. Position information was obtained via GPS sensors, and vehicle data such as SOC were collected through the in-vehicle telematics terminal.



Fig. 2.2-2. Small van-type PYEV

As an example of the data obtained, results from February 22, 2022, are shown. Fig. 2.2-3a presents the battery SOC data for that day. The battery, which had been depleted during deliveries the previous day, was charged from the morning to full capacity by noon. During deliveries conducted between just before 14:00 and after 16:00, the battery was observed to have been discharged by 62.5% (equivalent to 10 kWh). Fig. 2.2-3b shows the solar irradiance data on the roof of the demonstration vehicle for the same day. The weather was partly cloudy, and data collection, including during the delivery period (indicated by a red dashed box), was successfully conducted. Using the measured solar irradiance data, the generated electricity was estimated for a PV module with a conversion efficiency of 20% mounted on the vehicle roof, which has an area of approximately 2.7 m^2 (corresponding to a rated power of 540 W), resulting in an estimated energy output of 1.3 kWh, which corresponds to 13% of the battery consumption of 10 kWh described above.

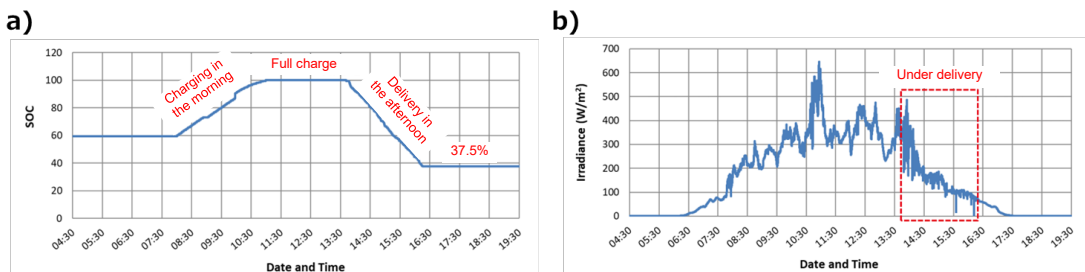


Fig. 2.2-3 a) Battery SOC data, b) solar irradiance data

By processing similar data on a daily basis (limited to days when deliveries were conducted), the daily PV supply ratio – defined as the ratio of estimated PV-generated electricity to battery consumption – was calculated, and the monthly averages are shown in Fig. 2.2-4. During winter months (December to February), battery consumption from driving as well as air conditioning (heater) resulted in PV supply ratios of approximately 10 to 20%. In contrast, during April and May in Japan, when PV power generation is particularly active and air conditioning usage during deliveries is relatively low, the PV supply ratio was suggested to potentially reach

approximately 60 to 70%. By averaging the monthly PV supply ratios over the entire year (February 2022 to January 2023), the annual PV supply ratio was estimated at 44%. This indicates that the corresponding reduction in electricity costs from grid charging could be achieved, suggesting that PV installation has the potential to provide significant long-term benefits.

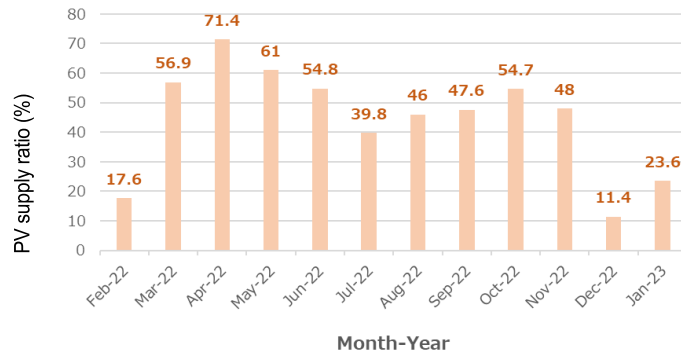


Fig. 2.2-4 Monthly PV supply ratio (product delivery use case)

The above discussion is based on a simple comparison between the estimated PV-generated electricity from solar irradiance and battery consumption, limited to days when deliveries were conducted; days without deliveries (i.e., days with zero battery consumption) were excluded. However, in actual product delivery services, there are days when no deliveries occur despite the expectation of significant PV generation (i.e., sunny days). For example, YORK-BENIMARU does not operate delivery services on weekends, and there are also weekdays with no orders. In such cases, if charging of the EV is not planned accordingly, PV electricity may not be stored because the battery is already fully charged, potentially leading to PV curtailment. In this product delivery service in particular, the EV is charged “from the morning until fully charged by noon” (see Fig. 2.2-3a). Ideally, the amount of PV-generated electricity available for charging before departure each day would be predicted (e.g., estimated at 10% SOC), and the charging starting in the morning would be controlled accordingly (stopping at 90% SOC) so that the SOC reaches 100% immediately before departure. Assuming such a smart EV charging operation, a re-analysis of the data was conducted. For the 365 days from February 2022 to January 2023, the total estimated PV-generated electricity was 490.4 kWh, and the curtailed electricity was calculated to reach 52.3 kWh (10.7%). This indicates that even with smart EV charging operations, PV curtailment cannot be completely avoided. To eliminate PV curtailment, it would be necessary to enable power transfer from the vehicle to other entities (grid, stores, etc.), i.e., by implementing V2X functionality.

(ii) Truck delivery

As a use case different from product delivery, a survey was also conducted on deliveries using EV trucks. With the cooperation of Teihoku Logistics Co., Ltd. (headquarters: Fukushima City, Fukushima Prefecture), a PV-module-type solar irradiance sensor was installed on the body roof of an EV truck (Mitsubishi Fuso Truck & Bus Corporation e-Canter, battery capacity: 81 kWh) used by the company, creating a truck-type PYEV. The exterior of this vehicle is shown in Fig. 2.2-5. Inside the vehicle, a CAN logger and GPS sensor were installed, allowing acquisition of vehicle data (SOC data) and position information similar to those obtained in the product delivery use case. Data collection was conducted over one year, from December 2023 to November 2024.



Fig. 2.2-5 A truck-type PYEV

Regarding the analysis of the data obtained, for the EV truck, it was assumed that a PV module with a conversion efficiency of 20% was installed on the body roof, which has an area of approximately 10 m² (corresponding to a rated power of 2 kW), and the same processing as in the product delivery use case was applied. That is, the daily PV supply ratio for days when deliveries were conducted was calculated, and monthly averages were then computed. The results are shown in Fig. 2.2-6. The PV supply ratio was lowest in December and particularly high in May and June, showing a trend similar to that observed in the product delivery case. The annual PV supply ratio, obtained as the average of the monthly PV supply ratios, was 35%, which is lower than that in the product delivery case. One reason for this is considered to be the difference in daily travel distance (approximately 30 km/day for the truck delivery in this case, compared to approximately 15 km/day for the product delivery).

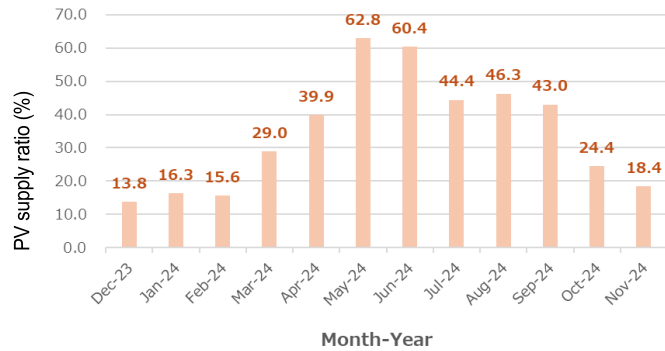


Fig. 2.2-6 Monthly PV supply ratio (truck delivery use case)

An estimation of PV curtailment was also attempted for truck delivery. In this case, the vehicles are typically in use from the morning, so the charging operation is conducted “starting in the evening after delivery operations and continuing overnight until fully charged by morning,” which differs from the product delivery case where the EV is charged “from the morning until fully charged by noon.” Therefore, in truck delivery, it is not necessary to predict the amount of PV-generated electricity for charging available before departure, as was required for product delivery; for example, setting the charging to always stop at 95% SOC is sufficient. Considering such a charging operation suitable for truck delivery and including PV-generated electricity of days when no deliveries were conducted, the estimated curtailed electricity was 95.5 kWh, corresponding to 0.8% of the total estimated PV-generated electricity of 1803.9 kWh. This is substantially lower than the 10.7% observed

in the product delivery case, likely because the vehicles are in use from the morning, allowing smooth utilization of PV electricity. This suggests that PVEVs are particularly effective in use cases where the vehicles are used from the morning.

(iii) Community bus

The previous two examples involved virtual estimations of PV installation effects using PYEVs, whereas for an actual evaluation using a PVEV, a community bus was considered. Fig. 2.2-7 shows the exterior of the PVEV used. A Toyota HiAce (10-passenger), originally a gasoline vehicle, was converted to an EV (battery capacity: 39.4 kWh) and configured to allow direct use of PV-generated electricity (rated power: 1.12 kW). This vehicle was operated under conditions simulating a community bus service in the Tatsugoyama district of Fukushima City, Fukushima Prefecture, and various data were collected from September 2023 to August 2024. The driving conditions consisted of a route of approximately 25 km driven once in the morning and once in the afternoon (total of approximately 50 km/day).



Fig. 2.2-7 Community bus PVEV

Fig. 2.2-8a shows an example of PV data. In this example, the total daily PV-generated electricity was 3.94 kWh. Fig. 2.2-8b shows the battery SOC data for the same day. The increase in SOC due to PV charging, the decreases in SOC from two driving sessions, and the increase in SOC from simultaneous charging from PV and the grid can be observed. The electricity consumed for driving on this day was 10.37 kWh. Therefore, the PV supply ratio for this day was calculated to be 28%. The same calculation was conducted using data obtained over 140 days under various weather conditions from September 2023 to August 2024, resulting in an average PV supply ratio of 13.5%. The lower value compared to the PV supply ratios in the product delivery and truck delivery cases is likely related to the shorter driving distances. On the other hand, the PVEV used in this experiment was a prototype, and there is significant room for improvement in the performance and weight of the PV modules as well as the internal power conversion system (e.g., DC-DC converters). By using a more refined PVEV, further improvements in PV supply ratio – leading to reductions in electricity costs and CO₂ emissions – can be expected.

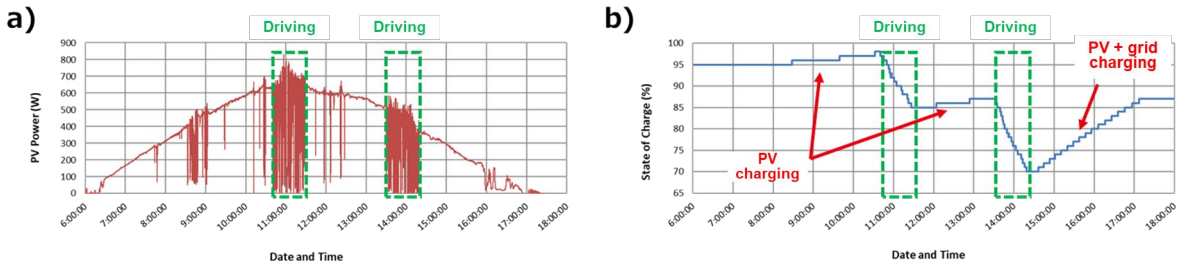


Fig. 2.2-8 a) PV data, b) SOC data

Finally, as a summary of points (i) to (iii) above, Table 2.2-2 presents a comparison of the PV installation capacity, PV supply ratio, and daily driving distance for each use case.

Table 2.2-2 Comparison of results for each use case

Use case	Product delivery	Truck transportation	Community bus
Vehicle			
PV installed capacity	0.54 kW (Planned)	2.0 kW (Planned)	1.12 kW (Actual)
PV supply ratio	44.0%	35.0%	13.5%
Distance traveled per day	15 km	30 km	50.0 km

(2) Development of PVEV system design technology

The PVEV system design technology, as illustrated in Fig. 2.2-9, refers to a tool that, given vehicle usage (operation data) for a particular use case, determines whether PVEVs can be effectively introduced under that use case. By utilizing the collected data from the various use cases described in the previous section, two elemental technologies required for the realization of such a tool were developed: a vehicle-integrated PV power generation estimation technology and an EV power consumption/charging-discharging simulation technology (the latter developed in collaboration with Waseda University). Furthermore, these outcomes were integrated to establish an estimation method (optimal design algorithm) for assessing the effectiveness of PVEV deployment.

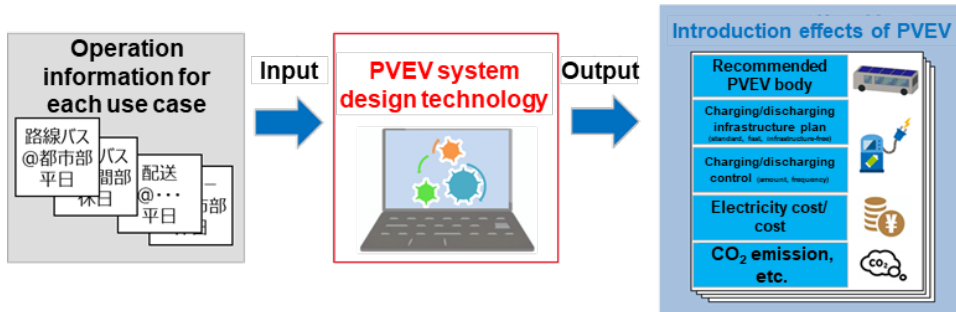


Fig. 2.2-9 Concept of PVEV system design technology

(i) Vehicle-integrated PV power generation estimation technology

In the case of vehicle-integrated PV, solar irradiance fluctuations are more dynamic compared to ground-mounted PV, requiring the establishment of an irradiance estimation method tailored specifically for vehicle-integrated applications. To address this, a method was developed that combines shading pattern simulation of driving routes using GIS (Geographic Information System) and DSM (Digital Surface Model) data with irradiance estimation based on satellite observations (AMATERASS data provided by the Solar Radiation Consortium). This enables time-series estimation of solar irradiance. Furthermore, a “solar irradiance-to-power generation logic” was established by incorporating the temperature characteristics of PV modules and the configuration and performance of downstream equipment (such as devices connecting the PV system with the EV batteries and motor, including MPPT efficiency and DC-DC conversion efficiency). By using vehicle location information as input data, this method enables the calculation of power generation estimates. A flowchart of the entire process is presented in Fig. 2.2-10.

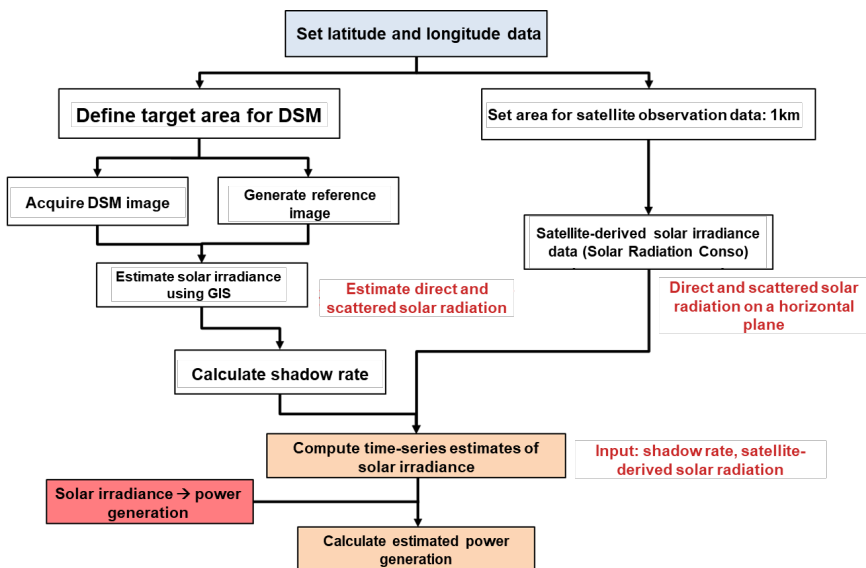


Fig. 2.2-10 Flowchart of vehicle-integrated PV power generation estimation

Fig. 2.2-11 shows an example comparison between the power generation estimates obtained using the developed method and the measured data. It is confirmed that the fluctuations in power generation during driving are reproduced relatively well. On the other hand, during vehicle stops, discrepancies with the measured data are observed in this example between 8:00 - 9:00 and 14:00 - 15:00. This is considered to be dependent on the accuracy of the DSM data used, since small structures not included in the DSM data—such as utility poles—could not be represented and therefore caused shading effects that were not reproduced. Thus, although there are certain limitations in reproducing detailed variations observed in the measurements, when results from other days are also taken into account, it has been confirmed that daily accumulated power generation can generally be reproduced with an accuracy within $\pm 10\%$. This indicates that the developed method is capable of providing sufficiently meaningful information for the final evaluation of PVEV effectiveness.

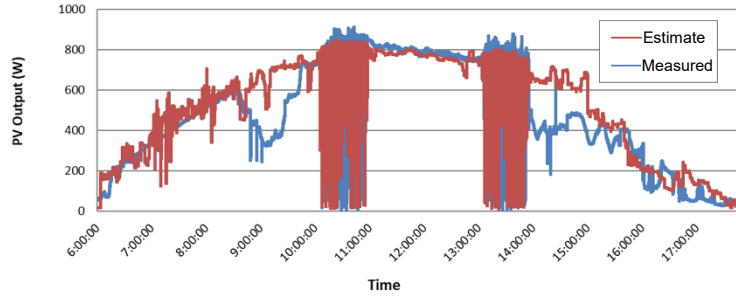


Fig. 2.2-11 Comparison between estimated vehicle-integrated PV power generation (red line) and measured PV data (blue line)

(ii) EV power consumption and charging-discharging simulation technology

Various simulation models for EVs have been reported to date, but most are based on the WLTC mode, and few models can be applied to real-world conditions, particularly those including the effects of ambient temperature or gradient roads in mountainous areas. To address this, a simulation model capable of estimating EV power consumption and charging-discharging amount under real-world conditions was developed based on the analysis of demonstration driving data from PV-powered EVs. A flowchart of the model is shown in Fig. 2.2-12. The method identifies the vehicle type and driving route, and by inputting road gradient, vehicle speed, and ambient temperature during driving, it calculates driving force and power consumption of both the drivetrain and auxiliary equipment based on the motion equation model of the EV powertrain, thereby determining the power consumption rate. Furthermore, it is possible to estimate the battery state of charge (SOC) based on the battery's charging and discharging power.

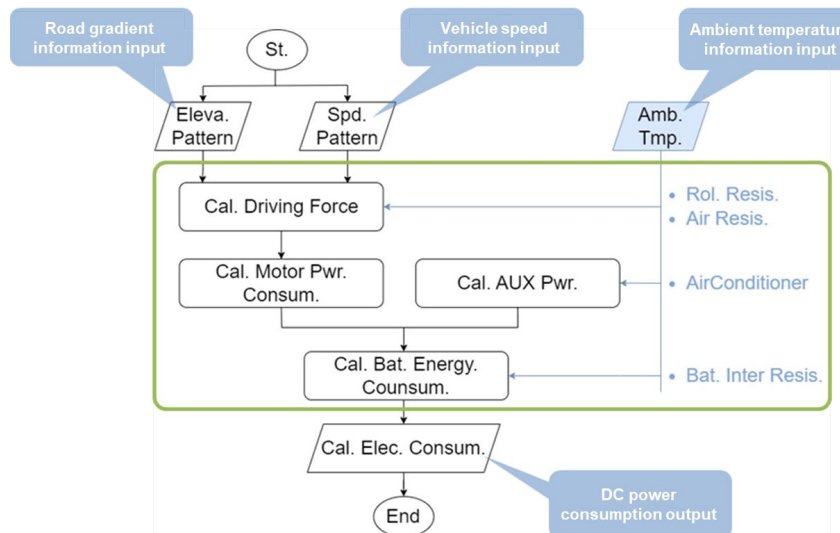


Fig. 2.2-12 EV power consumption and charging-discharging simulation flowchart

Fig. 2.2-13 presents an example of the evaluation results for the developed method. Here, the measured SOC data of a small van-type PYEV used in a commercial delivery use case is compared with the SOC simulation results obtained using the developed method. Fig. 2.2-13a shows that the simulation results (red line: SIM) are comparable to the measured values (blue line: DATA). Furthermore, comparative verification

was conducted for 30 trips under varying driving and weather conditions (trip distances: 1.5–3.9 km, ambient temperatures: -1.0 to $+32.3$ °C) as shown in Fig. 2.2-13b. For 26 of these trips, the maximum power consumption (1.127 kWh) was reproduced within a $\pm 10\%$ range, confirming the accuracy of the simulation model in estimating EV power consumption.

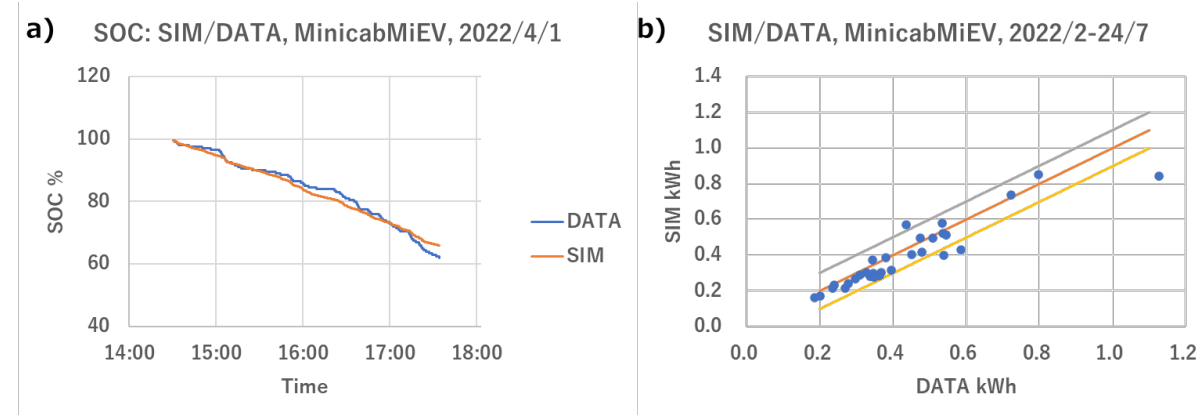


Fig. 2.2-13 Comparison between EV power consumption and charging–discharging simulation results and measured data: a) time series of SOC, b) correlation of cumulative values

(iii) Optimal design algorithm

By integrating the EV SOC simulations obtained from EV power consumption and charging–discharging simulations with the power generation data obtained from vehicle-integrated PV power generation estimation, it becomes possible to simulate the SOC of an EV equipped with PV systems. From these results, the PV supply ratio and the amount of curtailed PV power can be calculated, allowing the estimation of the PV installation capacity required to minimize PV curtailment, or, by allowing a certain degree of PV curtailment, the effects on economics (reduction of electricity costs), environmental performance (reduction of CO₂ emissions), and the improvement of charging operations (frequency and timing), among other effects, can be estimated. Furthermore, the information can be used to provide feedback for adjustments in battery capacity, vehicle weight reduction, improvement of energy efficiency, and the design of charging control mechanisms. Providing this information to vehicle users enables informed decisions regarding the introduction of PVEVs as commercial vehicles, while providing it to vehicle manufacturers can serve as design guidelines and material for evaluating market potential for PVEVs.

2.2.2 Installation of PV Systems on Internal Combustion Engine Trucks and Trailers

The project “[Demonstration of diverse commercial vehicle-integrated PV and development of effect prediction technology](#),” led primarily by SYSTECA CO., LTD., aims mainly to develop a methodology for quantitatively evaluating the effects of installing PV systems on commercial vehicles. The project targets the installation of PV systems on more than 200 diverse commercial vehicles, acquisition of demonstration data, and development of technologies for estimating PV-generated electricity amount and assessing the effects of its introduction, with a target accuracy of $\pm 20\%$.

[Research and Development Overview]

(1) Demonstration of vehicle-mounted PV in approximately 200 commercial vehicles (quantitative evaluation of PV benefits)
Installation in regions with significantly limited sunshine hours, such as Akita Prefecture, and in applications where effects are unclear (e.g., transport trucks, route buses): approx. 20 vehicles

Special-purpose vehicles (e.g., aerial work platforms, boom trucks, garbage collection vehicles): 10 vehicles
Various types of vehicles and operation modes, nationwide commercial vehicles: approx. 100–200 vehicles

* A new data logger will be designed for collecting power generation data.

(2) Development of technologies for quantitative evaluation of the above benefits

Evaluation methods linking driving patterns ⇔ power generation ⇔ fuel-saving effects, formulation of effective installation guidelines, estimation of effects using EV trucks

→ Expected R&D Outcomes

1) A first step toward CO₂ reduction in the transportation sector (potential: 7 million tons/year)

2) Effective introduction of PV-powered commercial vehicles through quantitative assessment of benefits across a wide range of vehicle types

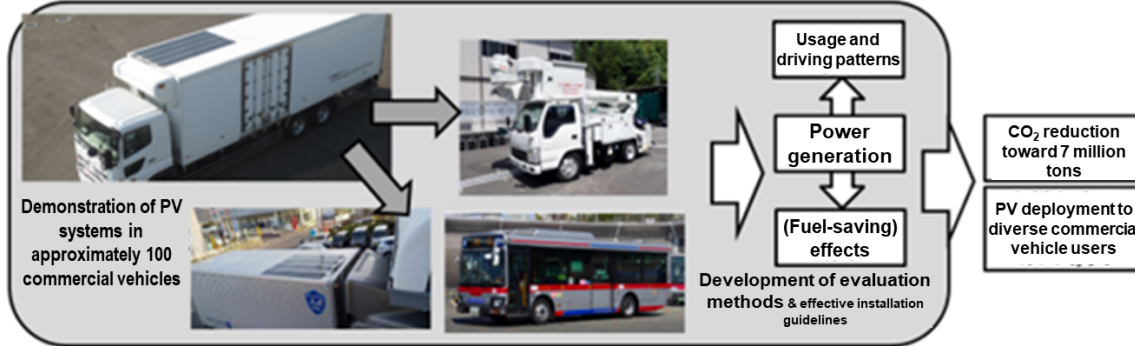


Fig. 2.2-14 Overview of the project “Demonstration of diverse commercial vehicle-integrated PV and development of effect prediction technology”

This section provides an overview of the comparison between predicted and measured PV-generated electricity amount in the project. To date, more than 100 commercial vehicles operating nationwide have been equipped with PV systems (film-type CIGS PV modules), and their power generation has been continuously monitored. This approach allows for the assessment of the potential of vehicle-integrated PV systems without route bias, while also providing validation of the previously developed prediction technologies for power generation amount of vehicle-integrated PV.

(1) Approach to Forecasting Power Generation

The perspectives and considerations underlying the measurement and collection of solar irradiance data for power generation forecasting are the same as those described in Section 2.1.1 for passenger vehicle-integrated PV systems. However, in the case of commercial vehicles, the phenomena are generally relatively simple. Therefore, for the measurement survey of vehicle-integrated PV systems on commercial vehicles, emphasis was placed on increasing the number of samples through simple single irradiance measurements and citizen science methods, in order to conduct fair and unbiased evaluations of the performance and power generation potential of vehicle-integrated PV systems (Table 2.2-3).

Approximately 200 trucks were ultimately equipped with PV, and both power generation data and driving data were collected via telephone networks. Because data collection was conducted in parallel with routine transport operations, detailed solar irradiance measurements were not performed. To evaluate the effectiveness of PV across a diverse range of trucks and commercial vehicles, transportation operators were selected through stratified sampling from various regions throughout Japan -from Hokkaido to Okinawa - with their cooperation secured for data acquisition. As the intent was to capture real-world operational data, no specific instructions were given regarding transport routes or schedules.

Data collection began on March 8, 2024. The driving records as of January 31, 2025, are shown in Fig.

2.2-15. Fig. 2.2-15 visualizes the GPS-based locations of monitored trucks, with median latitude and longitude points plotted at hourly intervals on a Geospatial Information Authority of Japan (GSI) map. While some areas, such as mountainous regions, were less represented, data on driving activity and in-transit power generation was successfully collected from nearly all parts of the country.

Table 2.2-3 Approaches to power generation forecasting in commercial vehicles

- Single pyranometer irradiance measurement (note 1)
- 200 vehicles (note 2)
- Random routes (note 3)
- Flat-plate solar cell
- No self-shading
- Minimal impact from partial shading
- Single-junction solar cell (CIS-based)
- Automatic measurement and data transmission via telephone line by truck drivers of cooperating transport companies
- Power generation fluctuations mainly due to shading during driving
- Power generation forecasting using a shading probability model → validation with measured power generation data

Note 1) The solar irradiance was estimated inversely from the power output of the solar cells. Since the vehicle roofs are frequently washed and continuously exposed to vibration and shock over long operating hours, it was deemed difficult to maintain the performance and accuracy of precision pyranometers without constant technical supervision. Therefore, pyranometers themselves were not installed.

Note 2) Installation of the solar cells and instrumentation systems began in February 2024, and operation commenced on March 8. Thereafter, the number of commercial vehicles (mainly trucks) equipped with the solar cells and instrumentation systems was gradually increased. As of December 2024, including self-financed installations, a total of 200 commercial vehicles had been equipped.

Note 3) The driving routes were determined solely within the scope of each transport company's business activities and were not deliberately randomized. By selecting transport operators across a wide range—from Hokkaido to Okinawa—and covering various categories such as local and long-distance transport, and by stratifying the trucks to be monitored, it was aimed at quantitatively assessing solar irradiance incident on the vehicle surface and performance of the vehicle-integrated PV under diverse driving modes throughout Japan without bias.



Fig. 2.2-15 Domestic driving records of 200 commercial vehicles used in the survey
(plotted from extracted GPS driving records on maps provided by the Geospatial Information Authority of Japan)

(2) Comparison between Predicted and Measured Power Generation

To estimate the potential amount of power generation by vehicle-mounted PV, applying a probabilistic model to driving data from random routes is considered an appropriate approach.

In this project, power generation and electricity usage during the routine operations were monitored. Electricity generated by PV does not always contribute directly to fuel savings. A portion is consumed by loads such as gate lifting and lowering, which reduces battery discharge and thereby suppresses alternator output and diesel fuel consumption. PV electricity generated is also used for charging the battery directly. To understand these power flows, monitoring was conducted using the measurement system shown in Fig. 2.2-16.

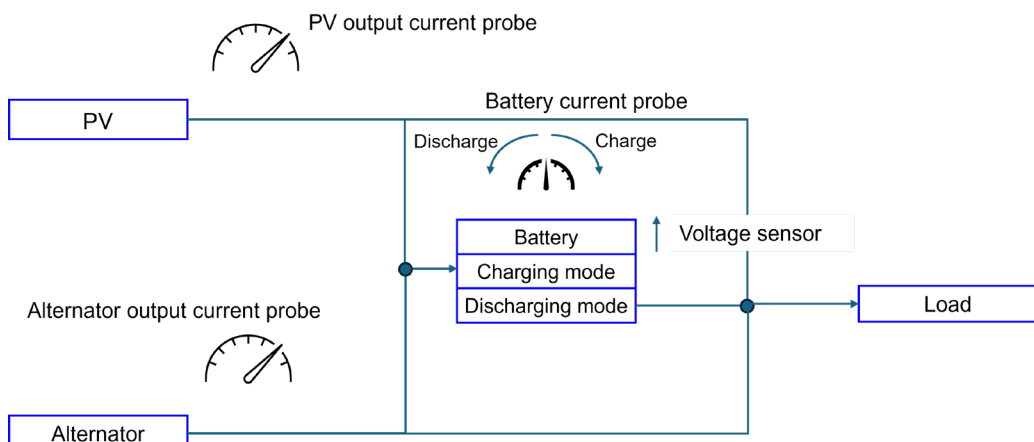


Fig. 2.2-16 Basic circuit diagram for PV power generation and output monitor

Fig. 2.2-17 shows an example of the results of power flow measurement. By comparing the flows of PV power and alternator power for the power load (i.e., by examining the ratio of PV power to load power), the PV power utilization rate can be calculated. The orange bands shown in Fig. 2.2-17 indicate periods when excess PV power was generated. This power was not supplied to the storage batteries or used by the commercial vehicle, resulting in so-called curtailed power generation. For the purpose of evaluating solar irradiance of vehicles-mounted surfaces, calculations must include the portion of generated PV power that was curtailed—that is, the nominal PV power generation.

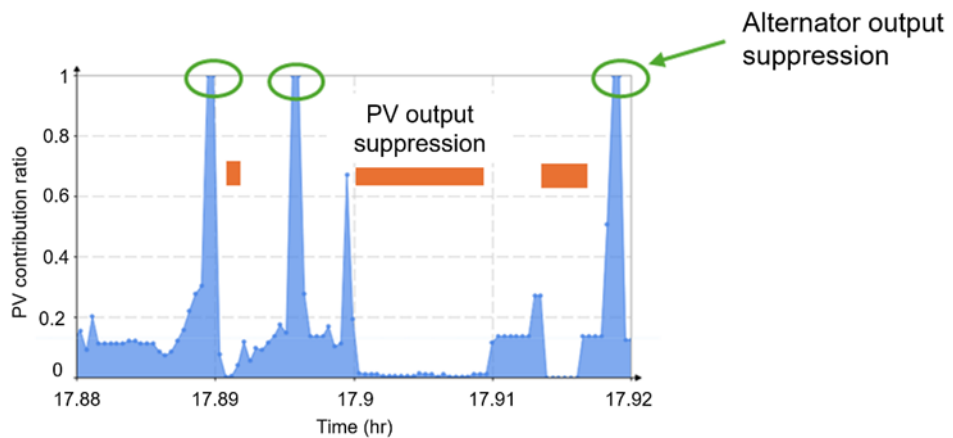


Fig. 2.2-17 PV and alternator output curtailment

To estimate nominal PV power generation, the cumulative duration of the orange-banded periods in Fig. 2.2-17 was calculated. It was assumed that during these periods as well, power would have been generated at a level equivalent to the average power for the entire one-hour interval. The relationship between the nominal PV power generation estimated in this manner and the actual generated power tends to be somewhat randomly distributed below the 45° line, as shown in Fig. 2.2-18.

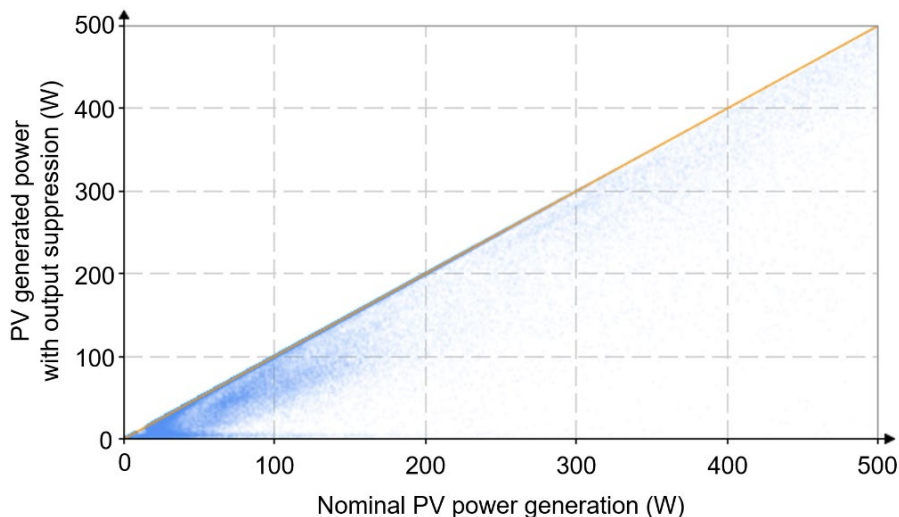


Fig. 2.2-18 Relationship between nominal power generation and actual power generation

The dense concentration of plots near 0 W can be attributed to the fact that many commercial vehicles operate 24 hours a day, and power generation data were collected from 4:00 a.m. to 10:00 p.m. for this research.

Of the nominal PV power generation following output curtailment, approximately 88% was used for alternator power curtailment and load supply—in other words, this portion contributed to fuel reductions—during the data collection period for this report (March 8, 2024 to January 31, 2025). The coefficient rises to over 90% during the summer when cooling loads are applied, but using this ratio generally doesn't pose any accuracy issues.

The following section proceeds to an analysis of the irradiance on the vehicle surfaces. Unless otherwise noted, figures are based on nominal PV power generation. References to “PV power generation” and similar terms below indicate the nominal power generation values as shown in Fig. 2.2-18 and Fig. 2.2-17.

Instrumentation systems were not installed in 200 trucks simultaneously; instead, the number of equipped vehicles was gradually increased through a process of trial-and-error. As shown in Fig. 2.2-19, the resulting dataset somewhat weighted toward the fall and winter seasons. Particularly, a large portion of data from March to June was recorded during morning and evening hours when solar elevation is low. Since the modeling of solar irradiance on vehicle surfaces and seasonal correction (solar elevation adjustment by time of day) relies on statistical models based on shade probabilities, care must be taken to assess whether any biases are present.

A demonstration research was conducted by equipping trucks operating across Japan (from Hokkaido to Okinawa) with vehicle-mounted PV and monitoring their power generation. To estimate the amount of solar irradiance on vehicle surfaces, road segments were categorized into three types according to their shade probability: (1) Areas with tall building or mountainous areas, (2) Residential areas, and (3) City outskirts. Shade probabilities were assigned based on solar elevation and were linked with meteorological data from nearby meteorological observatories, including global horizontal irradiance, sunshine duration, and temperature. The estimated solar power generation was then compared with the actual measured power generation. Based on these probability models, regional solar irradiance levels incident on vehicle-mounted PV were evaluated in accordance with local weather and shading conditions.

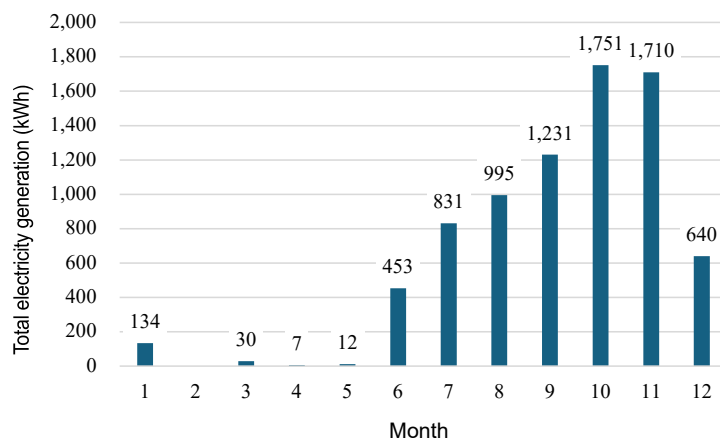


Fig. 2.2-19 Power generation performance of vehicle-mounted PV systems on commercial vehicles

Fig. 2.2-20 shows the correlation between the amount of generated power and predicted power generation based on solar irradiance estimates, calculated using the probability sunlight blockage on vehicle-mounted surfaces. The irradiance on vehicle-mounted surfaces was derived from the sum of the diffuse irradiance, calculated by applying the sky-view factor derived from surrounding structures to the global horizontal irradiance, and the direct irradiance, calculated from the expected value of the blockage rates. For the global horizontal irradiance and direct irradiance used as reference values, sunshine duration data from the nearby meteorological observatory were used. Each commercial vehicle was assigned a meteorological observatory based on the shortest distance from the median latitude and longitude of its driving route. Both global horizontal irradiance and sunshine duration data collected between 11:00 a.m. and 12:00 p.m. were treated as 12:00 p.m. data. For example, when the representative time for a commercial vehicle was 11:15 a.m., the values were interpolated by combining 25% of the 11:00 a.m. measurement with 75% of the 10:00 measurement. Although the actual truck locations were often several tens of km from the regional meteorological observatories that recorded solar irradiance, the values were considered sufficiently reliable. However, it was assumed that the overall deviation would not be significant, as random errors tend to be smoothed out when data is collected over a long period.

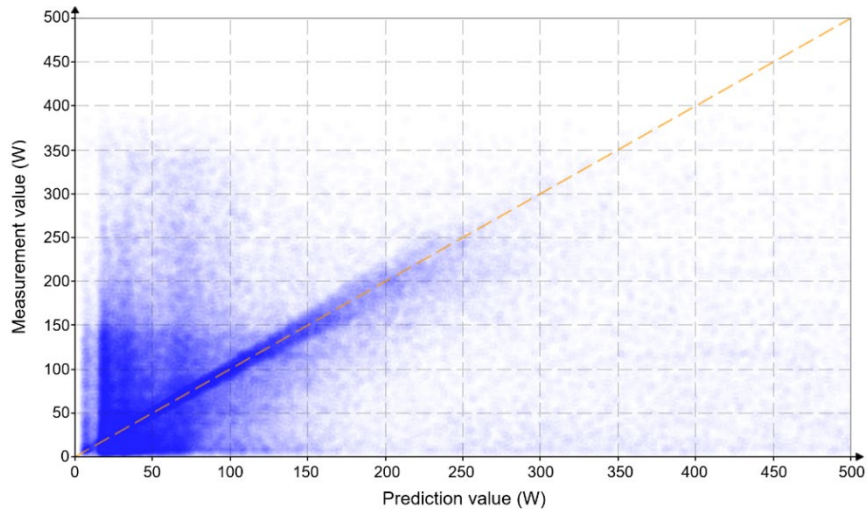


Fig. 2.2-20 Correlation between solar irradiance measurement and prediction values

When applying this estimation, it is essential to ensure that no bias exists in the factors that would affect solar irradiance calculations. For example, regarding solar elevation and the distribution of shading ratios, which influence sunlight obstruction, bias can be evaluated by examining whether prediction errors are evenly distributed with respect to latitude. The results are presented in Fig. 2.2-21. Although some bias was observed between Okinawa (power generation underestimated) and central Kyushu (power generation overestimated), the overall results suggest that no significant bias is present.

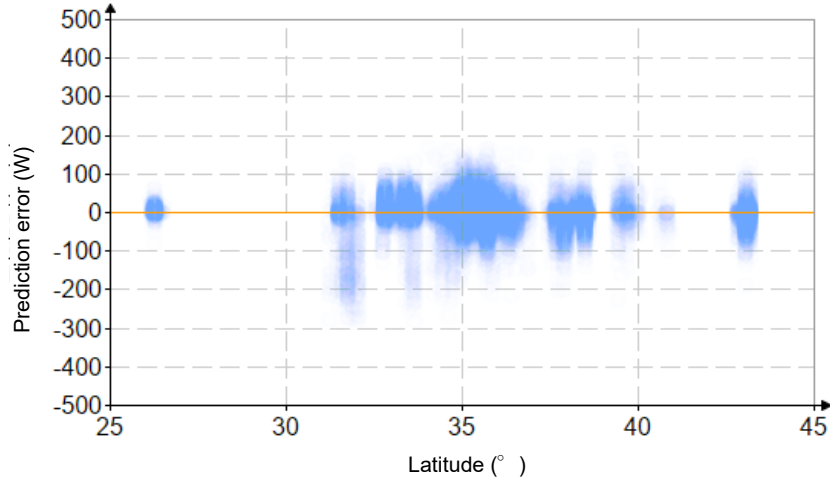


Fig. 2.2-21 Relationship between prediction error and latitude
(presence/absence of bias due to solar elevation)

With respect to weather—that is, the direct sunlight ratio—the presence or absence of bias can be confirmed by investigating the relationship between the sunshine probability and the prediction error. The results are shown in Fig. 2.2-22. It appears that the higher the sunshine probability, the higher the likelihood of overestimation, but the amount of bias does not appear to be that large.

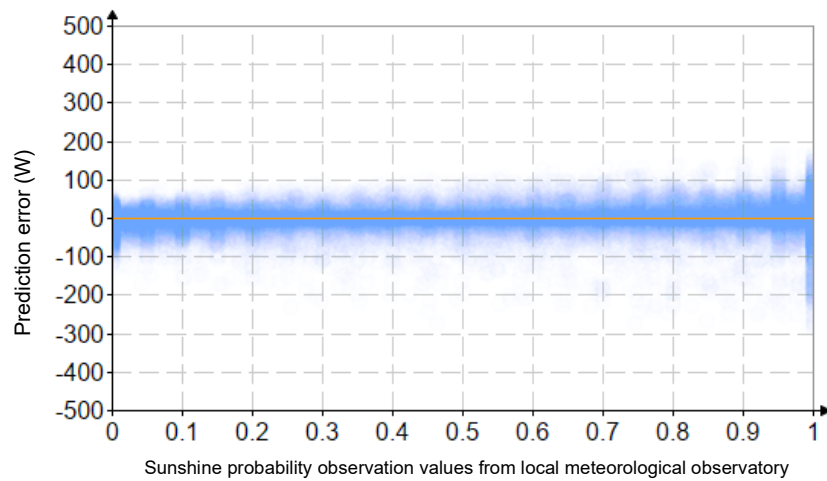


Fig. 2.2-22 Relationship between prediction error and sunshine probability (presence/absence of bias due to direct sunlight ratio)

Next, the difference between solar irradiance on vehicle-mounted surfaces and global horizontal irradiance was calculated. To prevent outliers and abnormal values from degrading the accuracy of the adjusted ratio, a filter was applied to the solar irradiance measurement records. These outliers and anomalies can result from various factors. The most common cause is a discrepancy in solar irradiance and weather conditions between the commercial vehicle's actual location and that of the regional meteorological observatory due to geographic distance. Additional factors include loading or unloading activities conducted indoors while the vehicle is stationary, poor GPS signal environments resulting in incorrect association with distant

observatories, and abnormal data due to instrument testing or malfunction. In this analysis, data points with a performance ratio below 0.5 or above 2.0 were treated as abnormal and excluded from aggregation.

Fig. 2.2-23 and Fig. 2.2-24 show a comparison of the predicted power generation amounts, tabulated for each month, and the actual power generation.

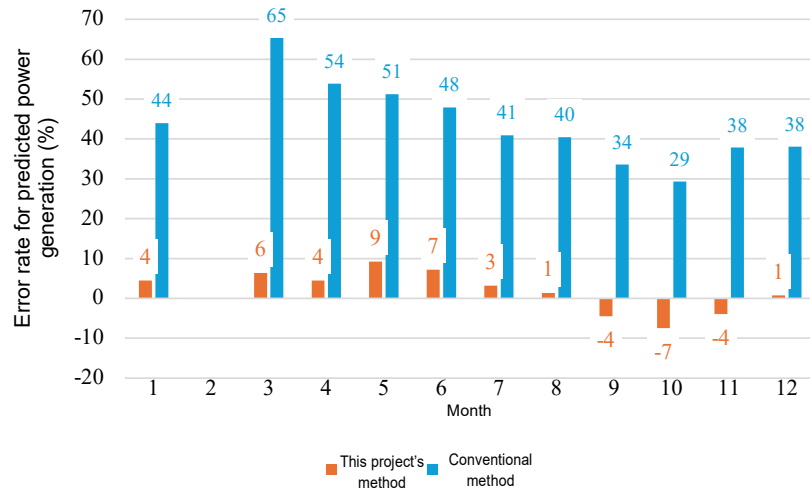


Fig. 2.2-23 Comparison of power generation predictions and actual measurements for random routes and sunlight probability model

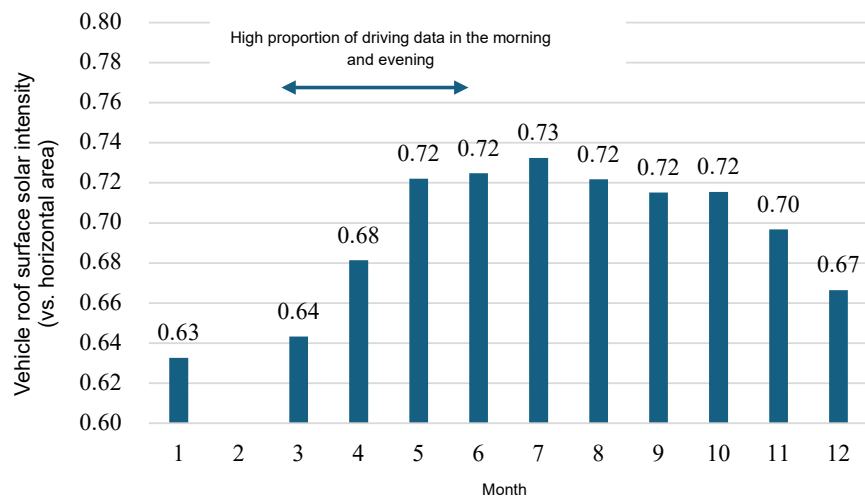


Fig. 2.2-24 Comparison of estimated vehicle surface solar irradiance and global horizontal irradiance

The conventional method for calculating power generation based on global horizontal irradiance does not take into account the effects of surrounding structures, slopes, or similar shading factors, resulting in overestimation. In contrast, the method used in this project corrects for this overestimation over the course of one year, though some seasonal fluctuation remains (Fig. 2.2-23).

Looking at the monthly solar irradiance ratios, the ratio is higher in summer when the solar elevation angle is higher, and lower in winter when the sun is lower and PV systems are more susceptible to shading (Fig. 2.2-24). It should be noted that data from March to June were limited, as this period immediately followed

the start of measurements, and a relatively high proportion of the power generation records were from the morning and evening hours—meaning the effective solar elevation was lower and the ratio slightly reduced.

The ratio of driving area types was as follows: (1) Areas with tall buildings or mountainous areas: 41%, (2) Residential areas: 13%, (3) City outskirts: 47%. From March to May, the number of trucks equipped with PV was low, and the data was slightly skewed toward early morning and evening hours. In any case, vehicle-mounted PV are affected by shading from roadside structures, and it should be kept in mind that solar irradiance on vehicle surfaces averaged around 70% of that expected from horizontal irradiance. (Actual power generation by vehicle-mounted PV during the above evaluation period was 71% of the power estimated using the conventional method.)

Furthermore, prediction errors showed no systematic bias not only by month, but also by latitude or weather conditions (Fig. 2.2-21 and Fig. 2.2-22). This indicates that the vehicle surface solar irradiance predictions generated by this model can be applied broadly across Japan, regardless of whether variation or solar elevation (which varies by latitude, time, and season).

The ratio of solar irradiance on a vehicle-mounted surface to that on a horizontal plane, as calculated for a Moderate Shading Zone (low-rise building and residential areas) under the Temperate Coastal climate category in the standard irradiance database defined by IEC61853-4, is 0.671. Given that a high proportion of the routes in this project were located in city outskirts with low shade probability, the observed irradiance ratio is considered approximately equivalent. Weighting the respective shade environment zones yields values of 0.455 for lightly shaded zones (city outskirts) and 0.904 for heavy shaded zones (high-rise buildings or mountainous areas). Applying these to actual route composition, $0.455 \times 0.41 + 0.671 \times 0.13 + 0.904 \times 0.47$, results in a composite irradiance ratio of 0.699, which closely matches the actual power generation ratio of 0.71 observed in this project. The degree of irradiance reduction varies depending on the driving environment—such as mountainous versus city outskirt routes—but the vehicle surface irradiance and power generation can be estimated using a unified model. However, for curved vehicle surfaces, such as those of passenger vehicles, additional loss factors unique to curved geometries (including partial shading and self-shading) must also be taken into account.

(3) Estimation of Fuel Savings from PV

The fuel savings are estimated based on the above power generation verification results.

PV power generation and fuel injection volume were monitored in selected trucks using a separate logger system. Synchronization of the power generation data (representing alternator operation suppression) and fuel injection data was achieved by identifying overlapping time periods using the GPS-based clocks in both systems. Truck fuel injection amounts can vary based on a wide range of factors. Drivers' habits and road surface conditions have little impact when trucks are idling or driving at low speeds, making it easier to see the mutual relationships between alternator power generation amounts and fuel injection amounts. For example, Fig. 2.2-25 shows the relationship between the amount of alternator power generation and the amount of fuel injection for a large, refrigerated truck while idling. The slope of the regression line corresponds to the amount of fuel consumption per unit of alternator power generated under these operating conditions. When idling, a large diesel engine must be operated at a light load, so the amount of fuel consumption is relatively high.

Fig. 2.2-26 shows an example of fuel reductions calculation based on driving data from seven trucks operated by a transportation company with a nationwide logistics network, monitored from late October. Although the measurement results are limited to November, the trucks traveled across regions from Hokkaido to Kyushu, making the data a valid representative sample.

Fuel reduction were primarily achieved by suppressing alternator operation during idling. The monthly diesel fuel reductions were calculated to be 62 liters per vehicle per month. This corresponds to a reduction of 162 kg in greenhouse gas emissions per truck per month. When converted into fuel efficiency terms, this represents an estimated 5% improvement.

This 5% improvement is based on actual power generation in November, when the solar elevation is low. If seasonal differences were taken into consideration, PV power generation and fuel reductions could be expected to be roughly 1.6 times higher. In other words, fuel reductions could improve by 8%.

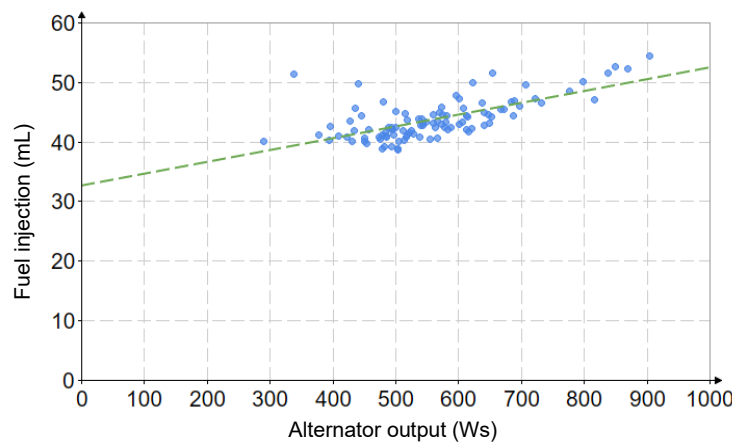


Fig. 2.2-25 Example of Measurement of relationship between alternator power generation and amount of fuel injection

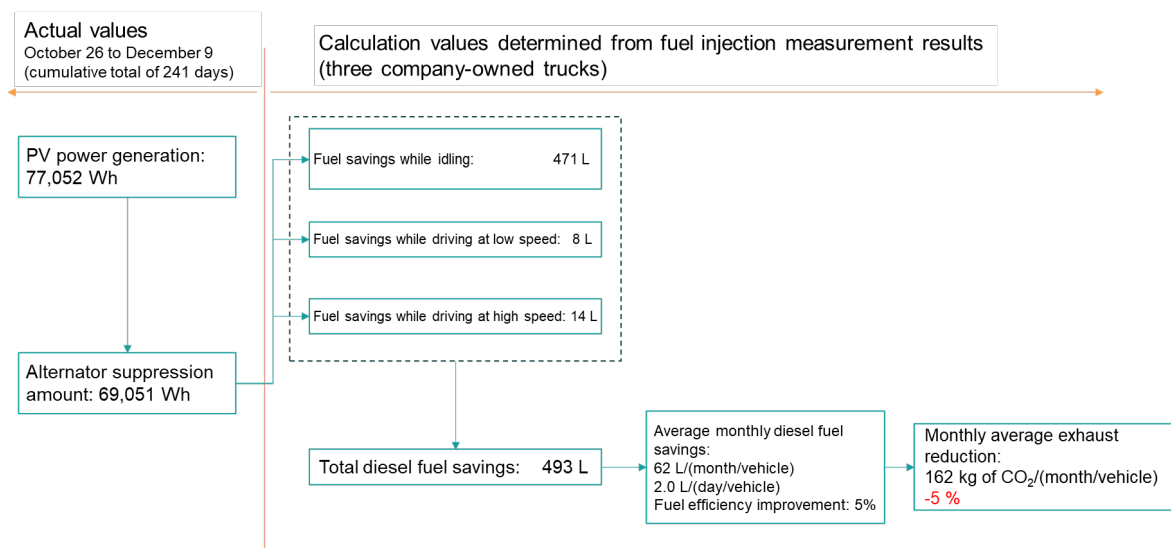


Fig. 2.2-26 November fuel savings calculation results for seven trucks owned by a transportation company with a nationwide network

2.3 Reliability Evaluation of PV Modules for Passenger Vehicles

2.3.1 Organization of Environmental Load Test Items and Points to Note

Vehicle-mounted PV are exposed to operating environments different from the conventional PV installed on building roofs or on the ground, so the expected requirements for durability and reliability differ. In this section, reliability assessment items to be met by vehicle-mounted PV, compared to terrestrial PV assessment items, are investigated, and assessment items and test conditions specific to vehicle-mounted PV are qualified²⁰.

Given that vehicle-mounted PV can be considered both derivatives of terrestrial PV and automotive components (electrical and electronic equipment, glass), the following international and Japanese standards (ISO, IEC, JIS, and JASO), which define reliability evaluation tests assuming their operating environments, were investigated. The results of the investigation are summarized below; for further details, the respective standard documents should be consulted.

Environmental load test standards for terrestrial PV modules

- **IEC 61730-2:2016**, Photovoltaic (PV) module safety qualification – Part 2: Requirements for testing
(**JIS C 61730-2:2020**, Photovoltaic (PV) module safety qualification – Part 2: Requirements for testing)
- **IEC 61215-2:2016**, Terrestrial photovoltaic (PV) modules – Design qualification and type approval – Part 2: Test procedures
(**JIS C 61215-2:2020**, Terrestrial photovoltaic (PV) modules – Design qualification and type approval – Part 2: Test procedures)
- **IEC 61701:2020**, Photovoltaic (PV) modules – Salt mist corrosion testing
- **IEC 62716:2013**, Photovoltaic (PV) modules – Ammonia corrosion testing
- **IEC 62938:2020**, Photovoltaic (PV) modules – Non-uniform snow load testing
- **IEC TS 63397:2022**, Photovoltaic (PV) modules – Qualifying guidelines for increased hail resistance
- **IEC 62759-1 ED2:2022**, Photovoltaic (PV) modules – Transportation testing – Part 1: Transportation and shipping of module package units
- **IEC TS 63126:2020**, Guidelines for qualifying PV modules, components and materials for operation at high temperatures

Environmental load test standards for automotive components

- **ISO 16750-2~5:2023**, Road vehicles – Environmental conditions and testing for electrical and electronic equipment – Part 2: Electrical loads, Part 3: Mechanical loads, Part 4: Climatic loads, Part 5: Chemical loads
- **JASO D 902:2012**, Automotive parts – Electronic equipment – Durability testing methods
- **JIS R 3212:2015**, Test methods of safety glazing materials for road vehicles

Table 2.3-1 categorizes the environmental load test items for terrestrial PV and automotive components into mechanical, climatic, electrical, and chemical loads. This section only contains test items intended for

maintaining essential performance. Items related to the safety protection of passengers and pedestrians against fire, electrical shocks caused by malfunction, collision, etc., are not included. The table contains the test numbers or section numbers of individual tests stipulated in the standards. Tests to which the entire standard applies are marked with "○". The assessment items that only apply to terrestrial PV, that only apply to automotive components, and that apply to both are colored green, red, and blue, respectively.

Tests stipulated exclusively for automotive components include mechanical shocks (e.g., curb strikes at high speed or mechanical loads from door operation) and thermal shocks, which are characterized by large load changes over a short period. Tests stipulated for "terrestrial PV only" as well as those stipulated for "both terrestrial PV and automotive components" (e.g., hail impact, constant temperature, damp heat, temperature cycling, salt and ammonia spray) are also considered necessary for vehicle-mounted PV. Among these, hail impact has been increasingly observed, requiring thorough evaluation and durability assessment. In the following, the characteristics of these tests are explained with a focus on their relevance to vehicle-mounted PV.

In the thermal shock test stipulated by JASO D902, the temperature of the specimen is varied between -40°C and 85°C at a rate of $25^{\circ}\text{C}/\text{min}$, which is approximately 15 times greater than that of the temperature cycling tests for terrestrial PV (IEC 61730-2 MST 51, IEC 61215-2 MQT 11) (see Fig. 2.3-2). PV modules are relatively thin structures, so temperature gradients through the thickness are unlikely to occur; however, different thermal stresses can act on the module materials depending on whether the environmental temperature changes rapidly or gradually. Therefore, verification through testing is considered necessary.

Vibration tests are stipulated both for terrestrial PV modules and for automotive components. In the case of terrestrial PV modules (IEC 62759-1 ED2), the tests stipulate vibration conditions assuming transportation loads, with a frequency range of 1–200 Hz. In contrast, for in-vehicle electrical and electronic equipment (ISO 16750-3, JASO D 014-3, JASO D 902), the standards stipulate detailed conditions for random vibration tests and mechanical shock tests according to the mounting position and vehicle type. For equipment mounted on the body of passenger cars, the vibration frequency range is stipulated as 1–2000 Hz, which differs significantly from terrestrial PV modules. Furthermore, in ISO 16750, the environmental test standard for in-vehicle electrical and electronic equipment, the tests for internal combustion engine (ICE) vehicles, hybrid electric vehicles (HEV), and battery electric vehicles (BEV) were consolidated in 2023, and the conditions were updated. When comparing the stipulated test conditions between ICE vehicles and HEV/BEV passenger cars, the maximum vibration frequency is 1000 Hz for ICE vehicles and 2000 Hz for HEV/BEV, meaning that the HEV/BEV conditions are stricter. In addition, for mechanical shock tests, the stipulated number of shocks for ICE vehicles has approximately doubled, regardless of the mounting position, and has been unified with the number stipulated for HEV/BEV vehicles.

Hail tests are stipulated for terrestrial PV modules in IEC 61215-2 MQT 17, in which ice balls are launched from a launcher to collide with the module. Special equipment is therefore required for this test. In the former JIS C 8917, a simplified test method was specified, in which a steel ball is dropped onto the module. This method is based on the test methods of safety glazing materials for road vehicles (JIS R 3212, 5.4 impact resistance test), using a steel ball of the same dimensions and weight. The purpose of the JIS R 3212 test is to determine whether safety glass has the minimum adhesion or strength required to withstand the impact of small hard flying objects, and the drop height of the steel ball is higher than the 1 m stipulated in JIS C 8917.

Since the tests described above are designed to simulate environmental loads specific to automobiles, it is desirable to conduct them for vehicle-mounted PV as well. However, there are very few reports of such environmental load tests applied to PV modules. In the next section, as an example, the results of vibration tests, mechanical shock tests, and thermal shock tests for vehicle-mounted electrical and electronic equipment, as well as hail impact (steel ball drop) tests for terrestrial PV, are presented for PV modules. For vehicle-mounted PV, module structures using resin instead of glass (resin modules) are also considered as candidates due to requirements for light weight and conformity to curved surfaces; therefore, the tests were primarily conducted on resin modules.

Table 2.3-1 Environmental load tests related to vehicle-mounted PV

Category	Reliability assessment items	Terrestrial PV								Automobile components			
		IEC (JIS C) 61730-2	IEC (JIS C) 61215-2	IEC 61701	IEC 62716	IEC 62938	IEC TS 63397	IEC 62759-1 ED2	IEC TS 63126	ISO 16750			
										-2	-3	-4	-5
Mechanical	Surface strength	MST 12									4.4		
	Hail / steel ball falling		MQT 17				○						5.4
	Static mechanical load	MST 34	MQT 16			○ (Snow)							
	Vibration							6.3 (Transportation)			4.1		6.4
	Mechanical shock										4.2		
	Gravel bombardment										4.5		
Climatic	Steady-state temperature	MST 37, 55, 56						○			5.1		5.8 5.19
	Dump heat	MST 53	MQT 13								5.7		6.3 5.10
	Thermal cycling	MST 51	MQT 11								5.3.1		
	Humid heat cycle (condensation)	MST 52	MQT 12								5.6 5.8		
	Solar radiation	MST 54	MQT 10								5.10		5.9 5.17
	Outdoor exposure		MQT 08										
	Salt corrosion			○							5.5		
	Ammonia corrosion				○								
	Thermal shock / ice water										5.3.2 5.4		6.2
	Mixed gas corrosion										5.9		
	Dust										5.11		
	Atmospheric pressure										5.12		
Electrical	Hot-spot endurance	MST 22	MQT 09							4.13			
	EMC												
Chemical											○		5.15

(Green: stipulated for terrestrial PV only; Red: stipulated for automobile components only; Blue: stipulated for both automobile components and terrestrial PV)

2.3.2 Implementation of Reliability Tests for Automotive Components

(1) Vibration Test and Mechanical Shock Test

A resin module was fabricated in which the top layer was composed of resin (polycarbonate: hereinafter PC). The resin module was configured, in order from the surface, as follows: PC / encapsulant / crystalline Si (c-Si) cells (2×2 array) / encapsulant / backsheet. As the c-Si cells, PERC cells with three busbars (width: 2.0 mm) were employed, having dimensions of $156 \times 156 \times 0.2$ mm (including electrode thickness). The cells were interconnected by ribbon wires (width: 2.0 mm, copper wire thickness: 0.15 mm, plating thickness: 40 μ m), and the ribbon wires were joined with tab wires (width: 6.0 mm, copper wire thickness: 0.23 mm, plating thickness: 40 μ m), so that all cells were connected in series. For comparison, a conventional glass module, with a typical layer configuration in which glass was used as the top layer, was also fabricated. The test apparatus and the appearance of the modules are shown in Fig. 2.3-1 (left). The modules were clamped around the entire perimeter by an aluminum alloy frame and were fixed to the vibration table. The power spectral density (PSD) of acceleration versus frequency for the random vibration test (JASO D 014-3: 2014) is shown in Fig. 2.3-1 (center). This vibration was applied for 8 hours in each of the X, Y, and Z directions. The acceleration profile versus time for the mechanical shock test (JASO D 014-3: 2014) is shown in Fig. 2.3-1 (right). Acceleration was applied 10 times in both positive and negative directions of each axis. The number of samples was three in each case.

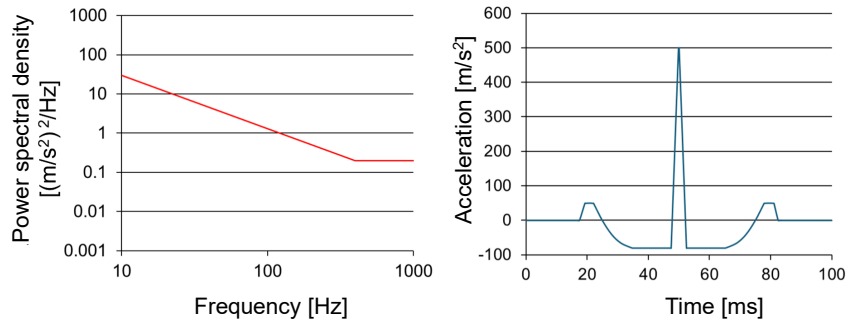


Fig. 2.3-1 Vibration and mechanical shock tests: device appearance (left), vibration test conditions (center), mechanical shock test conditions (right)

Tables 2.3-2 and 2.3-3 show the degradation rates of the module maximum power output, P_{\max} , before and after testing under Standard Test Conditions (STC). In the random vibration test (Table 2.3-2), the average degradation rate of the glass modules (Glass-1 to Glass-3) was -1.0% , whereas that of the resin modules (PC-1 to PC-3) was -3.2% , indicating a significant difference. In the mechanical shock test (Table 2.3-3), the average degradation rate of the glass modules was -0.47% , compared to -3.5% for the resin modules, again showing a significant difference similar to the random vibration test. The degradation of P_{\max} was primarily caused by a decrease in short-circuit current, while changes in open-circuit voltage and F.F. were small. The resin modules exhibited larger amplitudes and lower natural frequencies than the glass modules during both vibration and shock tests. These material characteristics are likely responsible for the observed degradation. Therefore, caution is required when using resin-based modules in vehicle-mounted PV.

Table 2.3-2 Results of random vibration test

Tested module	P_{\max} degradation rate [%]	Average degradation rate [%]
PC-1	-2.7	
PC-2	-2.5	-3.2
PC-3	-4.3	
Glass-1	-1.3	
Glass-2	-0.8	-1.0
Glass-3	-0.9	

Table 2.3-3 Results of mechanical shock test

Tested module	P_{\max} degradation rate [%]	Average degradation rate [%]
PC-1	-3.1	
PC-2	-3.5	-3.5
PC-3	-4.0	
Glass-1	-0.5	
Glass-2	-0.4	-0.47
Glass-3	-0.5	

(2) Thermal Shock Test

Three types of modules (2×2 cell arrays) were tested, with the top/bottom layers consisting of glass/backsheet, PC/backsheet, and PC/PC. The cells used and the electrical connection configuration were the same as those in “(1) Vibration test and mechanical shock test.” Fig. 2.3-2 shows the temperature variation inside the chamber during the thermal shock test for in-vehicle electronic components (JASO D 902:2012). For comparison, the temperature variation inside the chamber during a standard temperature cycle test for conventional PV modules (IEC 61215-2:2016) is also shown. In the thermal shock test, the chamber temperature changes from -40°C to 85°C (or vice versa) within 5 minutes, subjecting the test specimens to rapid temperature fluctuations.

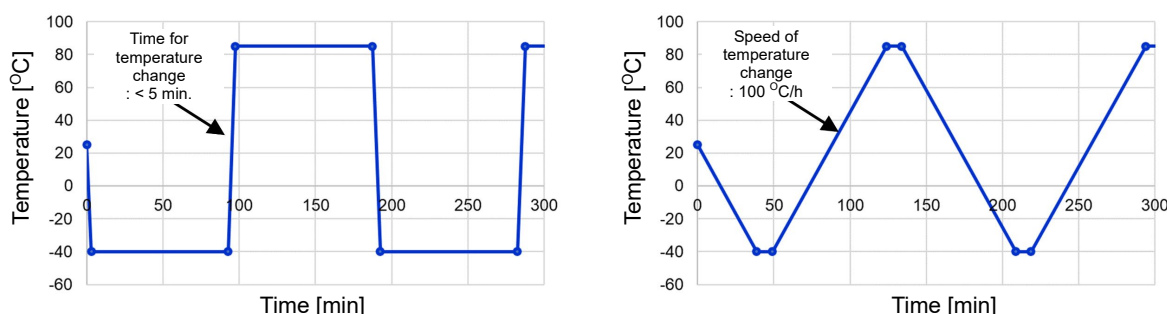


Fig. 2.3-2 Comparison of temperature variations: JASO D 902 thermal shock test (left), IEC 61215-2 temperature cycling test (right)

Fig. 2.3-3 shows the appearance, EL images, and P_{\max} degradation rates of each module before and after testing. Significant degradation was observed in the PC/backsheet and PC/PC modules. For the PC/backsheet modules, 2 out of 3 samples could not undergo IV and EL measurements after testing, while for the PC/PC modules, none of the samples could undergo IV and EL measurements after the test. In these resin-based modules, the thin ribbon lines connecting the cells and the thick ribbon lines where thin ribbons merge were broken due to deformation. In contrast, the glass modules showed no noticeable degradation in appearance or EL images, and the P_{\max} degradation rate was less than 1%. Since PC has a larger coefficient of thermal expansion than glass, the rapid temperature changes induced greater thermal stress and deformation, leading to ribbon line fractures. Therefore, when using resin-based modules in vehicle-mounted PV, attention must be paid to their durability against thermal shock, as well as vibration and mechanical shock.

	Glass/backsheet	PC/backsheet	PC/PC
Before testing			
After testing	 Average P_{max} degradation rate: -0.47% (n=3)	 P_{max} degradation rate: -53.9% (2 of 3: not measured)	 All 3 samples were not measured by disconnection

Fig. 2.3-3 Thermal shock test results

(3) Steel Ball Drop Test

A steel ball drop test was conducted based on the test standards for impact resistance against small, hard flying objects such as hail (JIS R 3212:2015: Safety glazing materials for road vehicles, JIS C 8917:2005: Terrestrial PV). Two types of flexible modules were tested: ETFE/crystalline Si cell and ETFE-PET-EVA/CIGS cell as combinations of top-layer resin and cells. The crystalline Si PV module was an inexpensive type available through online shopping sites. To simply simulate an add-on vehicle-mounted PV, the modules were attached to the roof of a passenger vehicle as shown in Fig. 2.3-4, and a steel ball was dropped onto the center of each cell from the heights indicated in the figure. For the crystalline Si PV module, a steel ball was dropped from four different heights for each string consisting of nine cells, while for the CIGS module, a steel ball was dropped from a height of 1.0 m onto each of twelve cells. The steel ball used had a mass of 225 g and a diameter of 38 mm, as specified in JIS C 8917:2005 and JIS R 3212:2015.

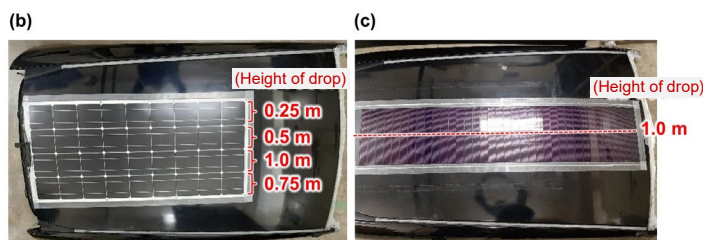


Fig. 2.3-4 Test modules attached to a passenger car roof and heights to drop a steel ball:
(a) roof appearance, (b) crystalline Si PV module, (c) CIGS module

Fig. 2.3-5 shows the EL images of the crystalline Si PV module before and after testing, along with pictures of representative cells. When the drop height was 0.75 m or greater, cracks occurred at the points of steel ball impact in all cells, and impact marks remained on the module surface. In contrast, as shown in Fig. 2.3-6, for the CIGS module, although impact marks remained on the surface after a steel ball drop from a height of 1 m, no significant cell damage was observed in the EL images. The thicknesses of the crystalline Si and CIGS modules were 2.0 mm and 2.5 mm, respectively, and differences in resin and cell thicknesses as well as mechanical characteristics are considered to have contributed to the observed differences in results.

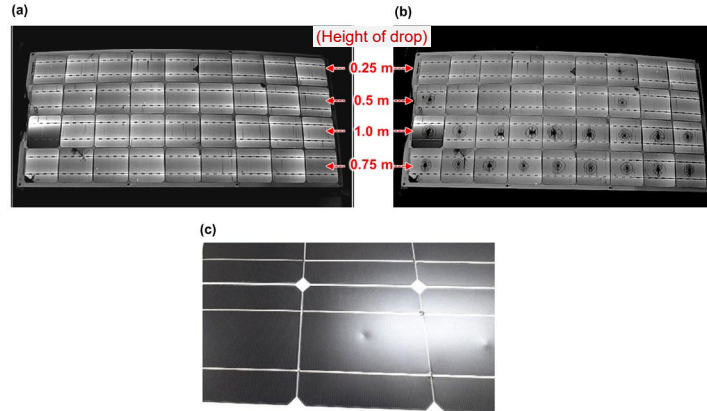


Fig. 2.3-5 Results of the steel ball drop test on the crystalline Si PV module:
 (a) EL before the steel ball drop, (b) EL after the steel ball drop, (c) picture of a representative cell

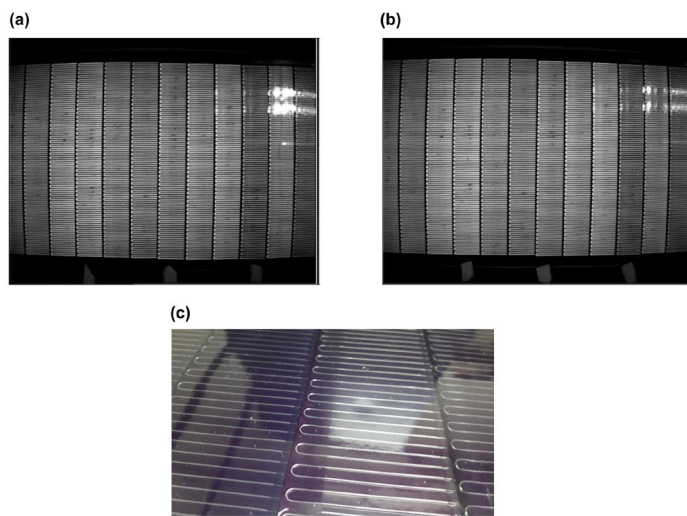


Fig. 2.3-6 Results of the steel ball drop test on the CIGS module:
 (a) EL before the steel ball drop, (b) EL after the steel ball drop, (c) picture of a representative cell

2.3.3 Summary

In this report, reliability evaluation items considered necessary for vehicle-mounted PV were investigated and examined, and representative examples of vibration and mechanical shock tests for in-vehicle electric and electronic components, thermal shock tests, and steel ball drop tests were conducted on PV modules. In all tests, performance degradation was observed; however, the degradation was more pronounced in resin-based modules compared to glass modules. These results indicate that degradation behaviors arising from environmental loads unique to automotive components differ significantly depending on the materials and structures of the modules. Therefore, it is desirable to conduct such tests as appropriate during research, development, and commercialization processes. In particular, when adopting materials and structures different from those of conventional PV modules, such as the resin-based modules tested here, or when curved module geometries are employed, stresses acting on the cells and their surrounding areas can be higher²¹, further emphasizing the necessity of these tests. Consequently, although the range of test items for vehicle-mounted PV is broader than that for stationary PV modules, the required service lifetime is shorter. This highlights the need for establishing more efficient testing methodologies.

2.4 Resilience Provided by Vehicle-mounted PV

One of the advantages of electric vehicles and PV modules is their potential use as emergency power sources during disasters. The resilience effect can be estimated based on the electricity generation of PV modules installed on vehicles (hereafter referred to as vehicle-mounted PV). However, regarding the effect of resilience, not only the supply side (electricity generation) but also the demand side (energy demand at disaster relief centers) and the process of transferring and transporting surplus electricity obtained from vehicle-mounted PV to the disaster relief centers are equally important. In particular, social behaviors during disasters can have a significant impact on energy distribution.

2.4.1 Resilience Scenario

Quantitative discussion requires numerical modeling. Such modeling also requires defining the “victory conditions,” that is, specifying under what disaster conditions, for which actions, and under what circumstances the system’s performance can be considered effective in terms of resilience. Based on the experience of lifeline restoration following the Great Hanshin-Awaji Earthquake, it was assumed here that emergency energy demand could be met for a period of seven days ($7 \text{ days} \times 24 \text{ hours/day} = 168 \text{ hours}$).

The timing of a disaster is difficult to predict, and it could occur at any time—24 hours a day, 365 days a year. Energy supply and demand also vary between summer and winter, and between daytime and nighttime. Quantitative models that take such uncertainties into account require probabilistic simulations (Fig. 2.4-1). In addition, probabilistic models allow for the quantitative assessment and avoidance of risks such as overinvestment in resilience measures, which could become obsolete if disaster preparedness equipment is never utilized.

In the social model regarding energy sharing, voluntary distribution was assumed. In the case of vehicle-mounted PV, electrical energy is stored in the onboard battery even if left unused, which is expected to lower psychological barriers to providing this energy as a public good. A survey conducted by University of Miyazaki targeting residents in neighboring school districts found that approximately 40% of respondents were favorable toward supplying stored electricity to disaster relief centers in the event of a disaster.¹¹

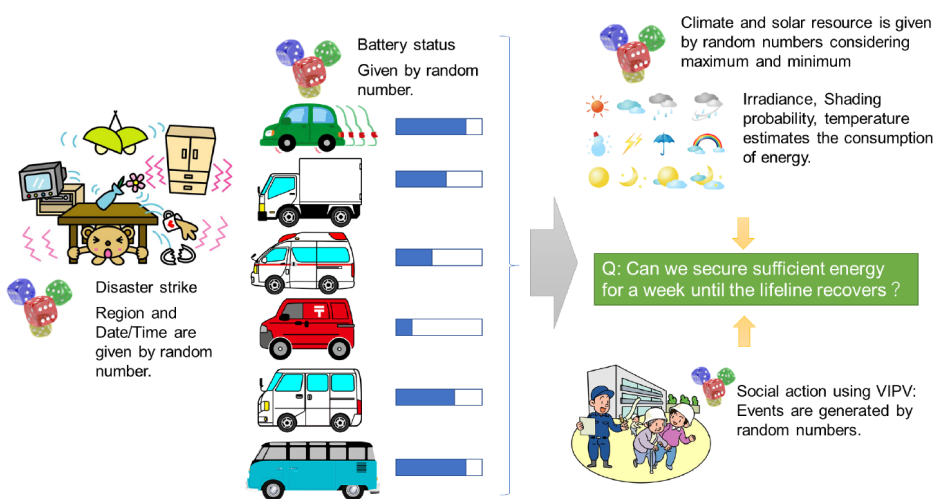


Fig. 2.4-1 Model for utilizing surplus electricity during disasters based on a probabilistic model

Voluntary energy provision is considered preferable when utilized in a way that leverages its characteristics as a public good, rather than being dedicated solely to disaster relief infrastructure established under municipal disaster prevention plans. Therefore, as illustrated in Fig. 2.4-2, its use is envisioned to complement conventional disaster prevention infrastructure, which is assumed to operate as emergency power sources.

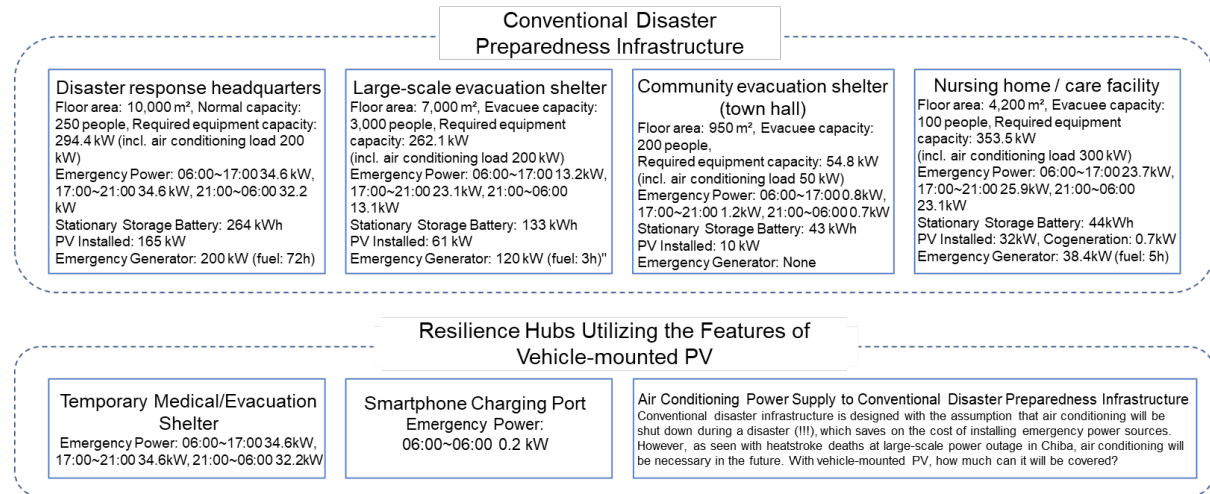


Fig. 2.4-2 Complementary role of resilience through voluntarily supplied energy

Table 2.4-1 lists the parameters used to estimate the resilience effect.

The target area was assumed to be a residential district in Miyazaki City, Miyazaki Prefecture, with the number of vehicles equipped with PV modules ranging from 200 to 1,600. The PV module capacity was set at 400 Wp, with a performance ratio of 0.9 accounting for curved surfaces. Electric fuel economy was assumed to be 8.33 km/kWh, and the onboard battery capacity was 40 kWh. Solar irradiance contributing to PV power generation considered factors such as road surface reflection (during snow melting) and shading from surrounding obstacles. On the demand side, electricity requirements included charging of mobile devices, spot air conditioning units, and temporary relief centers equipped with medical functions.

Table 2.4-1 List of parameters used for the calculations

Parameter	Explanation	Value
Target area	Miyazaki City, residential area	Index No. of METPV: 87376
Number of vehicles equipped with PV	Initial value for Monte Carlo simulation (integer)	200–1,600 vehicles
PV module rated efficiency		22%
PV module covered projected area		1.8 m ²
PV performance ratio	Curvature correction, etc. (temperature correction separately)	90%
Temperature correction coefficient		-0.328%/K
Power management efficiency		93%
MPPT efficiency		95%
Electric fuel economy		8.33 km/kWh
Battery capacity		40 kWh
Road reflectance	Reflectance to vehicle vertical surface	0.08
Road reflectance under snow	Reflectance from snow-covered surface to vehicle vertical surface (snow depth > 10 cm)	0.9
Reflectance of surrounding obstacles	e.g., building walls	0.25
Number of mobile device charging terminals	Deployed within walking range (1 km)	25
Required capacity per mobile device charging terminal	24 hours (constant value)	0.2 kW each
Number of spot air conditioners required		6 units
Spot air conditioner capacity	24 hours (constant value)	2.2 kW (6 hp)
Temporary relief center with medical functions		1 location
Power demand of temporary relief center with medical functions	Varies by time of day	0.36 kW 00:00 – 06:00 1.61 kW 06:00 – 17:00 4.47 kW 17:00 – 21:00 0.36 kW 21:00 – 24:00
Driving distance to public good supply location		5 km

2.4.2 Effectiveness of Vehicle-mounted PV as Resilience Hubs

The following scenario was assumed to examine the effectiveness of resilience provided by vehicle-mounted PV and the necessary conditions for their functionality:

1. A disaster occurs at a certain date and time in area V of city P (randomly assigned).
2. Within the first few hours, in addition to conventional disaster prevention infrastructure, the following facilities are established:
 - Temporary relief center: 1 location
 - Temporary mobile device charging stations: 25 locations
 - Power supply for air conditioning at public halls, etc.: 6 locations (4 hp each)
3. A portion of the electric vehicles that have moved to the temporary facilities voluntarily store energy in their onboard batteries.
4. As needed, vehicles move between temporary facilities to facilitate energy sharing.
5. Among vehicles equipped with PV systems owned by local residents (updates are performed hourly);
 - State of charge of the vehicle-mounted battery is 90% or higher
 - Of these, 5% of drivers share electricity with the above facilities
 - Travel to the supply locations using their own stored energy
 - Share electricity until the battery state of charge reaches 50%
 - Return using their own stored energy

This scenario assumes voluntary electricity provision, in which 5% of vehicle owners with nearly fully charged by vehicle-mounted PV supply their surplus electricity without coercion.

However, not all vehicles are necessarily fully charged at the time of a disaster, and sufficient solar irradiance may not always be available after the event. Some vehicles may remain in shaded areas at all times. Therefore, for each vehicle in the target area, the state of charge at the time of the disaster and shading conditions were assigned using a probabilistic model, with the initial state of charge for each vehicle determined randomly. In addition, whether each vehicle owner provides surplus electricity was also assigned randomly based on the above probability.

The results are shown in Fig. 2.4-3. With vehicle-mounted PV, electricity is stored even when left idle, making surplus electricity more likely to be generated, which reduces the number of battery-equipped vehicles needed in the disaster area by half.

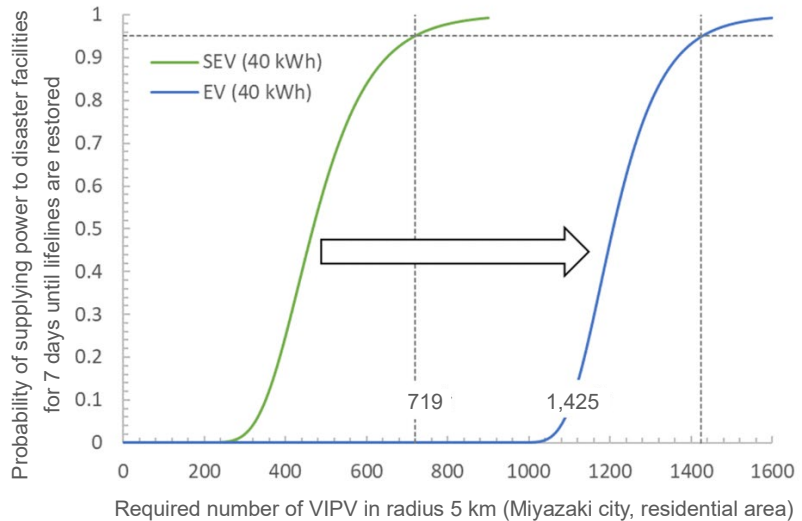


Fig. 2.4-3 Required number of PV-powered vehicles and EVs for the same battery capacity (within a 5 km radius)

2.4.3 Required Number of Vehicles According to the Amount of Surplus Electricity Shared from PV-powered Vehicles

In disaster situations, it is conceivable that, due to self-interested behavior, electricity stored in vehicle-mounted PV or EV batteries may be used for personal purposes rather than provided as a public good; such disaster scenarios are also possible. Therefore, assuming that vehicle owners first use electricity for themselves and then supply any surplus, a certain level of resilience can be achieved. Based on this assumption, the required number of vehicles was examined according to the amount of surplus electricity shared from PV-powered vehicles.

An example of the results is shown in Fig. 2.4-4. The definitions of the vertical and horizontal axes are the same as in Fig. 2.4-3. For example, “70–20%” indicates that if the battery has more than 70% surplus electricity, electricity is supplied with a 1% probability until the state of charge reaches 20%.

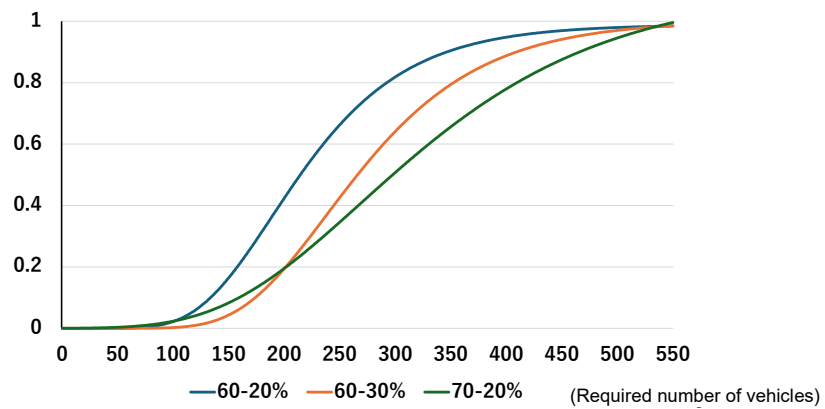


Fig. 2.4-4 Required number of EVs when surplus electricity from vehicle-mounted PV is first used by the vehicle owner

In this way, when vehicle owners first consume electricity for themselves and, due to self-interested

decisions, the probability of supplying to the public decreases, the opportunity to provide electricity as a public good is reduced. As a result, compared with Fig. 2.4-3, even with an increased number of EVs, the probability of maintaining the required electricity at disaster relief centers until lifelines are restored does not significantly improve. Parametric numerical experiments indicate that increasing the amount of electricity shared per PV-powered vehicle is effective. In other words, rather than limiting supply until the battery state of charge reaches 30% under a 60–30% scenario, or 20% under a 70–20% scenario, it is more effective to provide incentives that encourage sharing even when the battery remains at 60% or until it reaches 20%.

2.4.4 Summary

Equipping EVs with PV systems can enhance resilience compared with vehicles without such systems.

However, to realize this effect, it is important that policies assuming electricity as a public good incorporate appropriate incentive design. In particular, when the probability of supplying surplus electricity decreases due to self-interested decisions or similar behavior, it is crucial to implement a system that provides sufficient incentives to the providers.

【Chapter 2 References】

¹ IEA, World Energy Outlook 2002 (2022)

² T. Masuda, T. Nakado, M. Yamaguchi, T. Takamoto, K. Nishioka and K. Yamada, "Public road tests of Toyota Prius Prime equipped with high-efficiency photovoltaic modules with output power of 860 W", 49th IEEE Photovoltaic Specialists Conference (PVSC), 2022.

³ Araki, K.; Ota, Y.; Yamaguchi, M. Measurement and Modeling of 3D Solar Irradiance for Vehicle-Integrated Photovoltaic. *Appl. Sci.* 2020, 10, 872. <https://doi.org/10.3390/app10030872>

⁴ Ekins-Daukes, N., et al. "The Potential for Vehicle Integrated Photovoltaics." *Proceedings of the Asia Pacific Solar Research Conference*. 2020.

⁵ Wetzel, G., Salomon, L., Krügener, J., Bredemeier, D., & Peibst, R. (2022). High time resolution measurement of solar irradiance onto driving car body for vehicle integrated photovoltaics. *Progress in Photovoltaics: Research and Applications*, 30(5), 543-551. <https://doi.org/10.1002/pip.3526>

⁶ Sovetkin, E., Noll, J., Patel, N., Gerber, A., & Pieters, B. E. (2023). Vehicle-Integrated Photovoltaics Irradiation Modeling Using Aerial-Based LIDAR Data and Validation with Trip Measurements. *Solar RRL*, 7(8), 2200593. <https://doi.org/10.1002/solr.202200593>

⁷ Ota, Y., Masuda, T., Araki, K., & Yamaguchi, M. (2019). A mobile multipyranometer array for the assessment of solar irradiance incident on a photovoltaic-powered vehicle. *Solar Energy*, 184, 84-90. <https://doi.org/10.1016/j.solener.2019.03.084>

⁸ Macías, J., Herrero, R., San José, L., Núñez, R., & Antón, I. (2024). On the validation of a modelling tool for Vehicle Integrated PhotoVoltaics: Reflected irradiance in urban environments. *Solar Energy Materials and Solar Cells*, 277, 113060. <https://doi.org/10.1016/j.solmat.2024.113060>

⁹ <https://unit.aist.go.jp/rpd-envene/PV/ja/results/2020/poster/Mizuno-1.pdf>

¹⁰ Araki, K.; Ota, Y.; Nagaoka, A.; Nishioka, K. 3D Solar Irradiance Model for Non-Uniform Shading Environments Using Shading (Aperture) Matrix Enhanced by Local Coordinate System. *Energies* 2023, 16, 4414. <https://doi.org/10.3390/en16114414>

¹¹ Araki, K.; Ota, Y.; Maeda, A.; Kumano, M.; Nishioka, K. Solar Electric Vehicles as Energy Sources in Disaster Zones: Physical and Social Factors. *Energies* 2023, 16, 3580. <https://doi.org/10.3390/en16083580>

¹² NEDO, Press Release "Solar Battery Panel for Electrified Vehicles Using World-Class, High-Efficiency Solar Battery Cells", 6 July 2020 (https://www.nedo.go.jp/news/press/AA5_101326.html)

¹³ Y.Tomita, M.Saito, Y.Nagai, T.Tanimoto, T.Arai, and K.Nishijima, "MPPT operation performance of automotive photovoltaic system during driving", IPEC2022 ECCE ASIA, 19H1-2

¹⁴ NEDO, Solar Irradiation Database (<https://www.nedo.go.jp/library/nissharyou.html>)

¹⁵ NEDO, "PV-Powered Vehicle Strategy Committee Interim Report" (January 2018) (<https://www.nedo.go.jp/content/100961854.pdf>)

¹⁶ Y.Tomita, M.Saito, Y.Nagai, Y.Zushi, T.Tanimoto, and K.Nishijima, "Development of an Electric Vehicle with a High-Power Photovoltaic System", EVTeC 2021, 20214307 C1.4

¹⁷ SolarMoves brochure (<https://publications.tno.nl/publication/34642389/SKwCWv/tno-2024-solarmoves.pdf>) (Confirmed on January 9, 2025)

¹⁸ ASOM Press release, IM Efficiency receives € 2,651 million subsidy from Dutch government (<https://asom.solar/im-efficiency-receives-e-2651-million-subsidy-from-dutch-government/>) (Confirmed on January 9, 2025)

¹⁹ U.S.DOE, SETO, Silicon Solar Manufacturing and Dual-use Photovoltaics Incubator Funding Program (<https://www.energy.gov/eere/solar/silicon-solar-manufacturing-and-dual-use-photovoltaics-incubator-funding-program>) (Confirmed on January 9, 2025)

²⁰ Daisuke Sato, Hayato Kobayashi, Kenji Araki, Makoto Tanaka, Noboru Yamada, Assessment of PV module reliability against automobile-specific environment for design and standardization of vehicle-integrated PV, 33rd International Photovoltaic Science and Engineering Conference, 2022.11.17, Paper No. ThO-22c-03.

²¹ Daisuke Sato, Hayato Kobayashi, Taizo Masuda, Kenji Araki, Yukio Miyashita, Noboru Yamada, Structural design and demonstration of three-dimensional curved photovoltaic modules using crystalline silicon solar cells, Solar Energy Materials and Solar Cells 279, 113258, 2025. <https://doi.org/10.1016/j.solmat.2024.113258>.

Chapter 3: Conclusions (Findings and Future Challenges and Outlook)

Efforts to develop PV-powered vehicles have been gaining momentum both domestically and internationally. This report provides an overview of trends related to PV-powered vehicles, estimates the potential benefits expected from their widespread adoption, and presents a summary of outcomes from projects led primarily by NEDO aimed at the practical implementation of PV-powered vehicles, albeit partially. Below is an overview of the findings presented in each chapter, along with the future outlook, issues, and initiatives.

3.1 Findings

3.1.1 Trends in PV-powered Vehicles and Their Expected Benefits

PV was initially installed in passenger vehicles for ventilating the interior of the vehicle, but now the electricity generated is used for driving the vehicle. In recent years, in addition to increasing the output of PV, the range of vehicles equipped with PV has expanded, and interest in as well as expectations for the specific benefits have been growing.

- Passenger vehicles equipped with PV of approximately 200 W rated output have already been commercialized, and the application is beginning to expand to small vehicles, commercial vehicles as well as large vehicles such as trucks and trailers. The installation of PV on large vehicles is being demonstrated in pilot projects in Japan, the United States, and Europe, and market introduction is expected in the near future.
- Installing PV systems on passenger vehicles has somewhat plateaued, but efforts toward the commercialization of PV-powered vehicles with outputs on the order of 1 kW are continuing.
- In Japan, the expected benefits of PV-powered passenger vehicles (electric vehicles and plug-in hybrid electric vehicles) indicate that, in scenarios where adoption is promoted, the number of vehicles in use could exceed 30 million by 2050, with CO₂ emission reductions exceeding 500,000 tons per year during the 2040s.
- Furthermore, by 2050, a reduction of approximately 17 TWh in externally supplied charging electricity is anticipated. This would decrease the total number of external charging events by roughly 100 million, contributing to improved user convenience and a reduction in societal costs associated with charging infrastructure development.

3.1.2 Demonstration Driving of PV-Powered Vehicles for Passenger Use

The effects of installing PV systems vary depending on the PV output, vehicle driving patterns, driving and parking environments, and the specific vehicle model. Demonstration driving trials of PV-powered vehicles for passenger use are still being continuously conducted, and various results and issues will continue to be identified in the future. Based on the results obtained so far, the following findings have been obtained.

- (1) Plug-in Hybrid Vehicle (PV Cell Output: 860 W) (Evaluation of Generated Electricity and Driving Range, as well as Irradiance and Power Generation on Curved Vehicle-Mounted Surfaces)
 - For a demonstration drive conducted primarily in Nagoya City, in which the vehicle was driven 35 km

in the morning and another 35 km in the afternoon, mainly on expressways, the vehicle driving energy consumption rate was measured to be roughly 10.1 km/kWh. During daytime parking, the vehicle-mounted PV system charged the battery, which supplemented the power consumed during the morning drive. On the day of measurement in June 2020 (under clear skies), the amount of electricity generated by the PV system was roughly 4 kWh/day, which was confirmed to be sufficient to enable driving of 30 km per day.

- Based on measurements conducted in September 2021, the correlation between the amount of solar irradiation measured by pyranometers attached to the vehicle and the cruising distance was examined. It was found that the driveable distance using PV-generated electricity and the daily amount of solar irradiation were proportional, and the proportionality constant was 5.9 km/(kWh/m²/day) in this measurement. While seasonal variations in power consumption rates must be taken into account, for example, Tokyo receives approximately 1,200 kWh/m² of solar irradiation per year. Therefore, a vehicle equipped with an 860 W PV system would theoretically be able to drive approximately 7,080 km per year.
- From data obtained through demonstration drives in the south-eastern part of Shizuoka Prefecture (coastal to mountainous areas), the generation power correction coefficients accounting for the vehicle's curved surfaces, in addition to shading due to the driving environment, were analyzed. The resulting correction coefficients were as follows: engine hood: 0.952–0.971, front roof: 0.968–0.975, rear roof: 0.965–0.968, and rear section: 0.966–0.971.

(2) Battery Electric Vehicle (PV Cell output: 1,150 W) (Assessment of Generated Electricity, Reduction in Charging Frequency, and Performance under Solar Irradiance Fluctuations)

- Given the actual driving energy consumption rate determined by driving on public roads (roughly 6 km/kWh) and the estimated power generation amount based on a solar irradiation database (for Yokohama City), the driveable distance from PV power is 7,100 km per year. Due to seasonal variations in the amount of power generation and electricity consumption, the driveable distance from PV power is roughly half as much in winter as it is in summer.
- Charging frequencies were calculated from the PV power generation, power consumption rate, and driving distance obtained through demonstration driving. As a result, operation without charging by utilizing PV-generated power can only be achieved for driving distances up to 50 km.
- In the case of weekend-only use (assuming 25–200 km of driving per day), the electricity generated by PV during weekdays cannot be fully stored, and as a result, it is not sufficiently utilized. However, in a driving pattern with 5–100 km per day on both weekdays and weekends, PV-generated electricity can be effectively utilized, and even for driving distances exceeding 50 km per day, the number of annual charging events can be significantly reduced. For weekday commuting use, it was shown that no charging is required when the one-way commuting distance is 10 km, and even when the distance is 25 km one way, the number of annual charging events can be reduced by approximately 48%.
- With respect to the shade that falls on the vehicle when driving, to deal with shadows that move in front-rear direction, which are expected to occur frequently, cells could be arranged in series horizontally across the vehicle (perpendicular to the direction of driving) to maintain module voltage, reducing the

loss in power generation caused by a decline in module current.

- In conditions where the vehicle moves between sunlight and shade, the MPPT control initial search voltage could be raised to improve the MPPT control response. When the MPPT voltage is roughly 38 V, setting the initial search voltage between 20 and 35 V would raise the MPPT achievement rate to 97% or higher.

3.1.3 Demonstration Driving of Commercial Vehicles Equipped with PV Systems

Commercial vehicles encompass a wide variety of types and uses. In addition to vehicle configurations and operational patterns, the ways in which generated electricity is utilized also vary greatly. These factors significantly affect power generation performance and are expected to cause substantial variations in the effectiveness of PV installation. Efforts have been undertaken to estimate power generation while taking these factors into account, as well as to assess the potential market impact of deploying mobile units equipped with PV.

(1) Electric commercial vehicles (demonstration driving with PV-powered vehicles and development of design technologies)

- PV modules or pyranometers were installed on electric commercial vehicles to measure power generation, solar irradiance, and vehicle power consumption during actual driving, thereby obtaining data to verify the effects of PV installation.
- In demonstration experiments conducted with the cooperation of businesses in Fukushima Prefecture, assuming the installation of PV with 20% efficiency on a small delivery van (average driving distance: 15 km/day, roof area: approximately 2.7 m²) and a delivery truck (average driving distance: 30 km/day, roof area: approximately 10 m²), it was estimated that 44% of the annual vehicle power consumption for the small van and 35% for the delivery truck could be supplied by PV. For a community bus equipped with a 1.12-kW PV module (average driving distance: 50 km/day), it was estimated that PV could supply 13.5% of the annual power consumption.
- In parallel, a simulation model of vehicle power consumption and battery charge/discharge has been developed. By integrating this with PV power generation estimates, it becomes possible to simulate the state of charge (SOC) of the vehicle battery, enabling the assessment of the effects of PV installation and providing feedback for the design of battery capacity, charging control mechanisms, and related vehicle systems.

(2) Internal combustion engine trucks and trailers (development of quantitative evaluation techniques for the effects of PV Installation)

- PV systems (film-type CIGS PV modules: 300 W or 500 W) were installed on 200 commercial vehicles operating nationwide (as of December 18, 2024), and power generation was continuously monitored. This allowed for the assessment of the potential of vehicle-mounted PV without route bias, as well as the demonstration of previously developed techniques for predicting the amount of electricity generated by the vehicle-mounted PV.
- Solar irradiance on the vehicle decreases compared to stationary measurements depending on the driving

mode, such as whether the vehicle is operating in mountainous or suburban areas. However, it can be calculated using a common vehicle-mounted solar irradiance model and a power generation model.

- From the driving records of seven trucks, the fuel-saving effect was evaluated. Although the measurements were limited to November, fuel savings were mainly achieved by suppressing alternator operation during idling, resulting in an estimated 5% improvement in fuel efficiency. Considering seasonal variations, PV power generation and fuel-saving effects are expected to increase by approximately 1.6 times, corresponding to an expected fuel-saving effect of 8%.

3.1.4 Reliability Evaluation of PV modules for passenger vehicles

PV modules installed on vehicles are exposed to usage environments different from conventional PV modules fixed on building roofs or on the ground. Therefore, reliability evaluation items considered necessary for vehicle-mounted PV have been investigated and examined, and reliability tests for automotive components have been conducted.

- A comparison of evaluation items in general ground-mounted PV and automotive component standards shows that requirements for durability and reliability differ. For example, tests specified only for automotive components include mechanical shock and thermal shock. Vibration tests are specified for both ground-mounted PV and automotive components; however, for in-vehicle electrical and electronic equipment, the conditions for vibration and mechanical shock tests are detailed according to the mounting location and vehicle type.
- When vibration, mechanical shock, thermal shock, and steel ball drop tests were conducted on in-vehicle electrical and electronic equipment, more pronounced degradation was observed in resin modules compared to glass modules. This indicates that degradation behavior due to environmental loads specific to automotive components varies greatly depending on module materials and structure. Therefore, it is desirable to appropriately perform these tests during the research, development, and commercialization process.

3.1.5 Resilience Effects of Installing PV Systems on Passenger Vehicles

In emergency situations such as disasters, both electric vehicles and PV systems can serve as emergency power sources in areas experiencing grid outages. PV-powered vehicles can serve as efficient standalone power sources by combining PV electricity generated during the daytime with the storage batteries of electric vehicles that require external charging.

- One advantage of electric vehicles is their potential use as emergency power sources during disasters. The installation of PV systems can enhance resilience compared to vehicles without PV.
- The effect on resilience depends not only on the balance between supply and demand but also on the process of delivering and transporting surplus electricity obtained from vehicle-mounted PV systems to disaster relief centers. Social behavior during emergencies also influences the outcome.
- To fully utilize the benefits of vehicle-mounted PV, it is preferable to use them in a manner that leverages their public-good characteristics; however, the design of appropriate incentives is important.

3.2 Future Challenges and Prospects

In pursuit of carbon neutrality by 2050, there is a significant demand for the transportation sector, and initiatives in the automotive sector are particularly important. PV-powered vehicles can not only reduce CO₂ emissions by supplying driving power directly from PV systems, but also decrease charging frequency, which is considered one of the obstacles to the widespread adoption of electric vehicles, thereby improving convenience for users.

For passenger vehicles equipped with PV systems with an output capacity of approximately 1 kW, it is possible to achieve around 7,000 km of driving per year using PV electricity. This contributes to CO₂ emission reduction and minimizes the need for external charging, leading to energy savings and reduced charging frequency. Although the economic feasibility of installing PV system on passenger vehicles is currently limited relative to the expected benefits, the application of PV system to vehicles is expanding to small vehicles, commercial vehicles, and large vehicles such as trucks and trailers. The installation of PV on large vehicles is expected to achieve commercialization in the near future.

Electrical design technologies for the installation of PV systems on vehicles have improved, and methods for evaluating the effects of shading from surrounding buildings during vehicle operation, the area and location of PV module installation, and vehicle body curvature, as well as methods for predicting power generation, have also become more accurate. In addition, regarding storage batteries, which influence the effectiveness of PV installation together with vehicle driving patterns, simulation models are being developed to estimate the state of charge (SOC) of storage batteries when installing PV system on commercial vehicles. These models support the design of battery capacity, charge/discharge control, and related aspects, and are expected to be applicable to passenger vehicles as well.

Although PV modules for passenger vehicle roof mounting are still under development, degradation behavior caused by environmental loads specific to automotive components varies greatly depending on the module materials and structure. Compared to stationary PV modules, the required service life of vehicle-mounted PV modules is shorter, and a wide range of test items is necessary, making the establishment of efficient testing methods desirable.

Based on these findings, the challenges and prospects for the practical application of PV-powered vehicles are presented.

3.2.1 Future Challenges

Efforts toward the practical application of PV-powered vehicles are becoming increasingly active worldwide. In Europe, initiatives are being strengthened by establishing KPIs for technology development aimed at full-scale commercialization.

In Japan as well, through various technological developments, including demonstration driving on public roads, the effects and challenges of PV-powered vehicles have been confirmed and verified in real-field conditions, providing a variety of insights. However, for full-scale practical application of PV-powered vehicles, it is necessary to further accelerate efforts such as continuous data acquisition and analysis through demonstration driving, module design and development technologies, establishment of evaluation techniques and testing methods to support practical use, and cost reduction of the system, as illustrated in Table 3.2-1.

Continuous demonstration driving of PV-powered vehicles, including commercial vehicles, allows for the

acquisition of various data, and by improving the accuracy of data analysis, reliable effect predictions and design technologies can be derived. In addition, by accurately understanding and analyzing vehicle performance, including not only PV but also storage battery characteristics, it becomes possible to optimize vehicle design.

Furthermore, to accommodate a variety of vehicles, it is necessary to advance the design of PV modules of various types and shapes as well as system integration technologies. It is also essential to develop the performance of PV modules as power generation equipment and as automotive components, along with standardization and testing methods required for these functions. These efforts should ideally be established as guidelines and standard specifications.

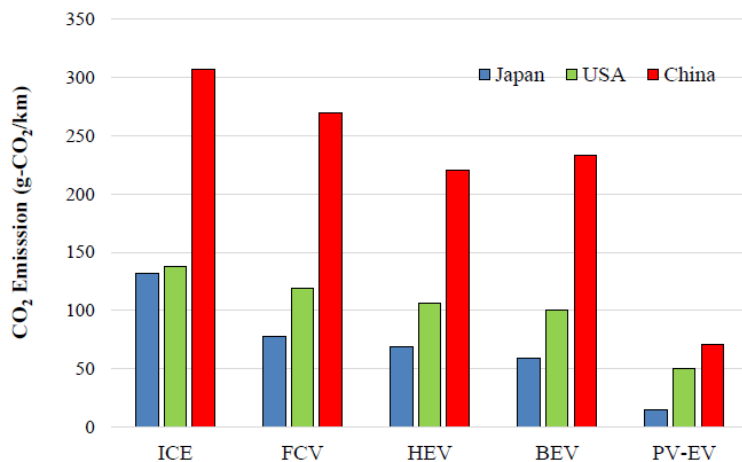
It is also extremely important to understand the price level of PV-powered vehicles acceptable to users, as well as that of the PV system itself, and to reduce costs accordingly to achieve this target.

Table 3.2-1 Challenges and initiatives for the full-scale practical application of PV-powered vehicles

Demonstration driving and verification of effects of PV-powered vehicles	<ul style="list-style-type: none"> - Development and demonstration of various types of PV-powered vehicles. - Data acquisition and analysis through demonstration driving under various regions, environmental conditions, and driving patterns. - Effect prediction using simulation models, etc.: <ul style="list-style-type: none"> Fuel consumption reduction, CO₂ emission reduction, electricity consumption reduction, economic effects, social effects, etc. - Verification of effects through demonstration driving and reflection of results in design technologies.
Establishment of design technologies for PV-powered vehicles	<ul style="list-style-type: none"> - Optimization of PV-powered vehicle design based on demonstration driving and effect verification: <ul style="list-style-type: none"> System design of PV-powered vehicle considering battery characteristics. Effective utilization of PV electricity when the battery is fully charged (external supply: V2X).
Development of module design, analysis, and system integration technologies	<ul style="list-style-type: none"> - Design and development of highly durable, ultra-light flexible modules: <ul style="list-style-type: none"> Modules resistant to mechanical stress and hail. Vibration countermeasures, partial shading countermeasures, and aesthetic adjustments for vehicle-mounted use. Improved flexibility (applicable to vehicles, agriculture, building materials, etc.). - Evaluation, demonstration data analysis, and optimal design technology development for 3D curved PV: <ul style="list-style-type: none"> Evaluation and analysis of internal stress in 3D curved PV. One-stop solution technology development balancing performance and durability according to vehicle body shape. System design leveraging the characteristics of next-generation solar cells such as perovskite.
Development of performance evaluation and testing methods	<ul style="list-style-type: none"> - Development and standardization of testing methods for electrical and mechanical performance of curved modules. - Identification of reliability evaluation items as automotive components and development and standardization of testing methods.
Cost reduction for practical application	<ul style="list-style-type: none"> - Setting module and system cost targets according to vehicle type and module type.

3.2.2 Future Prospects

Figure 3.2-1 shows a comparison of CO₂ emissions per km driven for various types of vehicles¹ in Japan, the United States, and China. Even for electric vehicles, which are expected to be clean vehicles, the introduction of renewable energy such as PV is essential. Against this background, the development of PV-powered vehicles is considered important. According to a scenario² by the U.S. Department of Energy, by 2050, PV is expected to account for 45% of electricity generation, with a cumulative installed capacity of 1,600 GW. Of this, the transportation sector is projected to account for 20%, corresponding to a cumulative installed capacity of 320 GW.



(ICE: internal combustion engine vehicle, FCV: fuel cell vehicle, HEV: hybrid electric vehicle, BEV: battery electric vehicle, PV-EV: PV-powered vehicle (electric vehicle))

Fig. 3.2-1 Comparison of CO₂ emissions per kilometer driven for various types of vehicles in Japan, the United States, and China

As vehicle-mounted PV, high performance is first required. Figure 3.2-2 shows the estimated required PV module installation area and module efficiency for PV-powered vehicles driving 30 km per day (calculated using the average solar irradiance in Nagoya, Japan, which has favorable insolation, 4 kWh/m²/day, and the vehicle's electricity consumption [km/kWh] as parameters)³. Even assuming full utilization of the roof and bonnet of current passenger vehicles, it is clear that a generation efficiency of at least 30% is necessary. Improving PV efficiency is effective not only for increasing driving range but also for reducing CO₂ emissions of PV-powered vehicles.

Figure 3.2-3 shows the impact of highly-efficient PV on the CO₂ emission reduction effect of electric vehicles equipped with PV systems⁴. CO₂ emissions from the transportation sector account for approximately 24% of global emissions, of which about 44% come from passenger vehicles⁵, highlighting the significance of reducing CO₂ emissions. In the case of electricity consumption of 10 km/kWh, installing a vehicle with PV module of 30% efficiency is expected to reduce CO₂ emissions by approximately 63%. As shown in Figure 3.2-3, in the case of a Prius demonstration vehicle equipped with a PV system (electricity consumption: 9.35 km/kWh), a CO₂ emission reduction of about 62% has been demonstrated⁶. Increasing PV efficiency is also effective in reducing charging costs and charging frequency for electric vehicles. For an electricity consumption of 10 km/kWh, installing a vehicle with a PV module of 30% efficiency is expected to reduce annual charging costs by approximately 150 USD⁴.

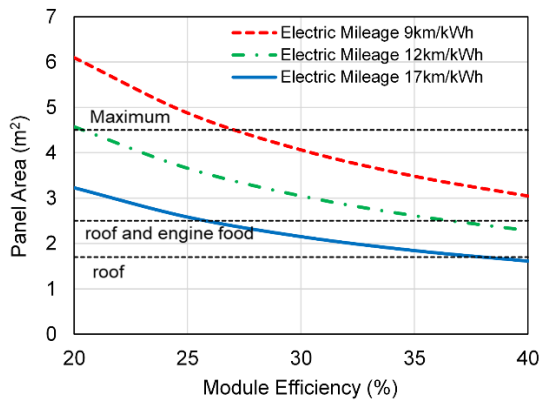


Fig. 3.2-2 Required PV module installation area and module efficiency for PV-powered vehicles driving 30 km per day

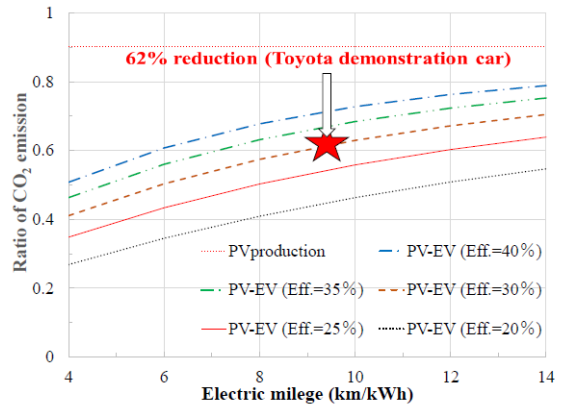


Fig. 3.2-3 Impact of highly-efficient PV on CO₂ emission reduction effect of electric vehicles equipped with PV systems

Reducing the cost of PV systems is also essential for the widespread adoption of PV-powered vehicles. According to a survey of 5,000 customers⁷ conducted by Toyota Motor Corporation, as shown in Figure 3.2-4, approximately half of the customers expressed strong interest if a PV-powered vehicle with 30% efficiency and a cost of 1.5 USD/W were developed.

Figure 3.2-5 shows the option prices of vehicle-mounted PV and directions for cost reduction. The option prices of installing PV systems for PV-powered vehicles sold by Toyota Motor Corporation (from the 2009 Prius to the 2022 bZ4X) ranged from 216,000 to 286,000 JPY, with costs decreasing from 4,000 JPY/W to 1,200 JPY/W. For a PV output of 200 W, as mentioned above, the attractiveness of PV-powered vehicles is low, and it is necessary to offer a 1 kW-scale PV system at 200,000–300,000 JPY. To achieve this, as also shown in Figure 3.2-4, it is considered necessary to realize module costs below 1.5 USD/W.

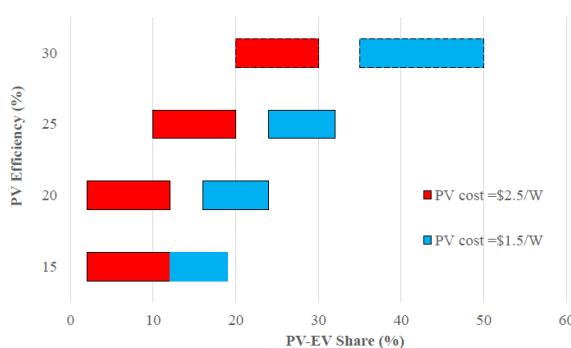


Fig. 3.2-4 Customer expectations for highly-efficient, low-cost vehicle-mounted PV among Toyota customers

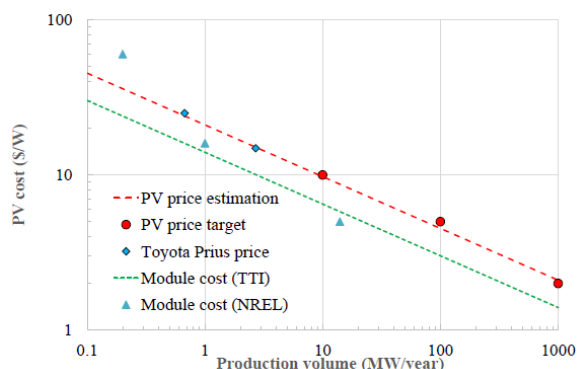
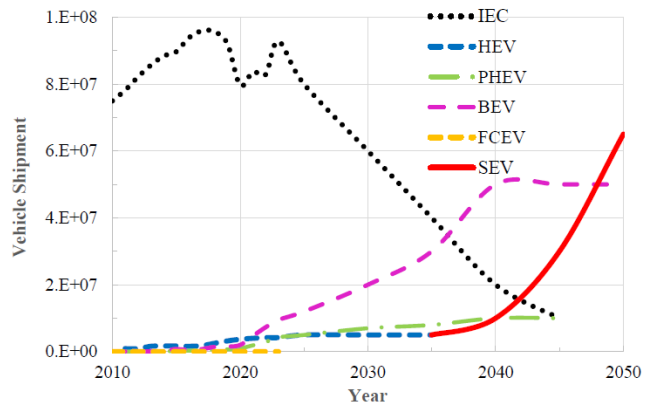


Fig. 3.2-5 Direction of vehicle-mounted PV cost reduction

For the full-scale practical application of PV-powered vehicles, it is necessary for companies and stakeholders involved in the development and manufacturing of both PV modules and vehicles to work together in an integrated manner. To this end, not only in terms of PV technology but also in mid-to-long-term roadmaps for vehicle driving technologies and markets, it is desirable that PV-powered vehicles be

positioned as key vehicles of the future, as shown in Figure 3.2-6.



(ICE: internal combustion engine vehicle, HEV: hybrid electric vehicle, PHEV: plug-in hybrid electric vehicle, BEV: battery electric vehicle, FCEV: fuel cell electric vehicle, SEV: solar electric vehicle (e.g. PV-powered vehicle))

Fig. 3.2-6 Transition of various types of vehicles⁸ and future projections

Although efforts toward PV-powered vehicles are becoming more active, the pathway to full-scale practical application is still at an early stage. Similarly to PV technology development, initiatives for electric vehicle development are intensifying worldwide, leading to increased competition.

It is expected that by continuously pursuing initiatives from both the PV and automotive perspectives, the widespread adoption of PV-powered vehicles can be realized, which in turn is anticipated to stimulate the domestic related industries through market expansion.

【Chapter 3 References】

- ¹ M. Yamaguchi et al., Prog. Photovolt. 29, 684 (2021).
- ² B. Jones, presented at the 49th IEEE PVSC, Philadelphia, June 5-10. 2021.
- ³ T. Masuda et al., Solar Energy 146, 523 (2017).
- ⁴ M. Yamaguchi et al., Energy and Power Engineering 13, 147 (2021).
- ⁵ T. Masuda et al., Proc. 49th IEEE PVSC, (IEEE, New York, 2022) pp. 467.
- ⁶ NEDO, PV-Powered Vehicle Strategy Committee Interim Report
(<https://www.nedo.go.jp/content/100885778.pdf>)
- ⁷ T. Hara et al., SAE Technical Paper 2016-01-1286, 2016, doi:10.4271/2016-01-1286.
- ⁸ IEA. Global EV Outlook 2024 (<https://www.iea.org/reports/global-ev-outlook-2024>)

PV-Powered Vehicle Strategy Committee

<List of committee members (as of 31 March 2025)>

Chair of committee	Kensuke Nishioka	Professor, Research Center for Sustainable Energy & Environmental Engineering, Faculty of Engineering, University of Miyazaki, Japan
Committee member	Kenji Araki	Distinguished Professor, Research Center for Sustainable Energy & Environmental Engineering, Faculty of Engineering, University of Miyazaki, Japan
	Masakazu Ito	Professor, Division of Engineering, Faculty of Engineering, University of Fukui, Japan
	Shinya Iwasaki	Assistant Manager, Carbon Neutral System Planning Dept., Carbon Neutral System Development Div., Carbon Neutral Engineering Development Center Toyota Motor Corporation, Japan
	Yuzuru Ueda	Professor, Department of Electrical Engineering, Faculty of Engineering, Tokyo University of Science, Japan
	Hiroyuki Juso	Division Manager, Compound Business Promotion Division, Sharp Energy Solutions Corporation
	Yosuke Tomita	Assistant Manager, EV System Laboratory, Research Division, Nissan Motor Co., Ltd., Japan
	Toshio Hirota	Ph.D., Adjunct Researcher, Research Institute of Electric-driven Vehicles, Waseda University, Japan
	Yukitaka Matsuoka	Ph.D., Senior Researcher, Electric System Research Group, Environment Research Division, Japan Automotive Research Institute, Japan
	Hidenori Mizuno	Chief Senior Researcher, Photovoltaic System and Application Research Team, Renewable Energy Research Center, Fukushima Renewable Energy Institute, National Institute of Advanced Industrial Science and Technology (AIST), Japan
	Masafumi Yamaguchi	Professor Emeritus, Invited Research Fellow, Toyota Technological Institute, Japan
Observer	Makoto Tanaka	Chief of Secretariat, Photovoltaic Power Generation Technology Research Association, Japan
	Akira Terakawa	Head of Technology Department, Photovoltaic Power Generation Technology Research Association, Japan
	Noboru Yamada	Professor, Department of Mechanical Engineering, Nagaoka University of Technology, Japan
	Daisuke Sato	Associate Professor, Electrical and Electronics Engineering Program & Green Transformation (GX) Research Center, Faculty of Engineering, University of Miyazaki, Japan
	Tatsuya Takamoto	Distinguished Professor, Vice Director, Green Transformation (GX) Research Center, University of Miyazaki, Japan
Secretariat	Atsuyuki Suzuki	Deputy Director, Solar PV System Unit, Renewable Energy Development, New Energy and Industrial Technology Development Organization (NEDO), Japan
	Hirokazu Nomoto	Project Coordinator, Solar PV System Unit, Renewable Energy Development, New Energy and Industrial Technology Development Organization (NEDO), Japan
	Kiyoshi Fukushima	Technical Researcher, Solar PV System Unit, Renewable Energy Development, New Energy and Industrial Technology Development Organization (NEDO), Japan
	Keiichi Komoto	Manager, Sustainability Consulting Division 1, Mizuho Research & Technologies, Ltd., Japan

Takahiro Kirihara	Manager, Sustainability Consulting Division 1, Mizuho Research & Technologies, Ltd., Japan
Naoto Takatsu	Senior Consultant, Sustainability Consulting Division 1, Mizuho Research & Technologies, Ltd., Japan
Ryohei Toyoda	Senior Consultant, Sustainability Consulting Division 1, Mizuho Research & Technologies, Ltd., Japan